personal buildup for

Force Motors Limited Library

MTZ worldwide 4/2012, as epaper released on 09.03.2012
http://www.mtz-worldwide.com

content:

www.MTZonline.com

MTZ WORLDWIDE

04 April 2012 | Volume 73

POTENTIALS and Limits of CO_2 Emissions of Gasoline Engines

FRICTION in Highly Loaded Journal Bearings

SOOT AND ASH Distribution in Diesel Particulate Filters

/// INTERVIEW

Peter Langen
BMW

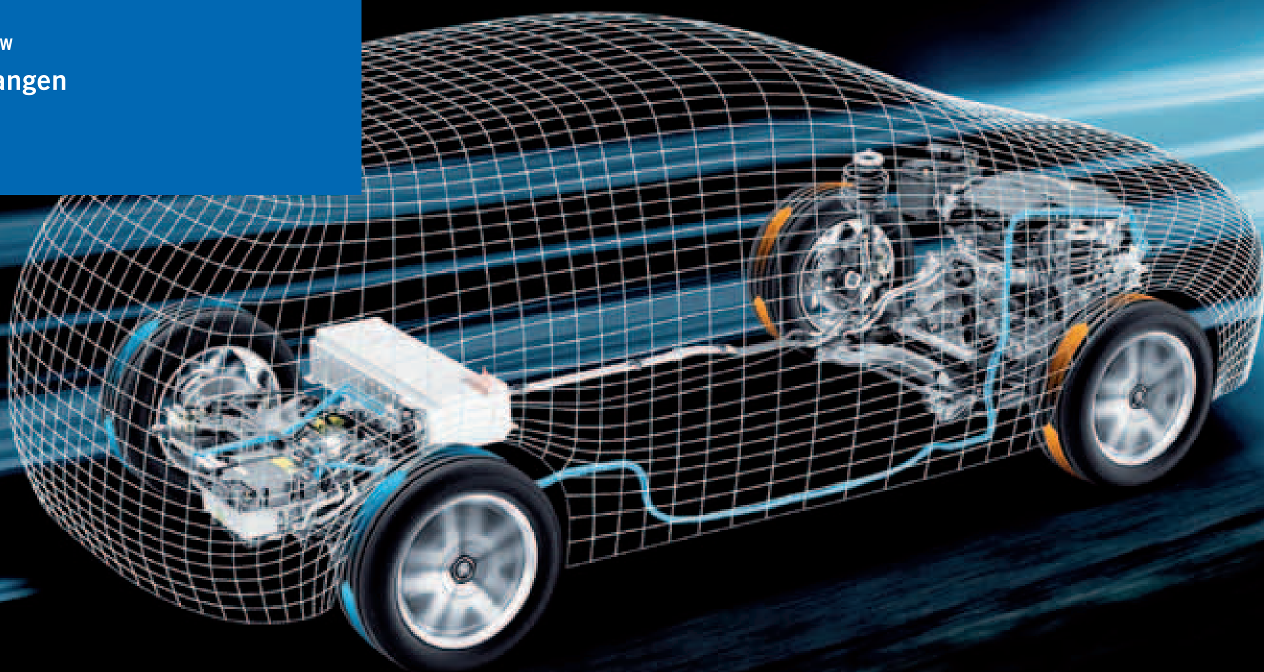

HYBRID DRIVES WITH LOWER EMISSIONS

CONTENTS

COVER STORY

HYBRID DRIVES WITH LOWER EMISSIONS

4, 12, 16 I The fuel consumption and emissions benefits that can be achieved by hybridisation of the powertrain are in competition with an increase in technical complexity – and therefore in cost. For that reason, the question of which hybrid configuration is suitable for which vehicle class can frequently be answered by a cost-benefit calculation. However, an isolated consideration of emissions alone does not always result in a direct improvement through hybridisation, as is shown by the example of the particulate emissions of a petrol hybrid powertrain. About hybrid strategies and questions of cost MTZ spoke with Peter Langen, Head of Powertrain Development at BMW.

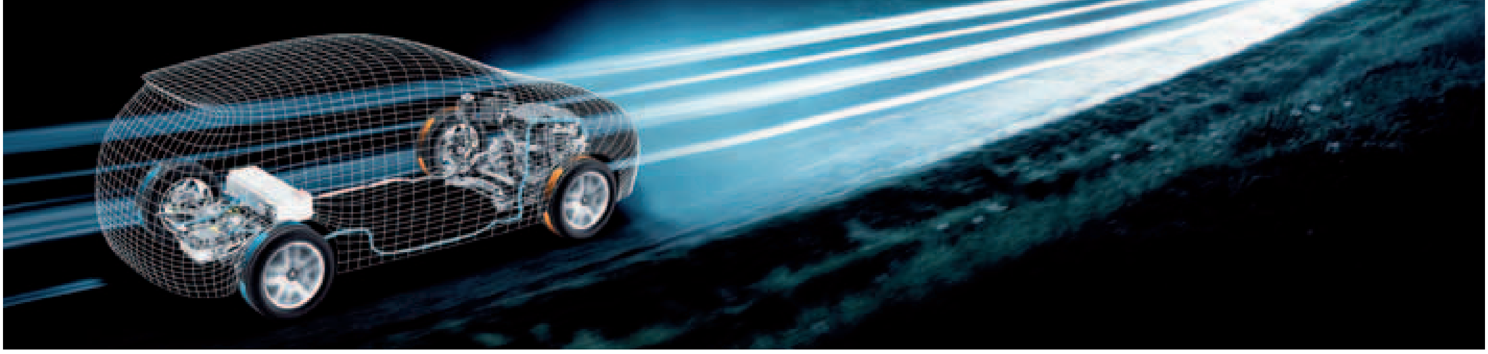

COVER FIGURE I FIGURE ABOVE © Peugeot

MTZ WORLDWIDE

Dear Reader,

Now in its 73rd year of publication, MTZ has lost none of its attractiveness for its users, as I am always pleased to hear and discover for myself. It is required reading for all engine technology specialists in their everyday work, and is the number 1 source of information among all the various media on offer. And amazingly, that is the case in more than 50 countries on all continents.

To ensure that more and more English-speaking readers can understand our content in full, MTZ worldwide was established as an e-magazine a few years ago, and has since acquired a wide readership. This electronic medium contains all of the specialist articles of MTZ in an English-language version. In future, even more articles from international engine development will be added. You can order a sample copy at springervieweg-service@springer.com. I would also be grateful if you would recommend this e-magazine to your colleagues, to enable this instantly accessible specialist medium to become even more popular.

For several years now, our event activities (ATZlive) relating to current issues in our technical field have been successful in networking our readers and bringing them together for a fertile exchange of experiences. I would therefore like to draw your attention to the following events in the second half of the year: 14th MTZ Conference "Virtual Powertrain Creation", 25/26 September in Esslingen; 5th MTZ Conference "Gas Exchange in the Internal Combustion Engine", 23/24 October in Stuttgart; 7th International MTZ Conference "Heavy-Duty, On- und Off-Highway Engines", 6/7 November in Nuremberg.

I would also like to take this opportunity to encourage you to make regular use of our many and varied online initiatives. ATZonline.de provides you with the very latest news from the automotive industry and you can also subscribe free of charge to our twice weekly newsletter to find more detailed reports. And if you have the time, please join in the discussion at the ATZblog to ensure an even more lively exchange of ideas.

Warm regards,

WOLFGANG SIEBENPFEIFFER,
Editor in Chief and Editor in Charge
Stuttgart, February 2012

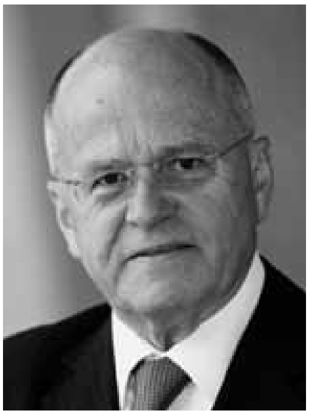

EMISSION POTENTIALS OF A DIESEL PLUG-IN HYBRID

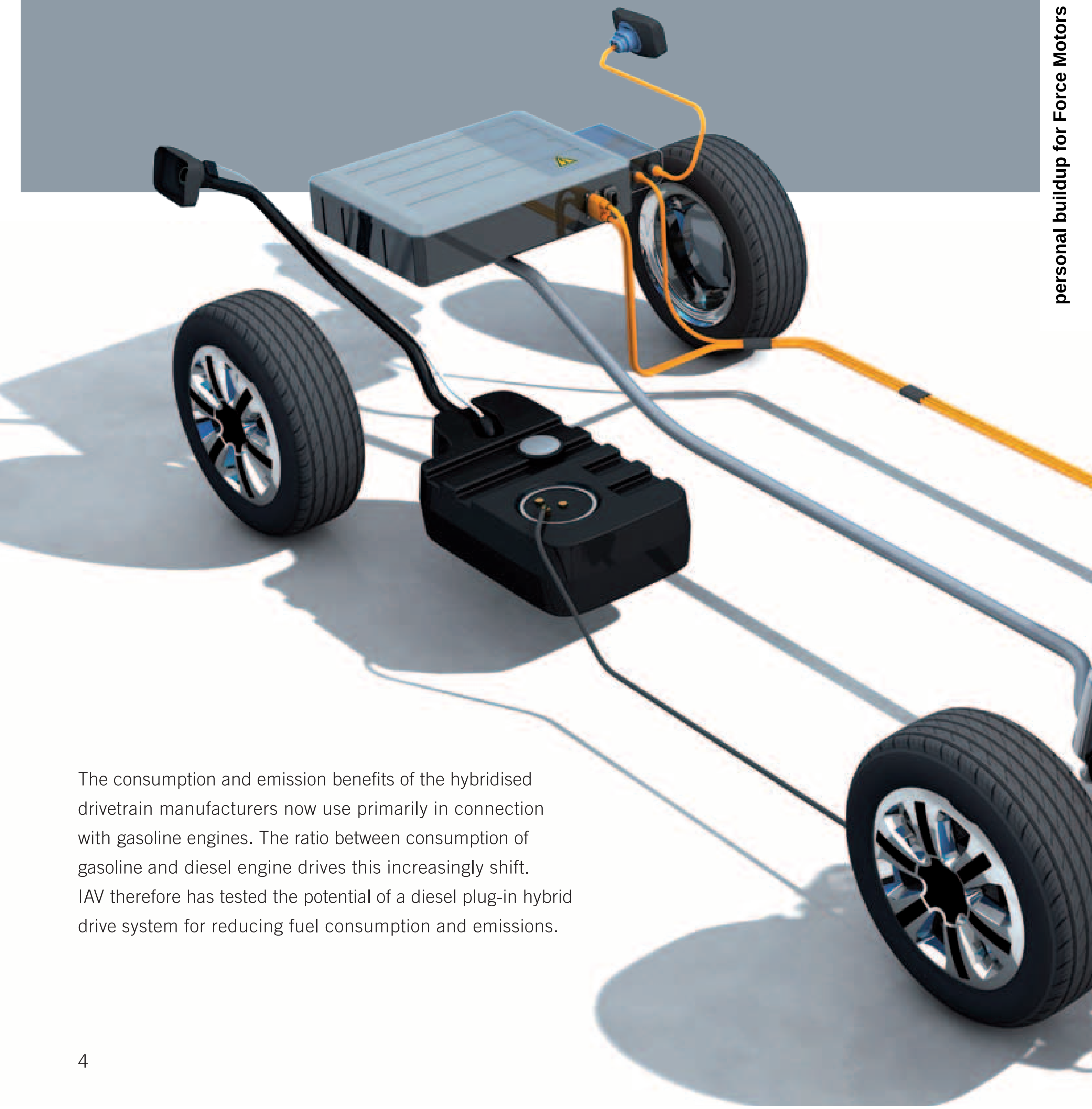

The consumption and emission benefits of the hybridised drivetrain manufacturers now use primarily in connection with gasoline engines. The ratio between consumption of gasoline and diesel engine drives this increasingly shift. IAV therefore has tested the potential of a diesel plug-in hybrid drive system for reducing fuel consumption and emissions.

AUTHORS

DIPL.-ING. MATTHIAS DIEZEMANN
is Technology Scout for the Powertrain Mechatronics Business Area at IAV in Berlin (Germany).

DIPL.-ING. CARSTEN VON ESSEN
is Consultant to the Management of the Powertrain Mechatronics Business Area at IAV in Berlin (Germany).

DIPL.-ING. MIRKO LEESCH
is Development Engineer in the Transmission and Hybrid System Concepts and Synthesis Team at IAV in Chemnitz (Germany).

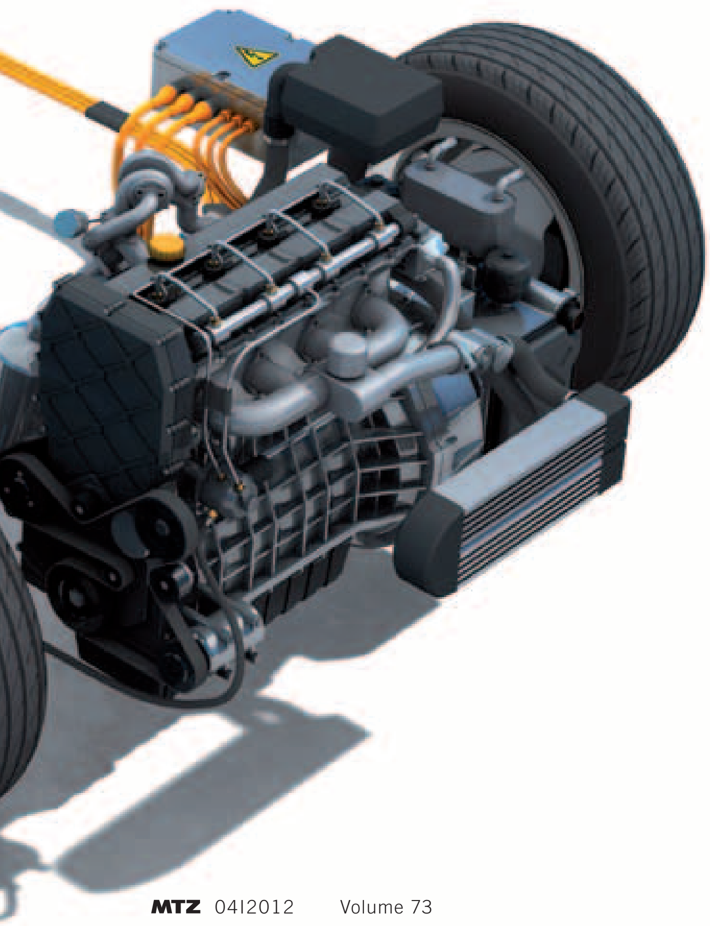

OPPORTUNITIES FOR HYBRIDISATION

In the gasoline engine segment, hybrid technology has reached the point where it is ready to go into mass production, providing many vehicle manufacturers with a component in the modular powertrain system for improving efficiency. Alongside electric drives, upgrading the hybrid drive to include plug-in hybrid electric vehicles (PHEV) is becoming increasingly important. The plug-in concept vehicles recently presented [1-3] confirm this trend.

Even today, various studies show that the demand for final energy will shift from gasoline to diesel fuel by 2030. This will result from less fuel being needed by hybridised gasoline-engine vehicles. It is also assumed that there will be a sharp rise in commercial-vehicle traffic, causing demand to rise for diesel fuel. Both influences will lead to a further shift in the gasoline-to-diesel ratio. The rising diesel share will see efficiency fall in the production process and have a negative impact on price development and the CO_2 balance [4].

Further hybridisation of the diesel engine in Europe makes sense from the aspect of stabilising the ratio between gasoline and diesel fuel.

The diesel engine segment has traditionally been accompanied by a trade-off between particulate and NO_x emissions. Introducing the legally binding CO_2 target of 95 g/km in average fleet consumption by 2020, European legislation is adding a further conflict between NO_x and CO_2 emissions.

Internal engine modifications to reduce NO_x usually produce a marked rise in CO_2. High-pressure EGR concepts come with far greater gas-exchange losses, retarded centres of heat release reduce internal process efficiency and, in the present state of the art, alternative process management approaches, such as status quo HCCI/PCCI, combine poorer process efficiency with inacceptable combustion noise from the diesel engine.

PHEV technology can help the engine to reduce NO_x emissions internally and, at the same time, cut the vehicle's CO_2 emissions by the level demanded. The energy mix used for generating charge power has a significant influence on the CO_2 balance from the energy source to the wheel (well-to-wheel analysis). As the legislator

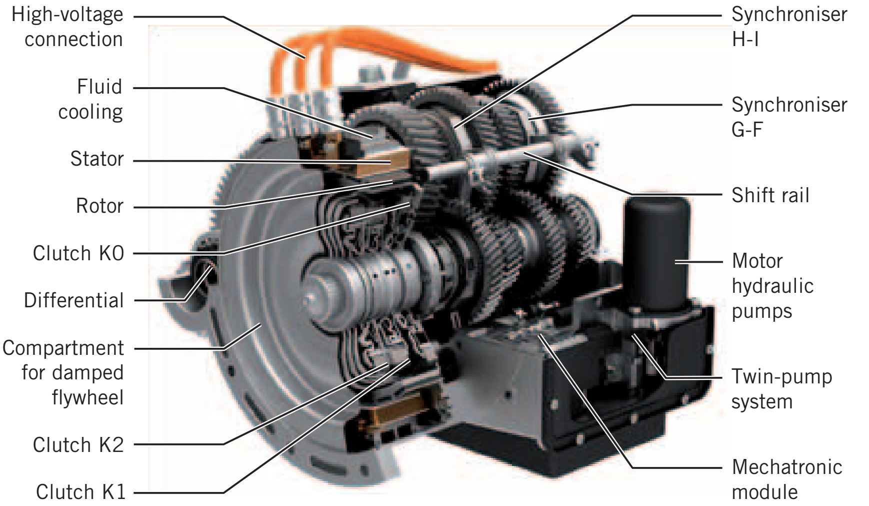

❶ Design draft for the IAV nine-speed hybrid dual-clutch transmission 9H-DCT450

ascribes emissions to the power producers on the polluter-pays principle, this is not negatively reflected in calculating the CO_2 emissions from PHEVs or electric vehicles.

Transient operation produces most of the NO_x emissions from the diesel engine. They are caused by the different time lags in feeding fuel and air into the combustion chamber. A load change is pre-controlled by the rapid fuel path. The fuel-air mixture diverges from the ratio ideal for minimal NO_x emissions until the slower air path has restored the ideal air-fuel ratio. This timing problem can be resolved in a plug-in hybrid by splitting the driver's torque request between combustion engine and e-motor. The load change is initially pre-controlled by the e-motor, and the combustion engine can slowly take over with the ideal air-fuel ratio.

PLUG-IN HYBRID TECHNOLOGY

Studies show that for 80 % of persons polled, an average daily mileage of 50 to 60 km is acceptable in Europe and of 60 to 70 km in the US [5]. Surveys among consumers have revealed that they also want a top electric driving speed of 80 km/h for overland journeys. For the concept, the electric motor's power output and battery capacity have been selected to meet these demands.

The electric machine is positioned between combustion engine and transmission and can be disconnected from the engine by a clutch. This provides the capability of electric driving, starting the engine from stationary as well as delivering or recuperating energy while the combustion engine is running. The battery used comes in the form of lithium-ion cells that provide an electric cruising range of 60 to 70 km.

IAV NINE-SPEED HYBRID DUAL-CLUTCH TRANSMISSION

The IAV 9H-DCT450 nine-speed hybrid dual-clutch transmission used is designed for front transverse application, ❶. The evolutionary development in the number of speeds from six to seven and then on to nine reflects the need to optimise the operating efficiency of combustion engines to meet the future CO_2 targets aimed for.

The transmission was developed for high-performance combustion engines delivering up to 215 kW of power, 450 Nm of torque and a rated speed of 7500 rpm. With this configuration, it can easily be used both for diesel and gasoline-engine applications. To meet the trend toward mild and full-hybrid applications, the electric motor is integrated into the IAV transmission at the input. The permanent-magnet synchronous motor provides a continuous output of 30 kW and 300 Nm. With its compact design length of 368 mm, the hybrid transmission can easily replace modern-day transmissions with six or seven gear ratios [6].

To ascertain the potential fuel saving from IAV's transmission, comparative cycle simulations were conducted on the basis of a C-segment vehicle in combination with a diesel engine and a six or seven-speed dual-clutch transmission, ❷. In the New European Driving Cycle (NEDC) of relevance to consumption, the nine-speed transmission is capable of achieving a fuel saving of 2.6 % over a six-speed transmission. A further 12.8 % saving can be obtained by using the electric motor. The hybrid advantage is clearly shown in the urban cycle and the benefit of wider spreading in the Artemis motorway cycle.

LI-ION TWIN-BATTERY CONCEPT

To cover significant distances on all-electric propulsion, plug-in hybrids have a larger battery than hybrid drive systems without charging function. It is, however, exposed to greater strain. This is why use is made here of a twin-battery concept comprising two lithium-ion batteries. The high-energy (HE) battery has a capacity of 15 kWh and the high-power (HP) battery a capacity of

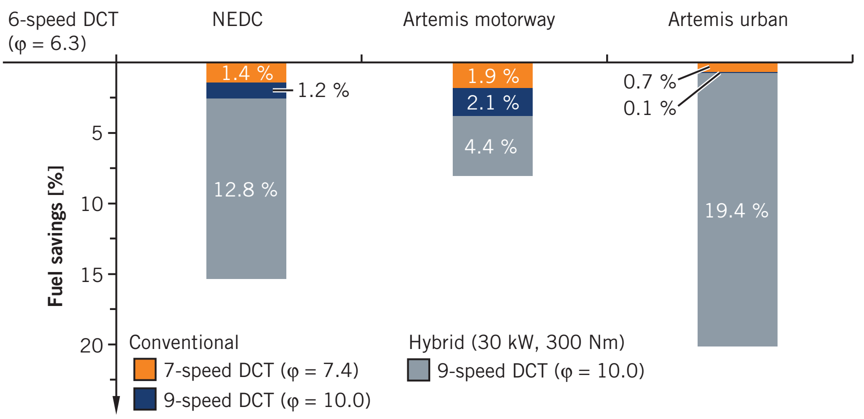

❷ Consumption-reducing potential from dual-clutch transmissions with various numbers of speeds for a C-segment vehicle with a 120 kW diesel engine

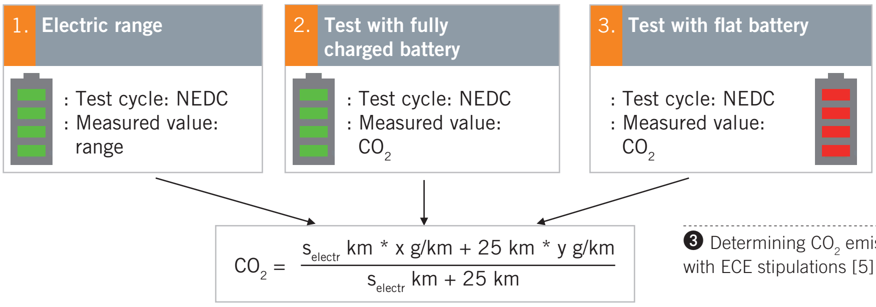

❸ Determining CO_2 emissions for plug-in vehicles in accordance with ECE stipulations [5]

1.5 kWh. An integrated charge manager keeps the charge balance of 10:1 between the HE and HP battery, i.e. energy is continuously passed from the HP to the HE side while charging and in the opposite fashion while discharging. This means the overall battery can utilise the benefit of rapid charging / discharging and the high level of efficiency of the slow battery.

STATUTORY REQUIREMENTS ON PLUG-IN HYBRID VEHICLES

Plug-in hybrids are bivalent vehicles, i.e. powered by fuel and electricity, which is why separate test regulations have been developed for them in European legislation. A core element here is the way in which CO_2 emissions are calculated from two cold-start NEDC test runs. One test run with high battery charge state (full battery) and a second one with low battery charge state (flat battery). CO_2 emissions are determined using the formula in ❸. The ceilings for emissions limited in law (NO_x/HC/CO/particulate) must be met for each in both test runs [7].

SIMULATING LONGITUDINAL DYNAMICS USING STEADY-STATE ENGINE MAPS

In terms of the components fitted in it, the diesel engine permits a huge diversity of options for realising a concept producing extremely low NO_x emissions (EU6). As the basis for the simulations conducted here, a single-stage supercharged fourcylinder engine delivering 100 kW of power was selected that uses high and low-pressure EGR. The engine was measured in steady state on the engine test bench in three engine-temperature ranges. 0-D Velodyn simulation software was used for simulating the powertrain’s longitudinal dynamics. The model allows for engine heat-up behaviour. The transmission, e-motor and battery are also modelled in Velodyn. A hybrid operating-mode manager is used for the operating strategy, ❹.

HYBRID OPERATING STRATEGY

Various operating strategies were produced during the course of the study. For the vehicle, the focus here was on keeping NO_x emissions under 80 mg/km and CO_2 emissions below 50 g/km. The exhaust-gas temperature behaviour of diesel plug-in hybrid vehicles was studied at length in [8]. The findings can be applied to this concept. The diesel-engine vehicle with seven-speed transmission is defined as the base variant.

Compared to the base, the maximum CO_2 potential can be realised in the NEDC all-electrically in a high battery charge state. Briefly oversupplying the e-motor is necessary for this variant. This variant must be regarded as a limit case. To determine CO_2 emissions with high battery charge state, variants were also simulated with differing degrees of all-electric driving-cycle components (e-drive cruising range) in order to define a balance between required e-motor power output

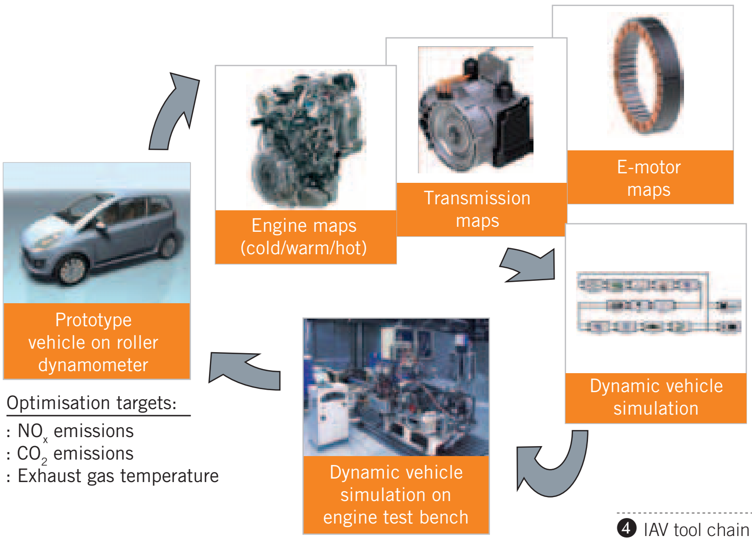

❹ IAV tool chain for simulating longitudinal dynamics

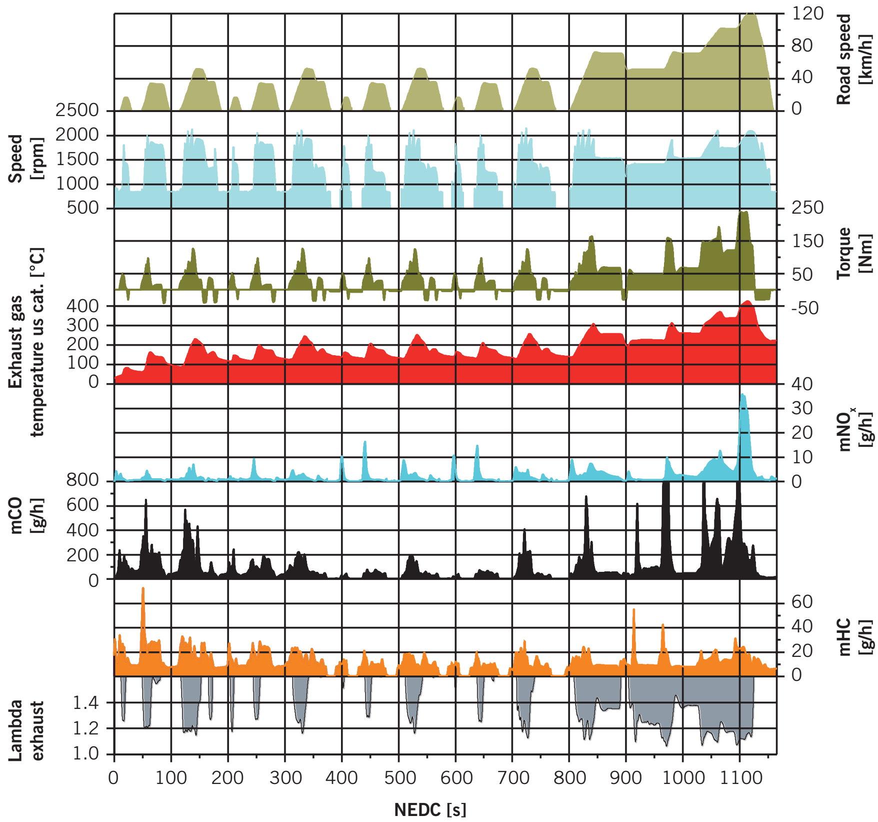

❺ NEDC driving-cycle measurement on the test bench for the base vehicle with 7-speed dual-clutch transmission

and e-drive travelling range. To ascertain the optimum in this context, the maximum all-electric driving speed was first increased from 50 kto 80 km/h, then to 95 km/h and finally to 105 km/h.

For the second test case with low battery charge state, various strategies of phlegmatisation were also simulated [9] that essentially support the combustion engine in acceleration cycles. The approach followed here aims to calm the air path on changing load and thus minimise engine emissions from transient load changes.

RESULTS OF DRIVING-CYCLE SIMULATION (NEDC)

Measurements were conducted on the engine test bench to compare the simulated base variant with a seven-speed dual-clutch transmission, ❺. The D-segment vehicle was shown to satisfy the EU6 emission limit values and achieve a consumption of 6.65 l/100 km (176 g CO_2/km).

By way of example, the curves are shown for the base without hybridisation, ❻, and, in the variant with e-drive V_{max} = 80 km/h, ❼, for the test with high battery charge state. In ⑦, the all-electric driving phases of the NEDC are marked in blue/grey. The combustion engine is activated in the orange areas.

❽ shows hybrid operation with low battery charge state. Operation with torque split between combustion engine and e-motor is plotted in the diagram at the bottom. The e-motor's high dynamic component calms the diesel engine's air path and results in only minor excursions in NO_x emissions. The engine speed plotted in red in the second diagram from the bottom illustrates the combustion engine's stop phases (stop-start function). NO_x emissions accumulate to 65 mg/km for the NEDC, thus remaining well below the EU6 limit value.

❾ presents an overview of the results for CO_2 emissions, with combined CO_2 emissions (low and high battery charge state) being shown for the e-drive variants. Although the e-drive variant with

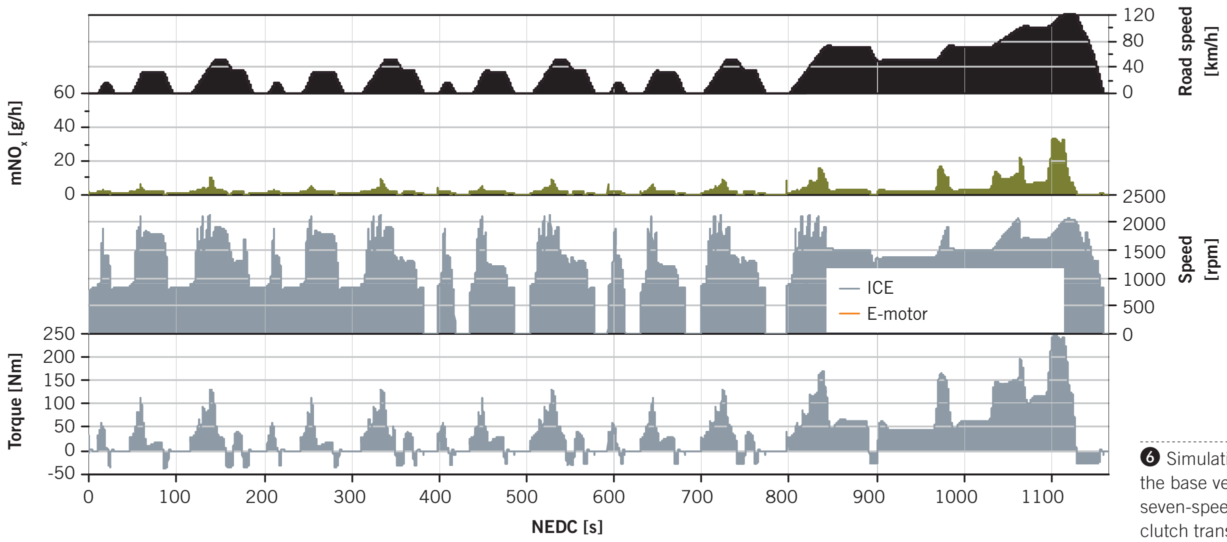

❻ Simulation result for the base vehicle with seven-speed dual-clutch transmission

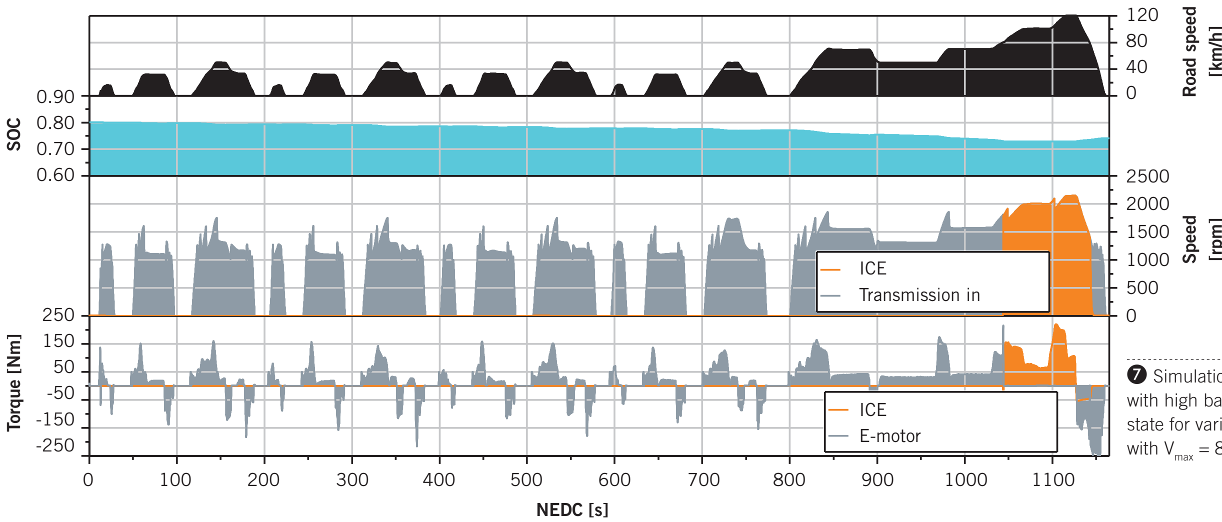

❼ Simulation result with high battery charge state for variant: eDrive with V_{max} = 80 km/h

V_{max} = 105 km/h provides an optimum in terms of electric cruising range and CO_2 emissions with high battery charge state, a peak output of 43 kW is demanded from the e-motor ($P_{nominal}$ = 30 kW) for 4 s while accelerating to 100 km/h. The V_{max} = 80 km/h e-drive variant is shown to provide the best compromise between practical suitability and CO_2 emissions with high battery charge state.

To meet the prescribed CO_2 target of 50 g/km, vehicle weight for the e-drive with V_{max} = 80 km/h can either be reduced or the e-motor's peak output can be adapted for the e-drive with V_{max} = 105 km/h.

SUMMARY

Through phlegmatisation, hybridisation provides the capability of significantly calming the air path and thus of reducing transient engine emissions. The results of simulations show a clear cut in NO_x emissions of 17 % for hybrid operation.

The CO_2 target of 50 g/km aimed for can be achieved through all-electric operation up to a speed of 105 km/h for the vehicle under study. The potential for cutting CO_2 is a compromise between all-electric travelling range and additional vehicle weight on the one hand and a compromise between battery capacity and additional vehicle cost on the other. A diesel PHEV can be produced in every automobile segment for the EU6 emission standard. CO_2 emissions can be significantly reduced and start-off behaviour improved. In economic terms, a PHEV can only hold its own from the C-segment and over.

At the same time, raising load (battery charge) provides the capability of managing exhaust-gas temperature in the way demanded as a means of actively supporting exhaust-gas aftertreatment [8].

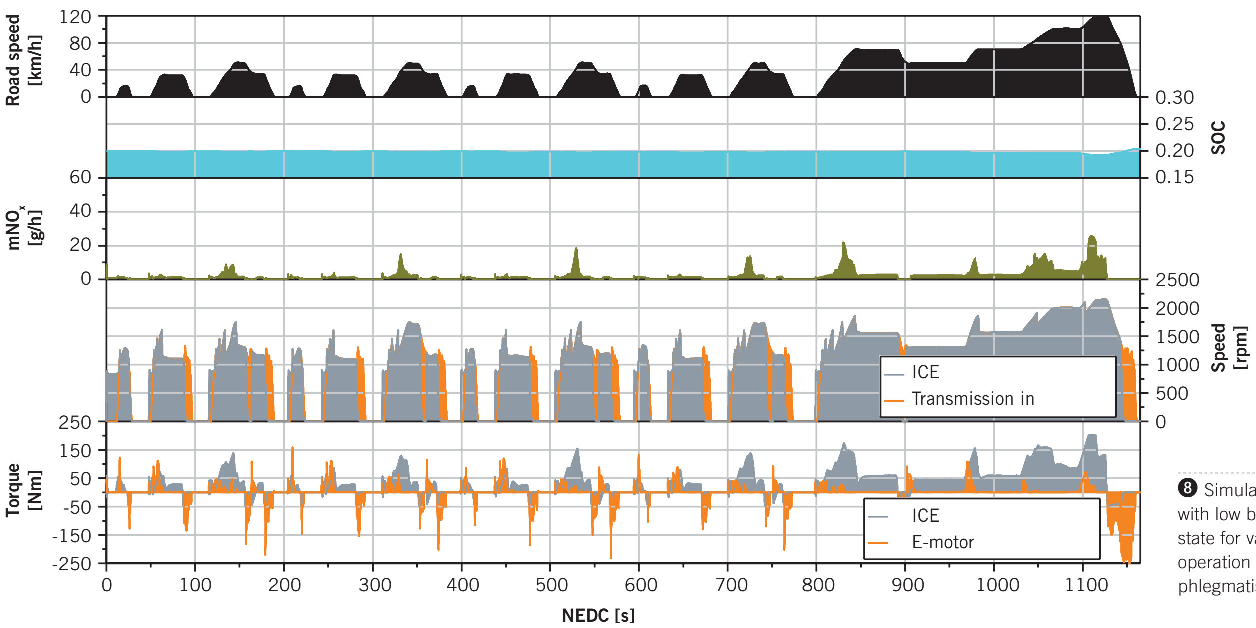

❽ Simulation result with low battery charge state for variant: Hybrid operation with 7 Nm/s phlegmatisation

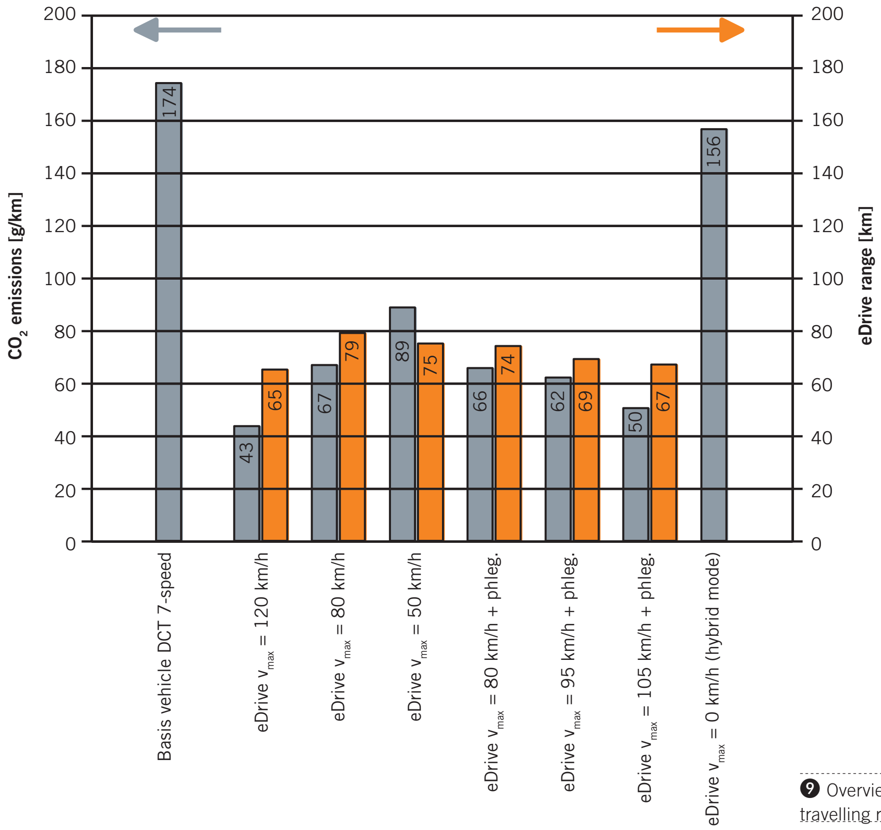

9 Overview of CO_2 emission and all-electric travelling range for the variants simulated

Consequently, plug-in hybrid technology is a key building block in meeting future emission targets and underpins the diesel engine in its quality of being the most efficient automobile drive system on the market.

OUTLOOK

At present, a diesel plug-in hybrid is a complex and costly technology with great potential for achieving low fuel-consumption and emission levels. Future driving cycles with their associated emission limits will determine the extent to which it spreads. The diesel plug-in hybrid will remain less expensive than the e-drive and also outmatch it in performance and cruising range. In comparison to the gasoline plug-in hybrid, the future consumption edge will be a crucial aspect. For provisional versions of the WLTP cycle [10, 11], initial simulations show that it will be necessary to shift drive power from the combustion engine to the e-motor. For future exhaust emission legislation tested in the WLTP cycle, a combination of active deNOxing and PHEV technology must be expected from the D-segment upwards for cost/benefit reasons.

REFERENCES

[1] http://www.volvocars.com/at/top/about/news-events/pages/default.aspx?itemid=40
[2] Toyota Prius als Plug-In-Hybrid, MTZ 70 (2009), No. 11
[3] http://www.automobilwoche.de/article/20110222/REPOSITORY/110229985/1056/REPOSITORY/porsche-ab-2015-alle-modelle-mit-plug-in-hybrid
[4] Dena-Studie 2011: Bedarf und Produktion von Mineralöl im künftigen Energiemix
[5] Takaoka, T.; Komatsu, M.; Killmann, G.: Toyota Motor Europe; Das neu entwickelte Toyota Plug-in Hybrid System und dessen Fahrleistung; 19. Aachener Kolloquium Fahrzeug- und Motorentechnik, 2010
[6] Leesch, M.; Müller, J.; Resch, R.; Paul, S.: A new 9-speed hybrid dual clutch transmission for transverse application up to 450 Nm input torque. 5th CTI Symposium North America 2011
[7] UNECE Vehicle Regulation No. 101, Revision 2 – Amend. 1-4
[8] von Essen, C.; Bunar, F.; Adelberg, S.; Donner, S.; Kramer, M.: Plug-in hybrid – emission-free in the city and efficient over land. 11th Stuttgart International Symposium Automotive and Engine Technologiy 2011
[9] Blumenröder, K.; Bunar, F.; Buschmann, G.; Nietschke, W.; Predelli, O.: Dieselmotor und Hybrid: Widerspruch oder sinnvolle Alternative? Wiener Motorensymposium 2007
[10] Heusler, H.; Müller, A.; Singh, T.: Investigation for a Global Fuel Consumption Drive Cycle, in 20. Aachener Kolloquium Fahrzeug- und Motorentechnik; 2011
[11] Study on cycle modification; 10th DHC subgroup meeting under GRPE/WLTP informal group; Belgium; 2011

"OUR HYBRID STRATEGY IS SUBJECT TO EVOLUTIONARY STEPS"

Is it possible to reduce the costs of the internal combustion engine when electrifying the power-train in a hybrid system? Probably not, says Peter Langen, Head of Powertrain Development at BMW in Munich. Lowering the costs of the electric drive system itself is the only possibility to make the hybrid cheaper in the future.

Dipl.-Ing. Peter Langen studied mechanical engineering at RWTH Aachen University from 1979 to 1984. He joined BMW AG in 1984, initially in engine advanced development. From 1987 to 1991, he worked in engine series development, and from 1991 to 1994 in powertrain advanced development. From 1994 to 1996, he was head of the natural gas vehicle project. From 1997 to 1999, he held overall responsibility for the development of fuel systems, from 1999 to 2004 he was head of powertrain advanced development, from 2004 to 2006 he was Director Driving Dynamics, and since 2007 has been Senior Vice President Powertrain Development at BMW in Munich.

MTZ _ Wouldn't it be a better idea to invest the development costs for the electrification of the powertrain in further developing the internal combustion engine?

LANGEN _ As far as the internal combustion engine is concerned, we have already reached a very high level, and in future we will only make relatively small steps with great effort. These steps are also important, but we will no longer be able to achieve the CO_2 reduction of up to 15 % that we have achieved with the hybrid.

Why doesn't BMW offer a diesel hybrid?

The diesel hybrid combines two very expensive drive units. A diesel engine is, in itself, already very fuel-efficient, and one can certainly achieve a little more through hybridisation, but we must ask ourselves whether the customer will be prepared to pay the additional cost involved. We are currently doing very well with our spark-ignition hybrid, for example in a new ActiveHybrid 5, also because we can market this concept internationally, which would only be possible to a limited extent with a diesel hybrid. We always make an effort to weigh up cost and benefit. Also against the background of our key markets, USA and Japan, each with a volume share of approximately 30 % for the ActiveHybrid 5, it makes good sense to focus on spark-ignition engines.

The ActiveHybrid 5 can be driven for a maximum of four kilometres fully electrically. Does that mean that the concept is not designed for inner-city areas with an emission-based congestion charge, such as Central London.

No, that is currently not possible because the power characteristics of the electric motor mean that the internal combustion engine would start up too frequently. It would only be possible with a much more powerful electric motor, and that would have to be combined with a larger battery system.

You combine a very powerful internal combustion engine with a relatively weak electric motor. Is that a reflection of BMW's hybrid strategy?

Our hybrid strategy is, of course, also subject to evolutionary steps. The ActiveHybrid 5 is what we can produce in series according to the current state of development. We achieve impressive fuel consumption targets with it. What we can't do at the moment is drive long distances fully electrically.

Will that always be the case?

We see potential there for future vehicle generations.

Will that be a result of your cooperation with PSA?

Our cooperation with PSA is currently concentrating on fully electric powertrains. Whenever we have more far-reaching hybrid concepts in the future, the components will certainly also come from this cooperation.

"We don't see major simplification potential for the internal combustion engine."

What electric range should a full hybrid have in your opinion?

That depends on the concept. If it is not a plug-in hybrid with a charging possibility, large battery capacities do not make much sense, because the battery would never really be fully charged through recuperation alone, and recharging by the internal combustion engine would mean consuming fossil energy resources. That doesn't seem to be the solution. However, if electricity from regenerative sources is used to recharge the batteries, this would lead to

Langen expects only relatively small steps to be made in reducing CO_2 emissions in internal combustion engines in the future

According to Langen, it makes good sense to focus on the petrol hybrid also because of international marketing possibilities

a completely different assessment of the CO_2 emissions. For such concepts, I consider an electric driving range of between 35 and 50 km to be appropriate.

When can we expect to see a plug-in hybrid from BMW?
We showed the study of an extended-wheelbase BMW 5 Series as a plug-in hybrid at a car show in Shanghai in 2011. At the IAA 2011 in Frankfurt, we unveiled the BMW i8 Concept also as a plug-in study.

Can customers really achieve the lower fuel consumption claimed for a hybrid car or does it exist only on paper?
That depends to a great extent on how the customer drives. The key domain of the hybrid is city traffic, and this is where customers will notice the fuel consumption benefits most clearly. Hybrids offer fewer advantages over long distances. Our Driving Experience Control feature, which is already fitted as standard on all new 1 Series, 3 Series and 5 Series models, including of course the ActiveHybrid 5, enables drivers to select an Eco Pro mode for particularly fuel-efficient driving.

How can the internal combustion engine benefit from the electric motor in a hybrid system?
It is difficult to fully master the efficiency of internal combustion engines in very low load ranges due to their basic design. The operating strategy must therefore be implemented in such a way that the electric motor supports the internal combustion engine in these low load ranges and provides the main source of power.

Does this mean that the internal combustion engine can have a simpler design?
We don't see major simplification potential for the internal combustion engine. On the one hand, it must be also able to cover large distances efficiently in the low load range, in other words it must have a high efficiency. On the other hand, the internal combustion engine must have excellent transient control in order to compensate for the surge in torque that occurs when the electric motor is activated. Our six-cylinder engine in the ActiveHybrid 5, with its fully variable valve control, turbocharging and direct injection, is highly developed. This results in low CO_2 emissions in the ranges directly above those in which the electric motor provides support as well as in good load control performance. We cannot compensate for this by using other components.

Not even with strong hybridisation?
One might consider using a smaller internal combustion engine, but it would also have to fulfil all the technical requirements of a large engine. Furthermore, one would also have to take the overall system weight into account. Obviously, a larger electric motor and bigger batteries would also mean considerably higher weight. Our BMW i8 Concept study uses a small 1.5-litre three-cylinder inline engine. An engine concept for a lightweight sports car.

If you have strong hybridisation, couldn't you then eliminate components in the exhaust system, or make them cheaper?
I don't see any savings potential in the exhaust system, for example by reducing the amount of precious metal used in the catalytic converter, because the internal combustion engine must still comply with emissions standards when it is used on its own to power the vehicle, in other words when the battery is flat. In the same way, in our experience it is not worthwhile shifting emission-critical load ranges of the internal combustion engine to the electric motor because the amount of effort required is too great in relation to the benefit achieved.

How do you want to make the price of a hybrid attractive in the future?
The only possibility is to make the electric drive system itself cheaper. That applies

"I am assuming that economies of scale will also take effect."

in particular to the electric motor and the battery. I am assuming that economies of scale will also take effect here.

To what extent does the emissions behaviour of the engine have an influence on the hybrid operating strategy?
We have an overall operating strategy that considers the areas of emissions, fuel consumption and power requirements. We pay great attention to the catalytic converter temperature, because a hybrid vehicle must never have poorer emissions than a conventional vehicle, even outside the certification range. The catalytic converters are thermally insulated accordingly, but it may well occur that the system management starts up the internal combustion engine in order to supply energy into the catalytic converter.

What does the ideal operating strategy for a hybrid powertrain look like?
Put very simply, each drive unit must do what it does best: the electric motor must support the internal combustion engine at low speeds, while the internal combustion engine must provide the necessary driving power at high speeds. The hybrid system should operate without the driver noticing it, in other words drivers should not be aware of the distribution of power between the electric motor and the internal combustion engine. This is based on a hybrid driving strategy with environment recognition and navigation support functions.

That sounds like a considerable development challenge.
Yes, implementing that in an operating strategy requires much more application effort than for a conventional vehicle. That is the case both for simulation and for test stand and vehicle testing.

What effects do different international emissions regulations have on the design of hybrid concepts?
With regard to the components, we have a worldwide powertrain, although we do have some country-specific applications. For example, the application will take particular account of US American emissions legislation.

What do you think the future of the hybrid will be?
We have already presented the most sporty hybrid derivative that we can imagine in our BMW i8 Concept. This concept combines a powerful and efficient three-cylinder spark-ignition engine with an electric motor that supports the internal combustion engine particularly in the low speed range.

Peter Langen, thank you very much for this interview.

INTERVIEW: Richard Backhaus
PHOTOS: Matthias Haslauer

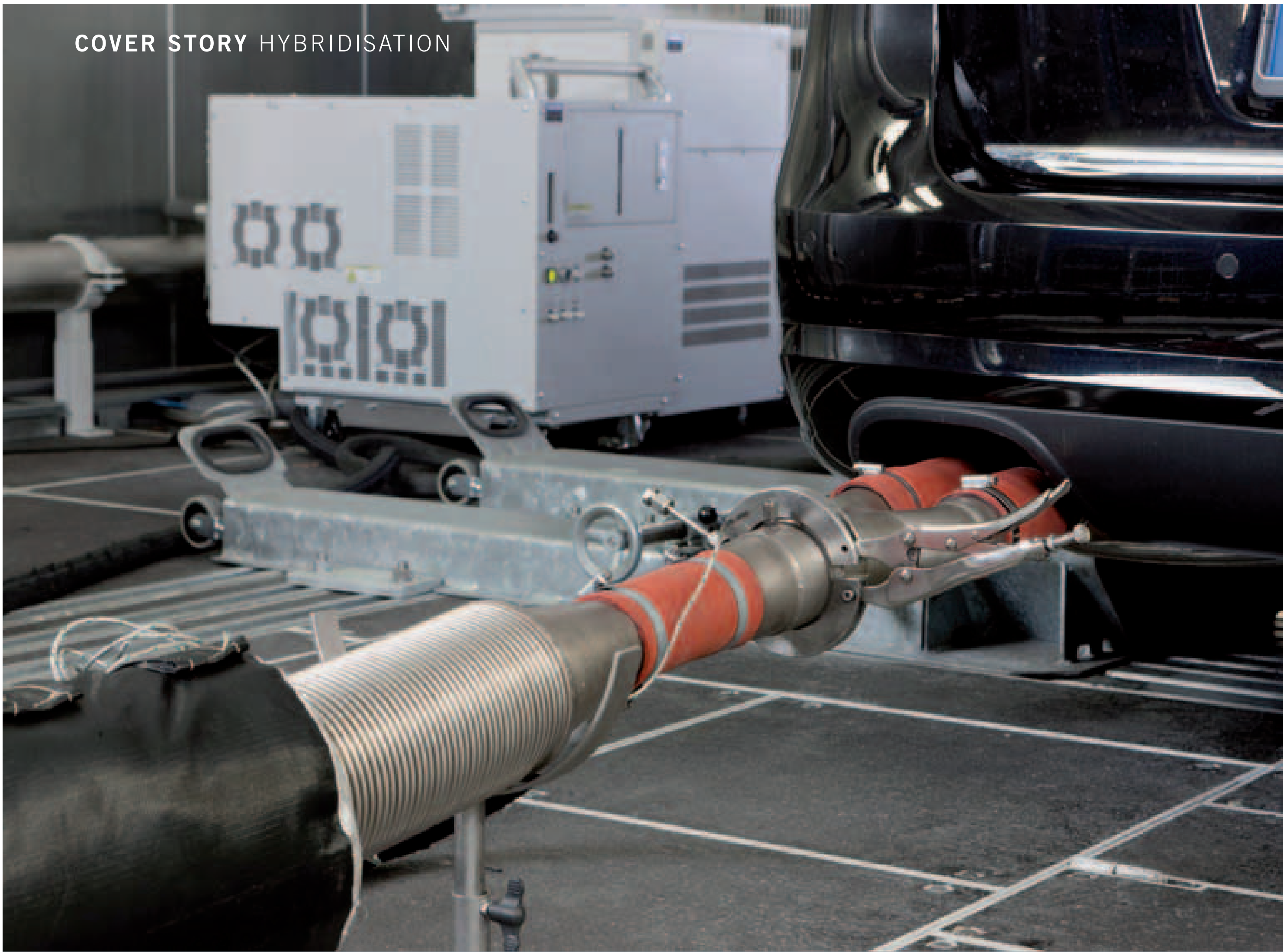

PARTICLE NUMBER EMISSIONS OF GASOLINE HYBRID ELECTRIC VEHICLES

Hybrid Electric Vehicles (HEV) are commonly reputed to be environmentally friendly. Different studies show that this assumption raises some questions in terms of particle number emissions. Against the background that upcoming emission standards will not only limit particle matter emissions but also particle number emissions for gasoline engines, the exhaust behaviour of downsized gasoline engines used in HEV should be investigated more extensively. A Horiba study compares the particle number emissions of a gasoline vehicle to those of a gasoline powered HEV.

AUTHOR

SCOTT PORTER
is Engineering Manager at Horiba Instruments Inc. in Ann Arbor, Michigan (USA).

BACKGROUND

Internal combustion engines emit soot mainly consisting of solid particles. These particles have negative effects not only on the environment – as soot is contributing to global warming – but also on human health [1, 2].

In the past, diesel engines were causing a large percentage of soot particle emissions. Thanks to stringent emission standards having come into effect in several countries within the last years – for example a standard affecting on-highway heavy-duty diesel engines in the USA since 2007 –, diesel particulate matter (PM) emissions have been cut by roughly 90 % compared to previous emission standards. Against this background, it has to be assumed that the fraction of PM emissions emitted by gasoline engines will increase significantly. As a countermeasure, the solid particle number emissions of gasoline engines have been limited starting with the Euro 5 standard. Since September 2011, Euro 5b already constrains the number of solid particles for diesel engines to 6 x 10^{11} particles per kilometre and regarding gasoline engines, a solid particle number (PN) restriction is planned with the introduction of the Euro 6 emission standard in 2014. Similarly, the California Air Resource Board (CARB) proposed a Low Emission Vehicle (LEV) III emission standard for light and medium-duty vehicles. For this standard which will be phased-in in 2014, particles will be measured either with a gravimetric mass or the solid particle number approach.

The standard approach for measuring PM involves weighing the overall mass of particles while the amount of particles is not counted. The number measurement principle counts the emitted particles in a specified size range (23 nm to 2.5 µm). Although a large number of solid particles smaller than 23 nm may be neglected [6-9], the PN approach has advantages such as good sensitivity, real-time measuring and a wide dynamic range.

OBJECTIVES

Evaluating solid particle emissions from a conventional gasoline vehicle and a gasoline powered HEV on a two-wheel chassis dynamometer; the study aims at investigating the feasibility of the Solid Particle Counting System (SPCS) compliant to the European Particle Measurement Programme (PMP) with regard to solid particle number measurement from gasoline engines. At the same time, the study has the objective to understand characteristics of solid particle emissions from gasoline engines in general.

TEST VEHICLES AND SETUP

The study analyses the emission behaviour of a 2009 model year HEV with a downsized 1.5-l engine compared to a vehicle with a 3.8-l gasoline engine in terms of solid particle number emission. Vehicle A, the conventional gasoline vehicle, is a minivan model year 1999 with a curb weight of approximately 900 kg more than Vehicle B, the HEV. The downsized 1.5-l gasoline engine of Vehicle B is oper-

	VEHICLE A	VEHICLE B
VEHICLE TYPE	Conventional gasoline minivan, auto transmission	Gasoline hybrid electrical passenger car, auto transmission
FUEL	California phase II reformulated	California phase II reformulated
MODEL YEAR	1999	2009
CURB WEIGHT [KG]	≈ 2700	≈ 1800
ENGINE CYCLE	Conventional Otto cycle	Atkinson cycle
ENGINE	6 cylinders, 3.8 l, SFI	4 cylinders, 1.5 l, SFI
AFTERTREATMENT	Three-way catalyst	Three-way catalyst
EMISSION CERTIFICATION	California ULEV	California ULEV II

❶ Technical data of the test vehicles

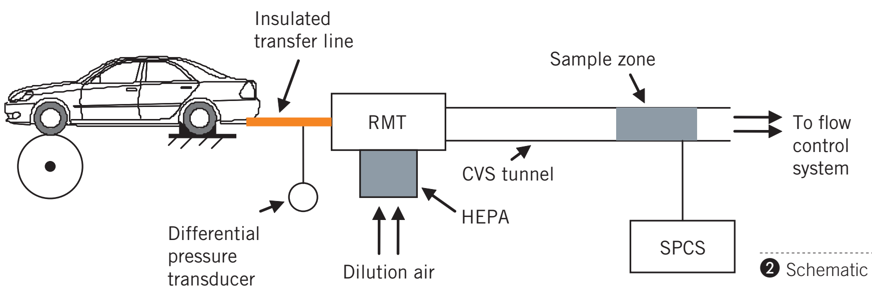

❷ Schematic for the experimental setup

CONFORMED STANDARD	UN/ECE regulation No. 83 CE, FCC
PND1 DILUTION RATIO	10 – 200
PND2 DILUTION RATIO	15
EVAPORATION TUBE TEMPERATURE (°C)	300 – 400
REMOVAL EFFICIENCY FOR 30 NM C40	> 99 %
ACCURACY OF TOTAL DILUTION RATIOS	Better than 10 %, and checked with gas analysers
PCRF CALIBRATION	Calibrated with NaCl particles
SIZE	434 (W) × 731 (B) × 600 (H) mm
WEIGHT (KG)	~ 115 kg (without transfer line, control unit and optional units)

❸ Specifications of the solid particle counting system

ated with the Atkinson cycle and uses a variable valve control. All technical details of the tested vehicles are depicted in ❶. During the test cycles the same fuel had been used for both vehicles.

For repeatable conditions the investigation is based on two standard drive cycles for dynamometer tests. The Federal Test Procedure (FTP) 72 is designed to simulate urban drive conditions at lower speeds, slower acceleration rates and with frequent stops. To simulate highway driving at high speeds with less acceleration and deceleration events, the Highway Fuel Economy Transient Cycle (HWFET) had been operated on the vehicles. As already mentioned above, the tests were conducted on a two-wheel chassis dynamometer. While the front wheels of the vehicles were placed on the dynamometer, the rear wheels were fixed during the test.

Via an insulated transfer line and a Remote Mix Tee (RMT), the vehicles exhaust tailpipes were connected to a Constant Volume Sampler (CVS) tunnel where the exhausts were diluted. Due to the emission level being different, Vehicle A

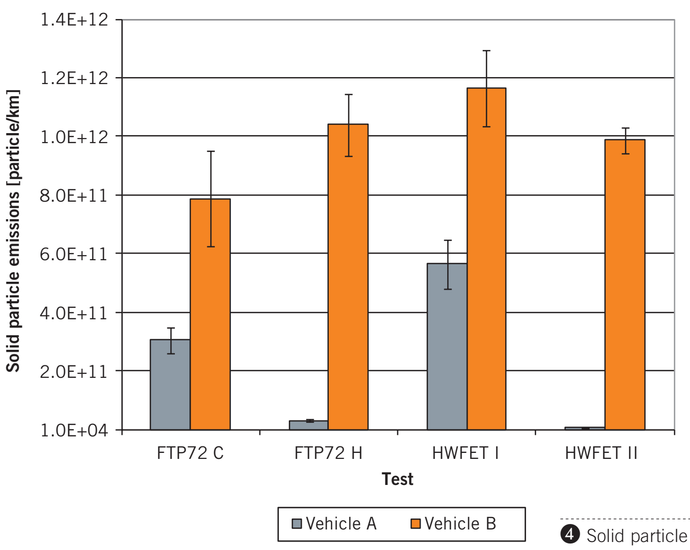

❹ Solid particle emissions from Vehicles A and B in comparison

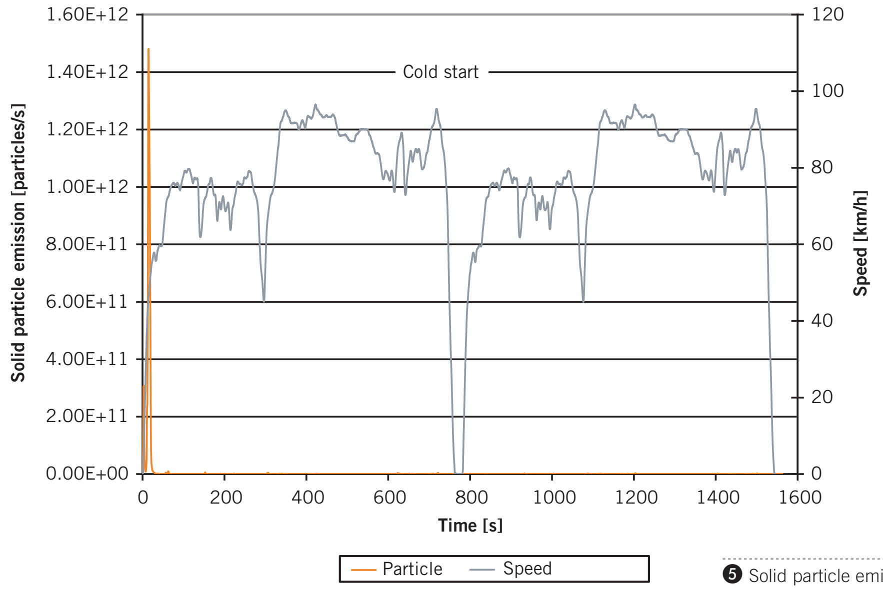

❺ Solid particle emissions from Vehicle A

was tested with a total dilution ratio of 150 while Vehicle B was tested with a dilution ratio of 300. The test configuration is shown in ❷.

For measuring solid particle number emissions in real-time, the engineers used the Horiba Mexa-2000SPCS, ❸. The system with a wide range continuous diluter takes sample from the sample zone on the CVS tunnel and measures the number of solid particles in engine exhaust gas using the Condensation Particle Counting (CPC) method. The analytical system of Horiba conforms to all requirements recommended by the European PMP. It covers all the applications from certification testing, meeting the Euro 5 and Euro 6 requirements, to engine research and development and exhaust particulate filter performance testing.

DISTINCTIONS IN HEV TESTING

In the case of Vehicle B, the HEV, some aspects have to be considered leading to distinctions in testing. Firstly, the vehicle has a traction control function which had to be disabled prior to the tests on a two-wheel chassis dynamometer. Therefore, Vehicle B was set into service mode to switch off traction control. According to engineers of the vehicle manufacturer, emissions under service mode should be identical compared to regular driving mode. Switching to service mode takes 30 to 90 seconds before standard drive cycles could begin and caused the combustion engine to start several times. Thus, there were some cold starts emissions uncollected for the tests of the HEV.

It is necessary to monitor the engine status of the HEV to understand the test results regarding particle emissions. Either driven electric motors or by the gasoline engine or both simultaneously, dependencies like driving speeds and battery status determine the operation mode of Vehicle B. As it was not possible to access the on board diagnose (OBD) system or the engine control unit (ECU) to monitor of the engine during all the tests, other approaches had to be found to identify whether the combustion engine is running or not. The engineers discovered that the analysed pressure differences between tailpipe and ambient air give information about the engine status. By means of a differential pressure transducer, also shown in ②, it is possible to detect engine starts and stops. Thus, the engine status may be obtained by monitoring the exhaust tailpipe pressures and without modifying the CVS tunnel or other testing equipments.

TEST RESULTS

The overall results regarding solid particle emissions per kilometre during the FTP 72 and HWFEET cycles are shown in ❹. The figure indicates significant differences between the two vehicles tested. While the conventional gasoline powered minivan (Vehicle A) in fact only emits a significant amount of particles while the engine is cold, Vehicle B, the HEV, emits a constantly high amount of solid particles independent from the engine temperature.

DETAILED RESULTS FOR URBAN TESTING

Regarding the conventional gasoline vehicle, a reason for high particle numbers at cold starts is the gasoline engine running rich when started. Combustion air may not be sufficiently supplied so the temperature in the combustion chamber is still low. As a result the air-fuel-mixing is not adequate and thus causes more solid particles. As long as the engine is cold (approximately 250 s), solid particle emissions are much higher in acceleration than deceleration phases. In total, Vehicle A emits over 90 % of its solid particles during the warm-up phase, ❺.

In urban driving conditions at low speeds, the HEV is driven by electric motors during most of the test cycle. Some measured spikes for solid particle emissions match well with peaks for tailpipe pressure, indicating that the combustion engine starts. Compared to Vehicle A,

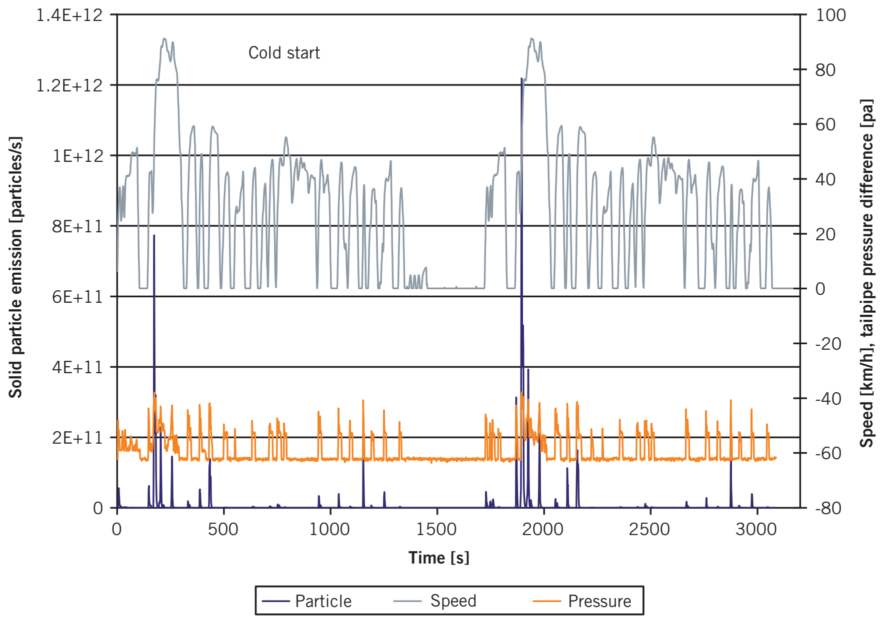

❻ Solid particle emissions from Vehicle B

the HEV emits two times more particle number emissions under cold starts. When fully warmed up it produces 30 times more particles than the conventional gasoline vehicle and emits 65 % more particles than in the first FTP 72 cycle. As it is possible that the state of charge (SOC) of the HEV battery has an influence on particle emissions Horiba tried to minimise this effect by running four FTP 72 cycles in series during a single test. The data collected show that only the first cycle differs largely while the last three test cycles produce similar results with higher solid particle emissions, ❻. To explain the lower solid particle emission from the first cycle, more studies need to be carried out in the future.

DETAILED RESULTS FOR HIGHWAY TESTING

As the vehicles are operated at high speeds during the HWFET cycles, the HEV is driven by the gasoline engine or the gasoline engine in combination with the electric motors for almost the whole duration of the cycle. Thus, the HEV operates very similar to the conventional gasoline powered car. Commonly, soot or solid particle emissions caused by gasoline engines are mainly detected at high engine loads and high engine speeds which may be found on highway driving conditions.

Compared to the conventional vehicle with an engine displacement of 3.8-litres, the HEV has a downsized 1.5-l engine. Downsizing usually offers several advantages such as better fuel efficiency, lower CO_2 emission, and lighter weight. However, by comparing the test results of both vehicles under highway conditions, it becomes obvious that the particle emissions of the two test vehicles differ even more significantly than under urban driving mode. On a fully warmed up HWFET cycle, Vehicle B emits approximately 200 times more solid particle emissions than Vehicle A, the conventional gasoline vehicle.

SUMMARY

The above described study shows that the gasoline vehicle causes solid particle emissions mostly at engine start and accelerations before the engine is warmed up. After the vehicle is fully warmed up, solid particle emissions are reduced significantly. The considerably higher amount of solid particle emissions produced by the HEV correlates with frequent combustion engine starts and accelerations under urban driving conditions and is influenced by the battery status as well.

Those test results support other studies indicating that new engine technologies reduce CO_2 emissions but may increase particle emissions simultaneously as a counter effect [3, 4, 5]. To reduce solid particle emissions from HEV and to fulfil upcoming emission standards limiting solid particle emissions of gasoline engines, the engine operation may need to be optimised.

REFERENCES

[1] Public workshop on proposed revisions to the low-emission vehicle program: emission limits for particle mass, solid particle number, and black carbon, California air resources board, El Monte, Californien, 18. Mai 2012
[2] Health assessment document for diesel exhaust, EPS/600/8-90/057E, Juli 2000, SAB review
[3] Andersson, J. et al.: Particle measurement programme (PMP) light-duty inter-laboratory correlation exercise (ILCE_LD) final report, Joint Research Centre, GRPE-54-08-Rev. 1, 2007
[4] Montajir, R. M.; Kusaka, T.; Kaori, I.; Kihara, N. et al.: Soot Emission Behavior from Diverse Vehicles and Catalytic Technologies Measured by a Solid Particle Counting System. SAE Technical Paper 2007-01-0317, 2007
[5] Zhang, S.; McMahon, W.; Toutoundijan, H.; Cruz, M. et al.: Particulate Mass and Number Emissions from Light-duty Low Emission Gasoline Vehicles. SAE Technical Paper 2010-01-0795, 2010
[6] Wei, Q.; Oestergaard, K.; Porter, S.; Ichiro, A. et al.: Real-Time Measuring System for Engine Exhaust Solid Particle Number Emission – Design and Performance. SAE Technical Paper 2006-01-0864, 2006
[7] Conclusions on improving particulate mass measurement procedures and new particle number measurement procedures relative to the requirements of the 05 series of amendments to regulation Nr. 83, GRPE-48-11-Rev. 1, 2004
[8] Amendments to UNECE regulations, Regulation No. 83, submitted by the expert from the United Kingdom, ECE/TRANS/WP.29/GRPE/2008/, 2008
[9] Herner, J. D.; Robertson, W. H.; Ayala, A.: Investigation of Ultrafine Particle Number Measurements from a Clean Diesel Truck Using the European PMP Protocol, SAE Technical Paper 2007-01-1114, 2007

DRIVELINE ELECTRIFICATION

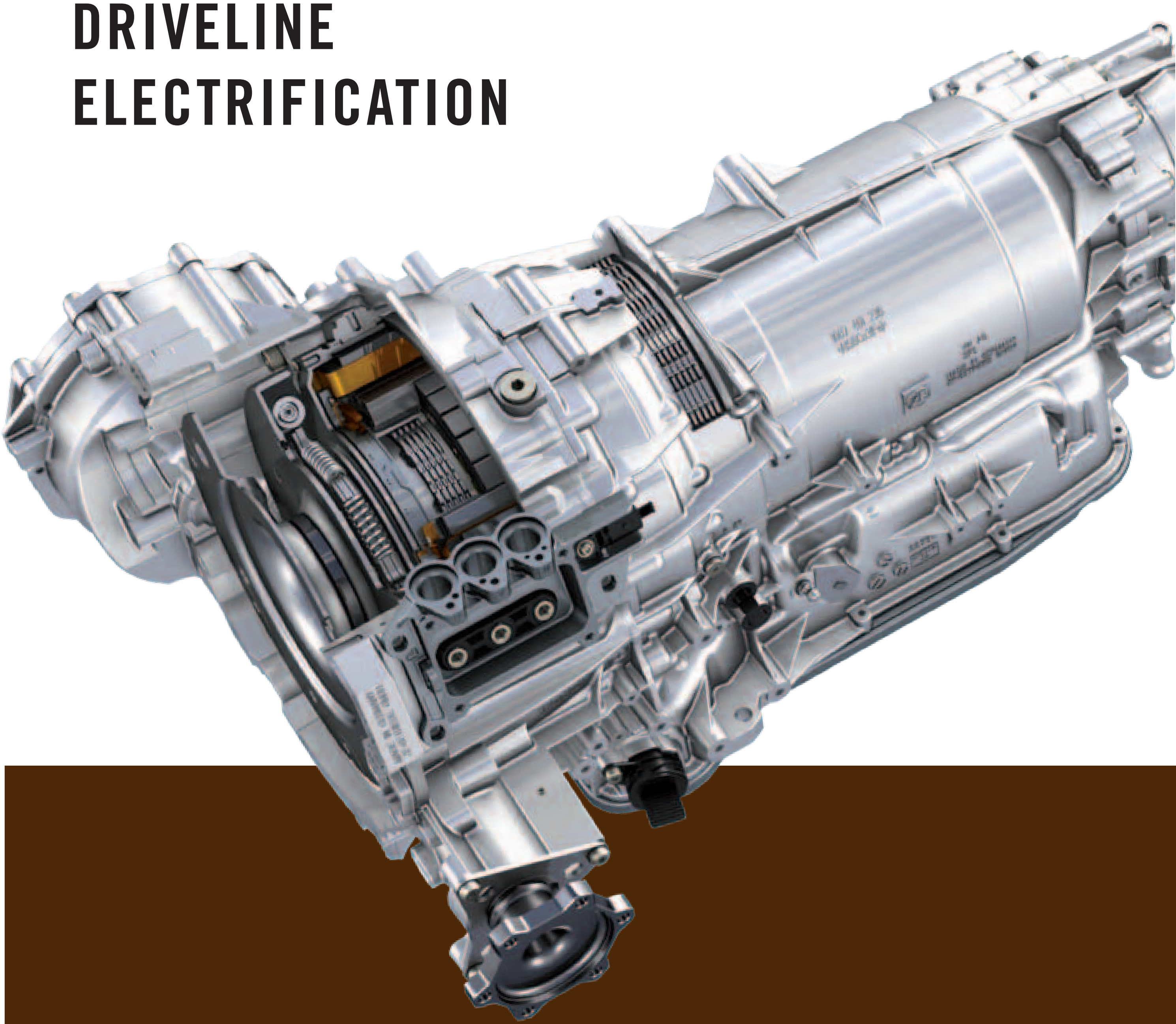

The hybrid powertrain is a technology that enables high energy-saving potentials to be achieved with relatively low costs. As ZF Friedrichshafen AG shows with its hybrid solutions, the concrete application determines which transmission configuration is the most promising in terms of efficiency.

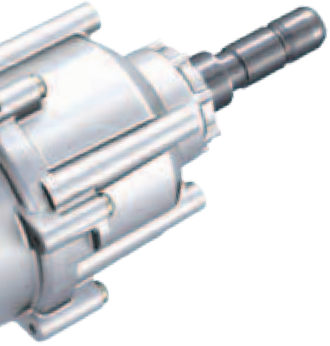

AUTHORS

DR. BERND VAHLENSIECK
is Manager Advanced Engineering Driveline at ZF Friedrichshafen AG in Friedrichshafen (Germany).

DR. RALF KUBALCZYK
is Director Development Hybrid Transmissions at ZF Friedrichshafen AG in Friedrichshafen (Germany).

HANS-JÜRGEN SCHNEIDER
is Director Electric Drives at ZF Friedrichshafen AG in Schweinfurt (Germany).

BERT HELLWIG
is Director Development Bus Driveline Technology at ZF Friedrichshafen AG in Friedrichshafen (Germany).

MOTIVATION

The trend towards more efficient vehicles – be it passenger cars or commercial vehicles – is omnipresent. There is not a single manufacturer who does not deal intensively with opportunities to obtain better energy efficiency. For suppliers like ZF Friedrichshafen AG this also means that, if they want to stay fit for the future, they have to supply new approaches for the mobility of tomorrow. Driveline electrification is a central starting point towards more economy: It reduces CO_2 emissions and gives manufacturers the technology required to meet the legal requirements of climate protection. Low CO_2 emission values are not only interesting from the aspect of climate change and saving resources – for the motorist, transport authority, or fleet operator they mean cash in the form of fuel savings. Life cycle costs are also the main area of conflict for automotive manufacturers and suppliers: An environmentally friendly that means economical drive must also pay off financially to be able to prevail. So we are not only talking about what is technically feasible but also what is sensible in terms of economy: The extra costs of the efficiency increase must not absorb the savings in operating costs, ❶.

Therefore the term temporary/bridge technology is problematic when talking about hybrid drives. It is often used when talking about electromobility as a major target of the automotive industry. These terms rule out per se that hybrid drives have a longer service life – before they are even used in a large scale. Here, the imagination of pure e-mobility goes at least one step too far. It is not only about getting away from fossil fuels. Doing without a combustion engine first of all only reduces local emissions. The question of how the batteries in the vehicle are charged, that means where the charging power comes from, is another story. In the foreseeable future it will not be possible to generate our power entirely without CO_2 emissions; not to mention the basically non-existent infrastructure for electric vehicles and the unsolved problem of energy density and, consequently, the limited range of conventional batteries.

In this regard, there is quite a large amount of development work to be done – also at ZF – in terms of energy management which means a long time until purely electric drivelines will have found extensive coverage. Driveline electrification, however, starts earlier. The electrification of the conventional driveline is part of practical reality already today. It allows for great fuel savings at economic cost. Apart from that, hybrid technology has

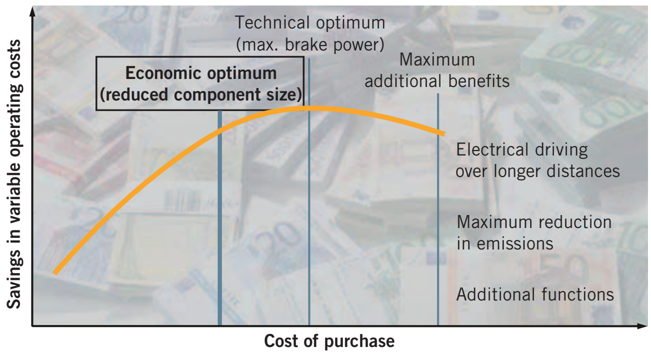

❶ Economic benefit over extra cost of hybrid drives not yet reached the end of its development scope; there are many unanswered questions and there is still room for improvement. Compared with the development history of the combustion engine which has its roots in the century before last, we have a relatively short learning process to look back on despite all the success we have had.

CLEAR STRATEGY BUNDLES COMPETENCE

Assuming that the combustion engine will remain the key component in the driveline for some time, the question arises of how consumption can be reduced efficiently via electrification and without causing considerable extra cost. This already starts when selecting the hybrid architecture. ZF is concentrating on the parallel hybrid, where the combustion engine and the electric motor are connected in parallel. The multi-ratio transmission used in this architecture takes over new functions when changing between operating modes. The advantage of the continuously variable approach which is typical for power-split hybrids is not as significant on the European market as it is in Asia. Also in terms of fuel savings and performance it does not lead to additional advantages compared to the hybridised stepped transmission. With full functionality, the parallel hybrid version has the advantage of being able to be used with planetary automatic transmissions in a modular design without requiring additional installation space. On the one hand, this plays a role for the platform strategies of the manufacturers in terms of construction – on the other hand, the hybrid transmission can be built with very many parts identical to the conventional transmission; this reduces the costs particularly with the currently still small quantities. One advantage in this regard is that, right from development start, ZF has been using flexible modular solutions that can be adapted to the most different vehicle designs. Additional applications that are developed around a specific basic transmission can be tested and adapted with reduced additional effort. Starting with all-wheel-drive applications, different starting elements, and an open software and interface structure, this also applies to hybrid versions: Based on the parallel hybrid architecture, for example, all hybrid power classes can be combined with the current eight-speed automatic transmission (8HP) from ZF – because it was developed right from the start with a modular hybrid design. Taking the kit as a basis, it is possible to provide innovative conventional basic transmissions which are then electrified according to the customers' requests via an add-on solution.

DIFFERENT HYBRID POWER CLASSES

In micro hybrids with automatic start-stop systems, the battery is charged in overrun mode to generate the energy required for frequent engine restarts. They are technically easy to implement with manual transmissions. This kind of electrification is not so easy to use with automatic transmissions because there is no hydraulic pressure for the shift elements when the engine is switched off and this considerably limits the quick-starting capability of the transmission. To solve this problem, ZF has developed the so-called Hydraulic Impulse Oil Storage (HIS) for the 8HP and at the same time introduced the first multi-ratio transmission with a start-stop function in the market. The integrated HIS works with the spring piston accumulator principle and swiftly presses the hydraulic oil required for starting into the shift elements of the transmission. This means that after engine shutdown, the vehicle is ready to set off again in just 350 ms. With the start-stop function, HIS, and further optimisations such as the increased spread, the eight-speed automatic transmission can achieve 11 % fuel savings compared to the second-generation six-speed auto-

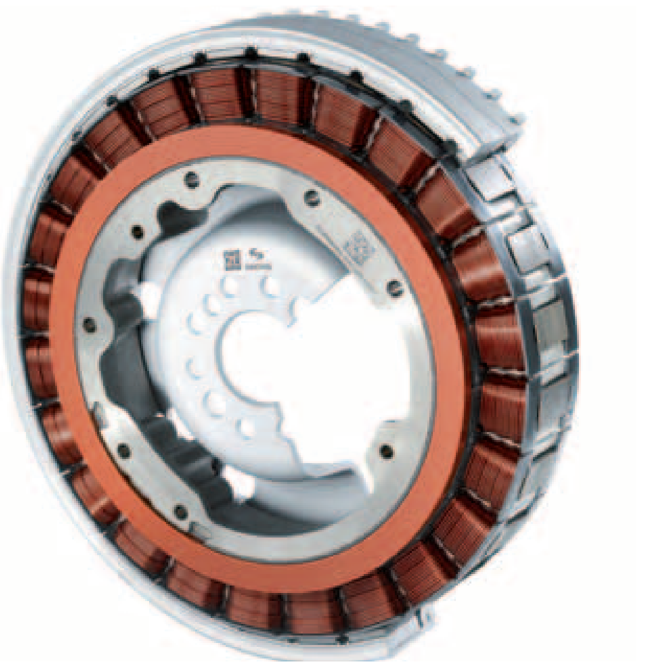

❷ Electric motor Dynastart

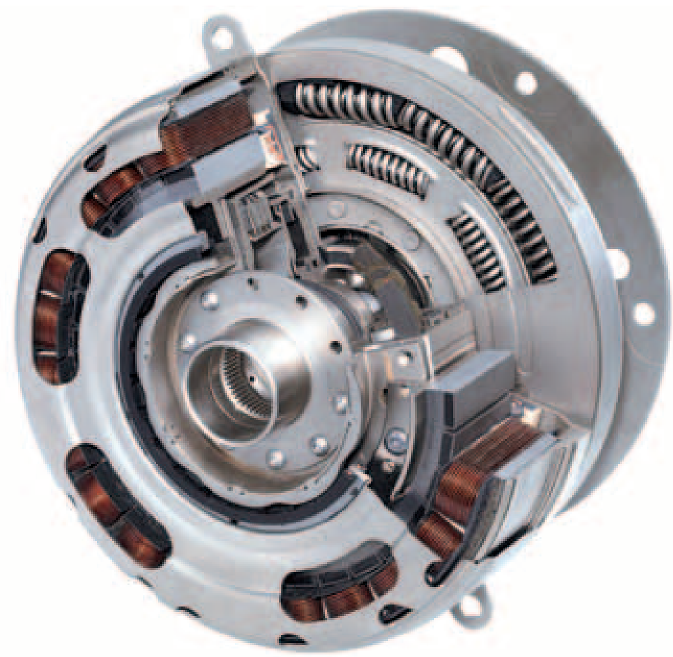

❸ Hybrid modul for passenger cars

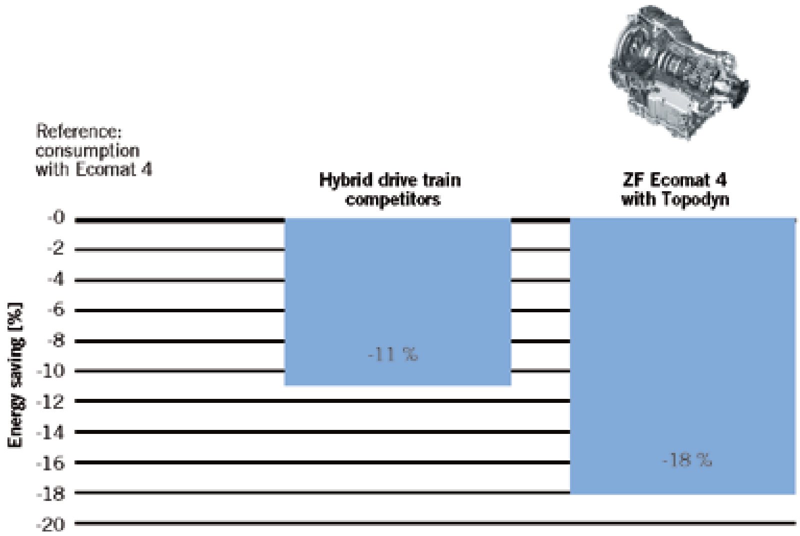

❹ Consumption with different driveline configurations in a US city cycle

matic transmission which has already been optimised in terms of fuel consumption.

ZF has the electric motor Dynastart in its modular kit as a core component for further hybrid configuration stages, ❷. It is integrated into the transmission and replaces the alternator and starter. Depending on the application, Dynastart can be obtained with different capacities: With the mild hybrid, the Dynastart in external rotor design supplements the 8HP torque converter and thus allows recuperation as well as torque support for the combustion engine. For full hybrid applications, Dynastart is available as a hybrid module with a powerful, inner-rotor electric motor and integrated separating clutch, ❸. Then it entirely replaces the torque converter and covers all hybrid functions right up to stealth mode. In this design, the hybrid driveline offers the best savings potential of up to 25 % compared to the 8HP basic transmission.

VARIOUS APPLICATION POSSIBILITIES

In general it is argued that hybrid drives only have a chance in vehicles that are moved in – what is generally referred to as – city cycles, which are characterised by frequent starting and stopping and thus have correspondingly many deceleration and acceleration procedures. Apart from passenger cars that were described before, this applies above all to delivery trucks and city buses. Also for such commercial vehicles, the portfolio from ZF already includes hybrid applications that consist of electrified basic transmissions (Hytronic-Lite and Ecolife-Hybrid). And this also applies as well as for passenger car transmissions – the more efficient the starting basis, the better: Practice has shown that an optimised conventional driveline can save more fuel than an inefficient hybrid driveline with an outdated transmission, ❹.

But hybridisation also makes sense for long-distance traffic: A relative savings potential of only around 5 % is possible but the high mileage and power of long-distance trucks mean major absolute savings. And there is also great potential in the field of commercial vehicles: Just think of the many electro(hydraulically) operated auxiliaries and the constant reversing of construction or agricultural machinery or cooling units of refrigerated trucks. A power outlet for the off-road machinery of industrial and handicraft businesses is also imaginable. To electrify all the different applications in the commercial vehicle sector at reasonable costs, ZF also relies on a modular kit system in the parallel hybrid architecture.

INTELLIGENT NETWORKING

In addition to the selection and targeted design of all components, efficient hybrid management is required for the hybrid drive to function smoothly. It enables the transmission hardware, the control software, and the power electronics to harmonise perfectly. The scalability of the power electronics must be just as versatile as the power classes. Therefore, it only makes little sense to focus on individual components when electrifying the driveline, the overall package must be right. An example from the area of passenger cars: Until now, the power electronics as the central connection between the electric motor and the battery is mounted at different places in the vehicle depending on the manufacturer. Based on the eight-speed full hybrid transmission, ZF has therefore developed an exemplary, scaled-down power electronics unit for passenger cars which can be integrated into the transmission irrespective of the installation space available, ❺. The direct installation of power electronics on the transmission holds many advantages: First of all, it is

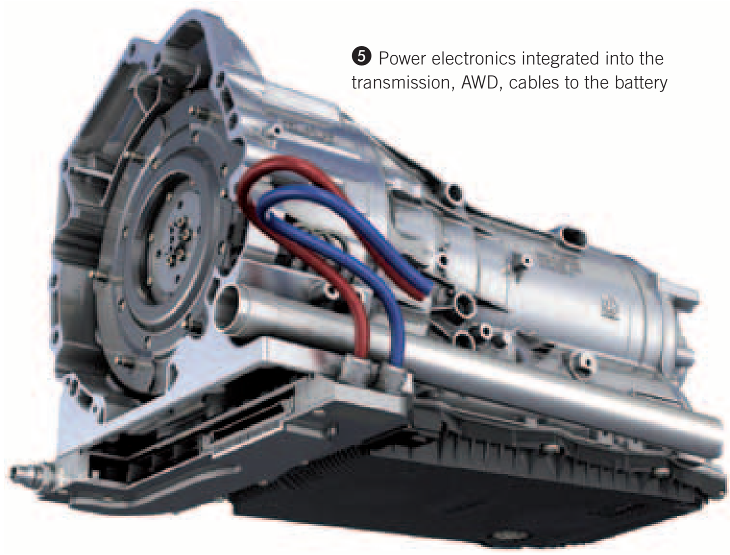

❺ Power electronics integrated into the transmission, AWD, cables to the battery closer to the electric motor which means fewer system interfaces and less wiring effort. In addition, it is possible to preassemble power electronics independently of manufacturer and platform. The vehicle manufacturers can install the hybrid transmission independently of the model – the power electronics is always already on board. At the same time, it is easier to service because the newly developed power electronics unit can be plugged into the transmission from below.

ADAPTIVE DRIVING STRATEGY

Apart from the design of the individual hybrid components and smartly integrated power electronics, the driving strategy has central importance: It not only determines how much fuel is saved but also the performance, driving comfort and, last but not least, the service life of the battery. The load-bearing capacity of all individual components must be adapted to the driving strategy. Of course, the main target is to select the driving strategy so that the respective hybrid modes (electric driving, boosting, recuperating) are perfectly fine-tuned, leading to the lowest possible fuel consumption. In doing so, the driving strategy does not follow a rigidly preassigned pattern that is called up on request. Instead, it must interpret the request from the driver and select the suitable action. Depending on the performance requirements – set via the accelerator and brake pedal – and depending on the charge status of the battery, the driving strategy decides on how to distribute the load between the combustion engine and the electric motor. This also means that the combustion engine has to be shut down at the right point in time and decoupled via a separating clutch; this means that the vehicle is operated without the high drag torque of the combustion engine both when driving electrically and during recuperation. At the same time, hybrid management decides whether the prerequisites are met for an efficiency-boosting load-point increase. Here, when the workload for the combustion engine is low, part of the torque is used for operating the electric motor as a generator to charge the battery. This means that the combustion engine always works with the best engine characteristics to save fuel. Apart from improving the hardware components, the complex driving strategy includes additional potential for optimising the efficiency of electrified drivelines. For both tasks, the component, interface, and systems expertise of a versatile supplier company like ZF is called for.

IMPRINT

MTZ

WORLDWIDE

www.MTZonline.com

Founded 1939 by Prof. Dr.-Ing. E. h. Heinrich Buschmann and Dr.-Ing. E. h. Prosper L'Orange

Organ of the Fachverband Motoren und Systeme im VDMA, Verband Deutscher Maschinen- und Anlagenbau e.V., Frankfurt/Main, for the areas combustion engines and gas turbines
Organ of the Forschungsvereinigung Verbrennungskraftmaschinen e.V. (FVV)
Organ of the Wissenschaftliche Gesellschaft für Kraftfahrzeug- und Motorentechnik e.V. (WKM)
Organ of the Österreichischer Verein für Kraftfahrzeugtechnik (ÖVK)
Cooperation with the STG, Schiffbautechnische Gesellschaft e.V., Hamburg, in the area of ship drives by combustion engine

04 I 2012 _ April 2012 _ Volume 73
Springer Vieweg I Springer Fachmedien Wiesbaden GmbH
P. O. Box 15 46 · 65173 Wiesbaden · Germany I Abraham-Lincoln-Straße 46 · 65189 Wiesbaden · Germany
Amtsgericht Wiesbaden, HRB 9754, USt-IdNr. DE811148419

Managing Directors Dr. Ralf Birkelbach (Chairman), Armin Gross, Albrecht Schirmacher I **Director Corporate Publishing, Corporate Content & Ad Sales** Armin Gross
Director Marketing & Direct Sales Rolf-Günther Hobbeling I **Director Production** Christian Staral

EDITORS IN CHARGE
Dr. Johannes Liebl, Wolfgang Siebenpfeiffer

EDITORIAL STAFF

EDITOR IN CHIEF
Wolfgang Siebenpfeiffer (*temporary*)
phone +49 611 7878-349 · fax +49 611 7878-462
wolfgang.siebenpfeiffer@springer.com

VICE-EDITOR IN CHIEF
Dipl.-Ing. (FH) Richard Backhaus (rb)
phone +49 611 5045-982 · fax +49 611 5045-983
richard.backhaus@rb-communications.de

MANAGING EDITOR
Kirsten Beckmann M. A. (kb)
phone +49 611 7878-343 · fax +49 611 7878-462
kirsten.beckmann@springer.com

SECTIONS
Electrics, Electronics
Markus Schötttle (scho)
phone +49 611 7878-257 · fax +49 611 7878-462
markus.schoettle@springer.com
Production, Materials
Stefan Schlott (hlo)
phone +49 8726 9675-972
redaktion_schlott@gmx.net
Research
Dipl.-Ing. (FH) Andreas Fuchs (fu)
phone +49 6146 837-056 · fax +49 6146 837-058
fuchs@fachjournalist-fuchs.de
Martina Schraad (mas)
phone +49 611 7878-276 · fax +49 611 7878-462
martina.schraad@springer.com
Transmission
Dipl.-Ing. Michael Reichenbach (rei)
phone +49 611 7878-341 · fax +49 611 7878-462
michael.reichenbach@springer.com

PERMANENT CONTRIBUTORS
Andreas Burkert (ab), Prof. Dr.-Ing. Stefan Breuer (sb), Dipl.-Ing. Jürgen Grandel (gl), Dipl.-Ing. Ulrich Knorra (kno), Prof. Dr.-Ing. Fred Schäfer (fs), Roland Schedel (rs)

ENGLISH LANGUAGE CONSULTANT
Paul Willin (pw)

ONLINE I ELECTRONIC MEDIA
Dipl.-Ing. (FH) Caterina Schröder (cs)
phone +49 611 7878-190 · fax +49 611 7878-462
caterina.schroeder@springer.com

Katrin Pudenz M. A. (pu)
phone +49 6172 301-288 · fax +49 6172 301-299
redaktion@kpz-publishing.com

SPECIAL PROJECTS
Managing Editorial Journalist
Markus Bereszewski (mb)
phone +49 611 7878-122 · fax +49 611 7878-462
markus.bereszewski@springer.com

Editorial Staff
Christiane Brünglinghaus (chb)
phone +49 611 7878-136 · fax +49 611 7878-462
christiane.bruenglinghaus@springer.com

ASSISTANCE
Christiane Imhof
phone +49 611 7878-154 · fax +49 611 7878-462
christiane.imhof@springer.com
Marlena Strugala
phone +49 611 7878-180 · fax +49 611 7878-462
marlena.strugala@springer.com

ADDRESS
Abraham-Lincoln-Straße 46 · 65189 Wiesbaden
P. O. Box 1546 · 65173 Wiesbaden, Germany
redaktion@ATZonline.de

MARKETING I OFFPRINTS

PRODUCT MANAGEMENT AUTOMOTIVE MEDIA
Sabrina Brokopp
phone +49 611 7878-192 · fax +49 611 7878-407
sabrina.brokopp@springer.com

OFFPRINTS
Martin Leopold
phone +49 2642 907-596 · fax +49 2642 907-597
leopold@medien-kontor.de

ADVERTISING

HEAD OF SALES MANAGEMENT
Britta Dolch
phone +49 611 7878-323 · fax +49 611 7878-140
britta.dolch@best-ad-media.de

KEY ACCOUNT MANAGEMENT
Rouwen Bastian
phone +49 611 7878-399 · fax +49 611 7878-140
rouwen.bastian@best-ad-media.de

SALES MANAGEMENT
Volker Hesedenz
phone +49 611 7878-269 · fax +49 611 7878-140
volker.hesedenz@best-ad-media.de

MEDIA SALES
Frank Nagel
phone +49 611 7878-395 · fax +49 611 7878-140
frank.nagel@best-ad-media.de

DISPLAY AD MANAGER
Petra Steffen-Munsberg
phone +49 611 7878-164 · fax +49 611 7878-443
petra.steffen-munsberg@best-ad-media.de

AD PRICES
Advertising ratecard from October 2011

PRODUCTION I LAYOUT
Heiko Köllner
phone +49 611 7878-177 · fax +49 611 7878-78177
heiko.koellner@springer.com

SUBSCRIPTIONS
Springer Customer Service Center GmbH
Haberstraße 7 · 69126 Heidelberg · Germany
phone +49 6221 3454-303 · fax +49 6221 3454-229
Monday to Friday, 8 a.m. to 6 p.m.
springervieweg-service@springer.com

YOUR HOTLINE TO MTZ

Editorial Staff
☎ +49 611 5045982
Customer Service
☎ +49 6221 3454-303
Advertising
☎ +49 611 7878-395

SUBSCRIPTION CONDITIONS
The eMagazine appears 11 times a year at an annual subscription rate 199 € for private persons and 299 € for companies. Special rate for students on proof of status in the form of current registration certificate 98 €. Special rate for VDI/ÖVK members on proof of status in the form of current member certificate 172 €. Special rate for studying VDI members on proof of status in the form of current registration and member certificate 71 €. Annual subscription rate for combination MTZworldwide (eMagazine) and MTZ (print) 398 €. All prices include VAT at 7 %. Every subscription comes with access to the ATZonline archive. However, access is only available for the individual subscription holder. To obtain access for your entire company/library/organisation, please contact Rüdiger Schwenk (ruediger.schwenk@springer.com or phone +49 611 7878-357). The subscription can be cancelled in written form at any time with effect from the next available issue.

HINTS FOR AUTHORS
All manuscripts should be sent directly to the editorial journalists. By submitting photographs and drawings the sender releases the publishers from claims by third parties. Only works not yet published in Germany or abroad can generally be accepted for publication. The manuscripts must not be offered for publication to other journals simultaneously. In accepting the manuscript the publisher acquires the right to produce royalty-free offprints. The journal and all articles and figures are protected by copyright. Any utilisation beyond the strict limits of the copyright law without permission of the publisher is illegal. This applies particularly to duplications, translations, microfilming and storage and processing in electronic systems.

Springer Vieweg is a brand of Springer DE. Springer DE is part of Springer Science+Business Media.

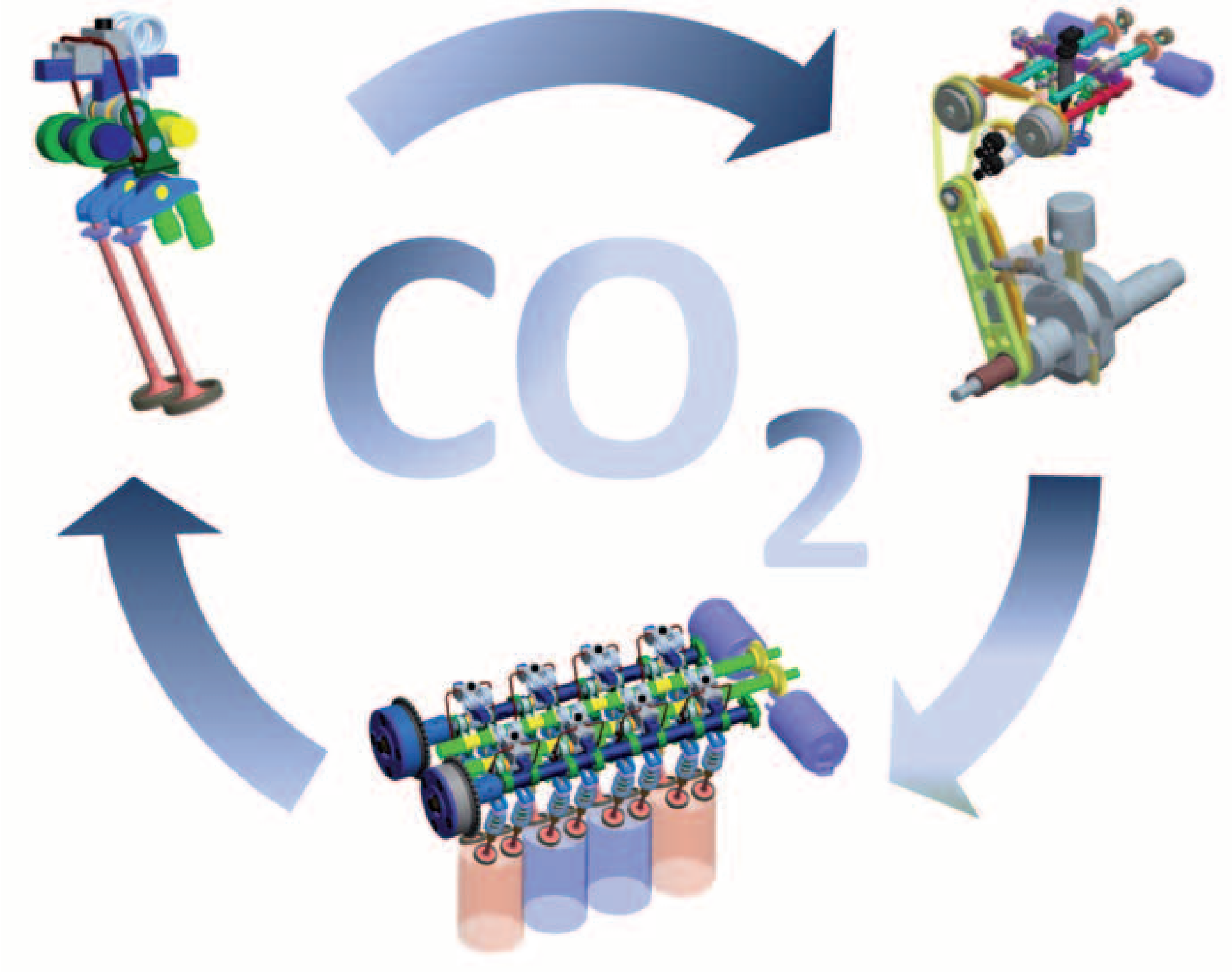

POTENTIALS AND LIMITS OF CO_2 EMISSIONS OF GASOLINE ENGINES
PART I: MECHANIC TECHNIQUES

In the following, Technical University of Kaiserslautern and Karlsruhe Institute of Technology (KIT) present and discuss the potentials and limits of the further development of gasoline engines. Thermodynamic approaches to optimise engine process via valve train variability shall be evaluated and compared for a homogenously and stoichiometrically operated gasoline engine. Therefore, the possible application of cam phasers, discretely staged valvelift shifters and fully variable systems will be separately examined. Additionally, the possibility to reduce fuel consumption with cylinder deactivation and throttle free load control will be demonstrated. The second part of the article in MTZ 5 will present stoichiometric and stratified lean operation mode as well as future combustion processes like HCCI and their potentials.

AUTHORS

PROF. DR.-ING RUDOLF FLIERL
holds the Chair of Internal Combustion Automotive Engineering at the University of Kaiserslautern (Germany).

DIPL.-ING. FREDERIC LAUER
is Research Associate at the Internal Combustion Automotive Engineering Department at the University of Kaiserslautern (Germany).

DIPL.-ING. STEPHAN SCHMITT
was Research Associate at the Internal Combustion Automotive Engineering Department at the University of Kaiserslautern (Germany).

PROF. DR.-ING ULRICH SPICHER
holds the Chair of Reciprocating Engines at the Karlsruhe Institute of Technology (KIT) (Germany).

MOTIVATION

Reducing fuel consumption as well as CO_2 emissions has been the primary concern guiding ongoing research and development activities of combustion engines for many years now. The recent regulations for CO_2 emissions in the New European Driving Cycle (NEDC) and the introduction of penalties for exceeding the fleet limit values have added further emphasis to these investigations. In fact, they have provided the rationale to utilise new technologies that had so far been considered too expensive for mass production. The transport demands of today's society cannot be met by a purely electric engine without the additional utilisation of a combustion engine, for example as a range extender. Research has thus focused on increasing the efficiency of combustion engines.

Different technologies have been furthered by car manufacturers. That is why it is important and necessary to critically evaluate the potentials of these different approaches with regards to questions of fuel consumption and CO_2 emissions. In most cases these technologies are examined using different engines with diverse displacements, rated power and emission limits. Therefore, the published results are not directly comparable. This paper contrasts different technologies with each other, with the knowledge that some of the fuel consumption results are estimations.

INITIAL POSITION

The comparison is based on the performance of two engines, a 2.0-l four-cylinder naturally aspirated engine and a 1.6-l four-cylinder turbo engine. Both engines were equipped with a cam phaser on the inlet side. To approximate the NEDC the following operating points were examined: firstly, the naturally aspirated engine at n = 2000 rpm, BMEP = 2 bar and secondly, the turbocharged engine at n = 2000 rpm, BMEP = 3 bar. ❶ shows the respective values for fuel consumption.

STAGED VALVE LIFT SHIFTING SYSTEMS

Depending on layout design, valve lift shifting systems on the inlet camshaft allow a complete closure of either one or several valves or the choice of one or several cam profiles. This is the case in, for example, Honda's VTEC system [1] or AUDI's AVS system [2, 3]. The usage of a cam profile which offers advantages at part load, with a reduction of the inlet valve opening time in the shifting stage, allows a decrease in the charge cycle work in an area of the corresponding engine map. Thereby, the engine load can be effectively controlled through the usage of the lower valve lift, inlet cam phasing and throttle flap. According to the layout design of the lower valve lift, throttle-free load control is possible

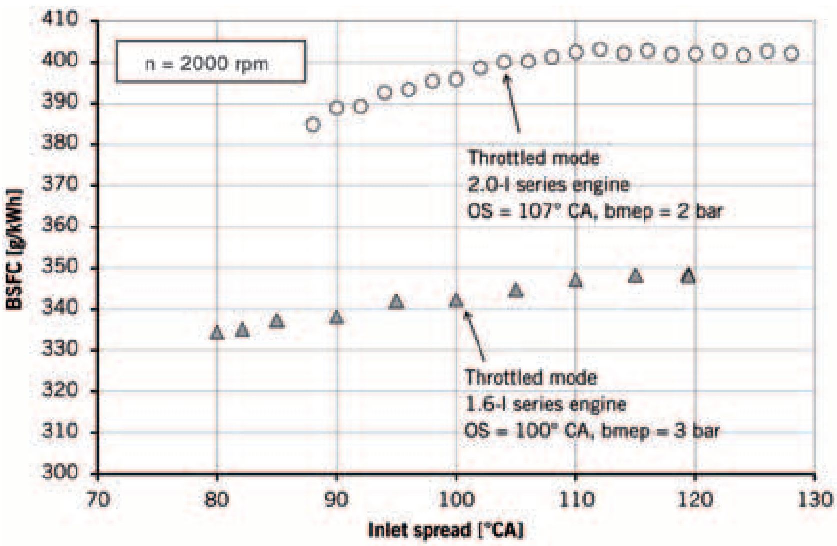

❶ Specific fuel consumption using throttled load control

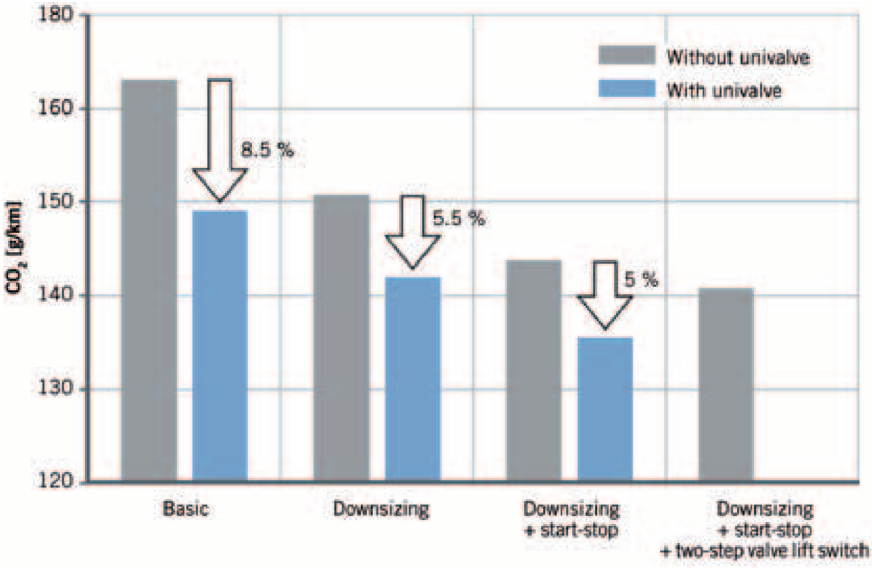

❷ CO_2 emissions within the NEDC when using different engine operation strategies [4]

at one singular engine operation point which is located either at higher to lower loads depending on the event timing of the lower cam profile.

Since both inlet valve lift and inlet valve opening timing can only be optimised for one engine operation point, an evaluation at fixed load points would thus not be relevant. To differentiate between the effects of shifting systems and alternative technologies, an evaluation of the fuel consumption within the parameters of the NEDC should therefore be taken into account. ❷ demonstrates the CO_2 emissions produced by a vehicle with 1.6-l engine, double cam phase adjustment, direct fuel injection and different concepts to reduce fuel consumption within the parameters of the NEDC. The test results were determined using the mechanically fully variable valve train system Univalve as well as a valve lift shifting system.

The attainable effective fuel consumption depends strongly on the adjusted inlet valve lift and inlet valve spread. With the chosen valve lift shifting system, the CO_2 emissions at NEDC were reduced by approximately 2 % through the utilisation of a valve lift shifting mechanism.

The higher the pressure in the intake manifold is increased through the usage of short inlet valve timing at constant load – the more the throttle losses decrease. Early inlet valve opening and closing as well as high amounts of residual gas backflow are necessary to decrease charge-cycle-work losses and thereby also fuel consumption. During engine operation at load points below the layout point, the engine equipped with a valve lift shifting system equally must be throttled. This again influences the amount of charge-cycle losses [5].

So when suiting a part valve lift to a discretely working shifting system, the conflict of aims must be solved between not only a broadly covered engine map through the small valve lift, but also the needs to have the most optimal effect within the parameters of the NEDC. For this reason the load band through which advantages can be achieved with part lift curves can only be relatively small. Additionally the area in the engine map which can be covered by the reduced inlet valve timing and a respectively smaller inlet valve lift is depending on the chosen engine concept. In the case of a turbocharged engine, this engine map area is larger than that of a naturally aspirated engine. ❸ illustrates how the load with a

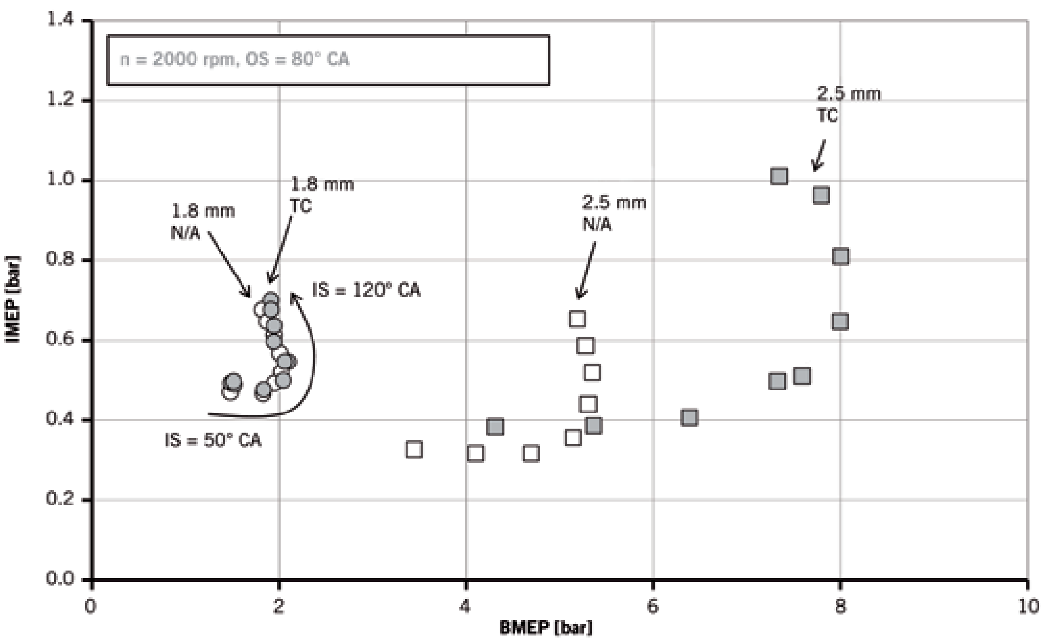

❸ The reachable load area and the occurring charge-cycle-work losses with discrete inlet valve lifts and variable inlet spread, illustrated with and without turbocharging constant inlet valve lift varies through the modification of the inlet spread. An increase of the charge-cycle work losses when using small inlet valve lifts advantageous at part load, leads to higher fuel consumption at higher engine loads. The choice of the part load cam lobe therefore presents a compromise achieved from the advantages at low loads, the effects within the NEDC and at customers as well as the drivable engine-map range. Hannibal et al. furthermore analyse in [6] the different demands that arise during application of discretely working and fully variable valve train systems.

THROTTLE-FREE LOAD CONTROL THROUGH MECHANICALLY FULLY VARIABLE VALVE TRAINS

In the case of mechanically fully variable valve trains which are utilised today by BMW (Valvetronic), Toyota (Valvematic), Mitsubishi (Mivec), Nissan (VVEL) and by the KSPG AG (Univalve), the valve lift/valve timing as well as the inlet- and outlet spread have to be controlled in fully variable mode to attain the optimal fuel consumption, ❹. The inlet spread (IS) and the inlet valve lift determine the instants of time for the opening and closing of the inlet valves. These are the very moments which influence the amount of charge-cycle work and hence the effective fuel consumption, ④. The outlet spread determines the exact time for the closure of the outlet valves which, in turn, influences not only the amount of residual gas backflow, but also the amount of charge-cycle work losses (which are also influenced by the amount of residual gas) and the effective compression ratio. Thus the effective fuel consumption is also essentially shaped by the choice of the outlet spread (OS), as illustrated in ④.

The lowest achievable effective fuel consumption is limited in a naturally aspirated engine at part load by the residual gas compatibility of the combustion chamber and the available outlet valve opening duration. Using throttle-free load control in a 2.0-l naturally aspirated engine, the specific fuel consumption can be decreased at an operating point of n = 2000 rpm, BMEP = 2 bar from approximately 385 to around 355 g/kWh.

Turbocharged four-cylinder engines under the use of monoscroll systems are equipped with a short outlet opening duration. This is particularly important for the separation of firing order which is necessary at full load and low driving speeds. This short outlet valve opening duration leads to disadvantages in the charge-cycle work and fuel consumption at part load [7]. An outlet valve timing which is designed for high low-end torque opens up a potential for fully variable valve trains to reduce fuel consumption by about 4 to 5 %. When the outlet valve opening time is optimised through the application of, for example, a twin-scroll-turbocharger, a fuel consumption potential of up to 10 % is possible.

MECHANICALLY FULLY VARIABLE VALVE TRAINS ON THE INLET- AND OUTLET SIDE

If a further mechanically fully variable valve train system is used on the outlet side in addition to that on the inlet side, the conflict between low-end-torque and minimal fuel consumption at part load of a four-cylinder turbocharged engine can be successfully solved. Compared to shorter, full load compatible outlet event

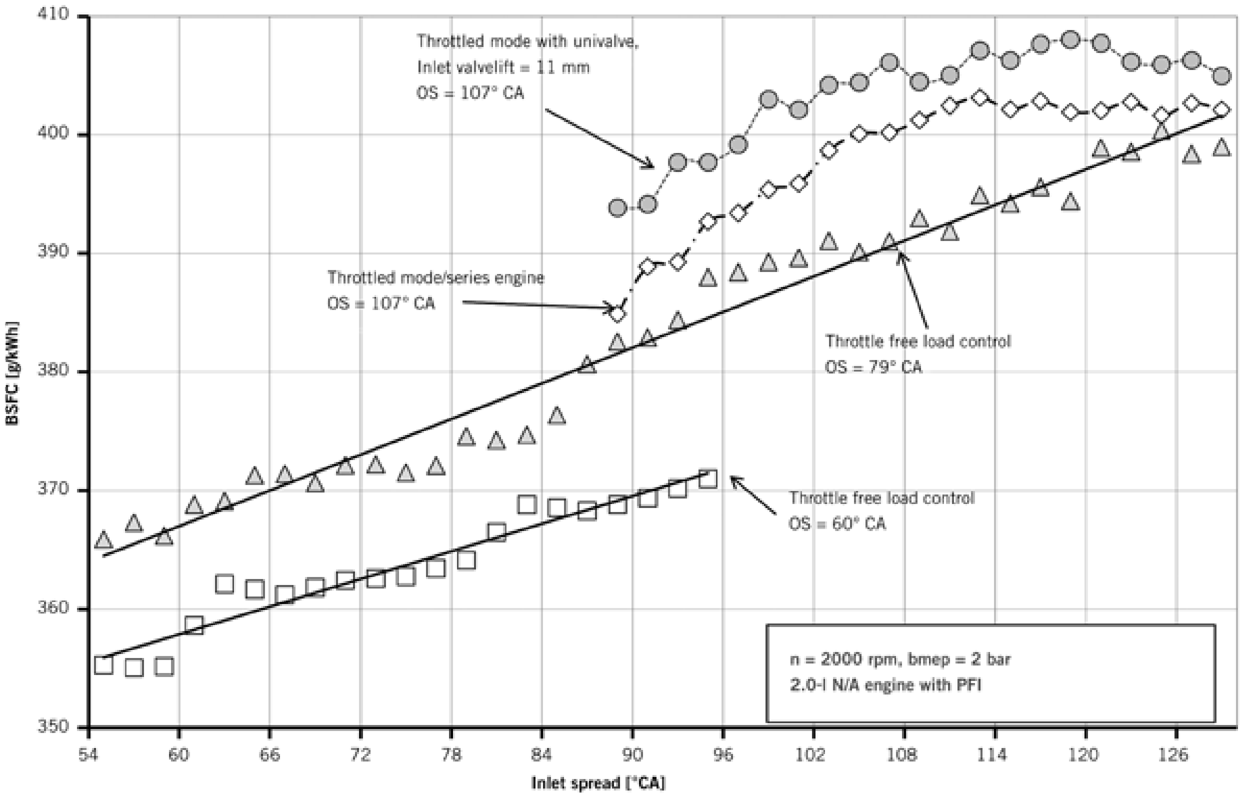

❹ Effective fuel consumption at throttle-free load control

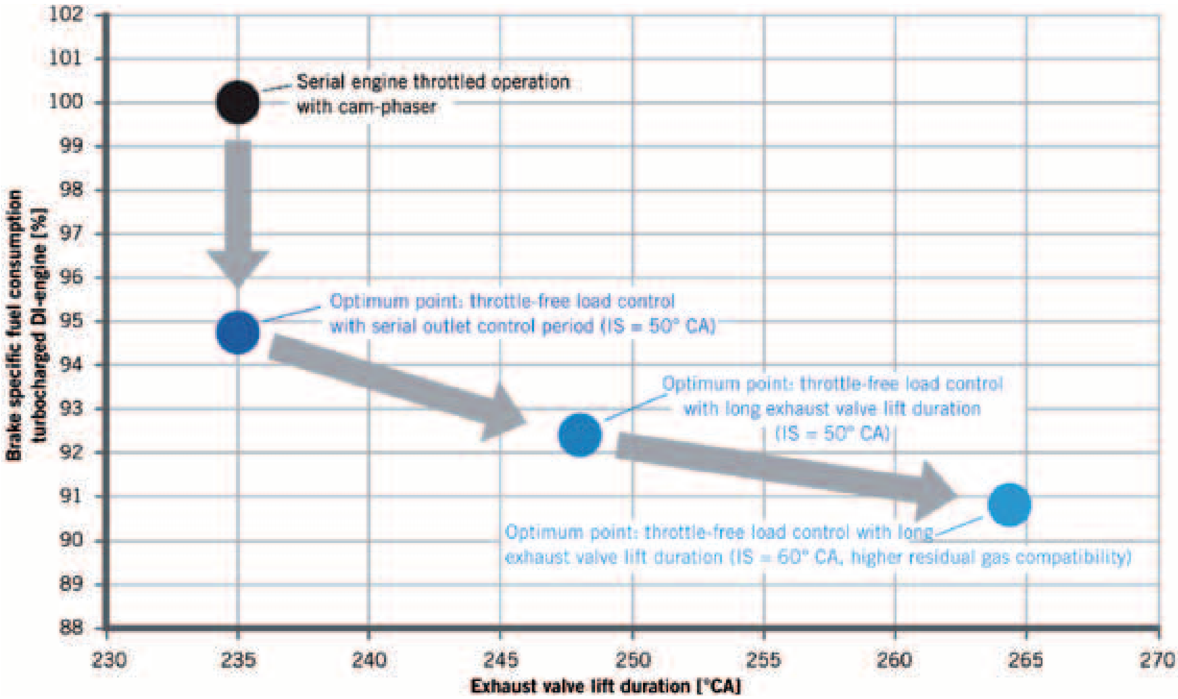

❺ Influences on fuel consumption through a fully variable outlet valve train with throttle-free load control [4]

duration, fuel consumption can thereby be improved by about 5 %, ❺ [7]. Due to the residual gas compatibility of the combustion chamber, potential to improve fuel consumption at lower engine loads is limited. The fully variable valve train system has to vary outlet valve timing between 230° and 270° CA to solve the conflict of aims between full load and part load. In terms of naturally aspirated engines, the conflict of outlet camshaft application is distinctively less apparent between part- and full load. It is here that the application of a fully variable outlet valve train can only attain an improvement of fuel consumption ranging up to 2 %.

MECHANICALLY FULLY VARIABLE VALVE TRAIN AND CYLINDER DEACTIVATION

Through utilising a fully variable valve train on both, inlet- and outlet side, a cylinder deactivation can also be implemented insofar as the valve train system allows zero valve lift. When deactivating two cylinders at constant engine load, the load of the active cylinders is elevated with the effect that the entire engine runs on reduced effective specific fuel consumption. Furthermore, in cylinder-deactivation mode charge-cycle work is reduced due to the throttle-free load control compared to the throttled mode. An effective consumption of 304 g/kWh can be achieved through combining this technology with inlet- and outlet phase adjustment on a 1.6-l turbocharged engine at an engine operating point of n = 2000 rpm, BMEP = 3 bar. Compared to throttle-free operated four-cylinder engines with short outlet valve opening durations, an additional advantage of 5.5 % can be deduced due to cylinder deactivation. Taking this result as the basis for a 2.0-l naturally aspirated engine with an engine operation point at n = 2000 rpm, BMEP = 2 bar, approximately 330 g/kWh are to be expected, ❻ [8].

Such achievable reductions of fuel consumption depend strongly on the engine load. Particularly at lower loads, cylinder deactivation is an effective way to reduce fuel consumption. On a 1.6-l turbocharged engine at 2000 rpm, improvements up to BMEP = 5 bar were reached, ❼ [8].

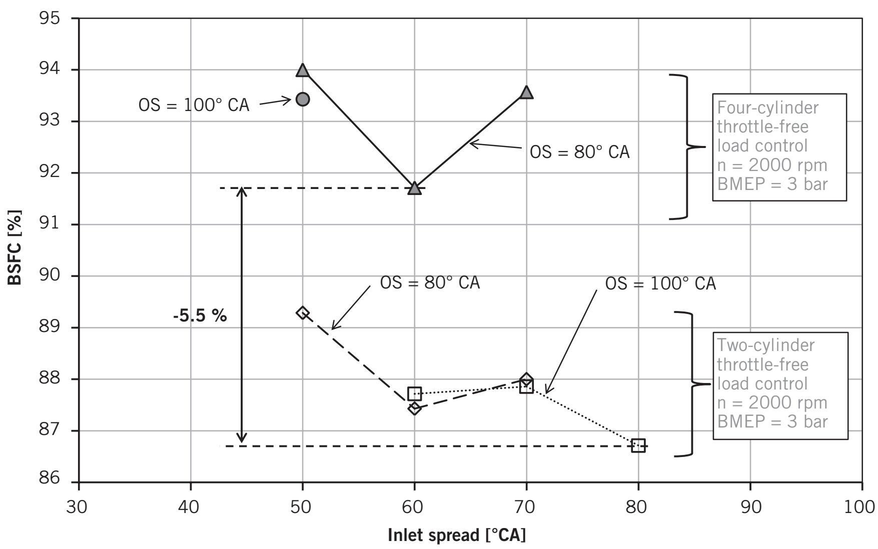

❻ Influence of cylinder deactivation on fuel consumption with trottle-free load control

VARIABLE COMPRESSION RATIO AND MECHANICALLY FULLY VARIABLE VALVE TRAINS

On a single-cylinder research engine with variable compression ratio and a fully variable valve trains on the inlet and outlet sides [9], the indicated fuel consumption was reduced by around 9 % through the variable compression at an engine speed of n = 1100 rpm, BMEP = 3 bar, ❽. During stationary engine dynamometer testing, the energy expenditures of the actuating elements are not taken into account. Therefore at an operating point of n = 2000 rpm, BMEP = 2 bar, an additional effective fuel consumption advantage of approximately 5 to 6 % is estimated in comparison to the throttle-free engine mode. The consumption potential within the parameters of the NEDC is even further influenced through the energy expenditures of the actuator.

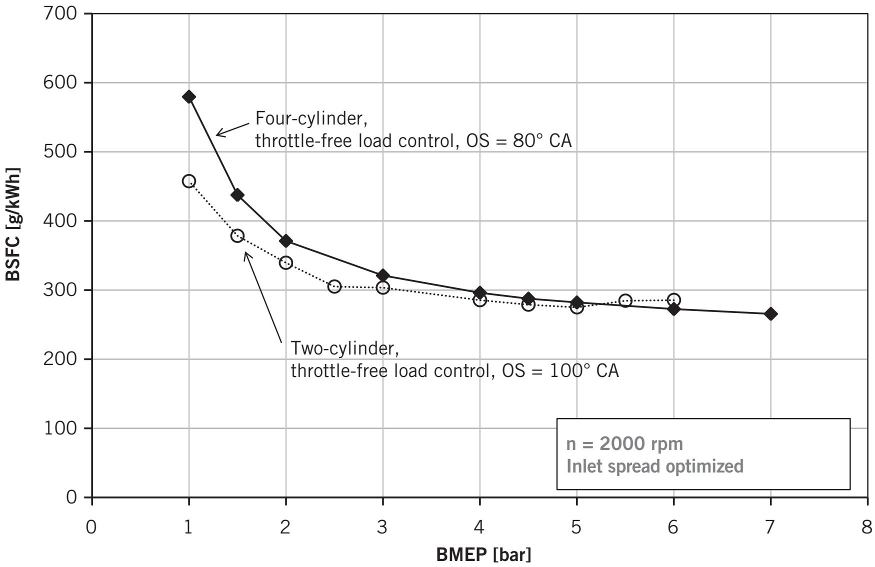

❼ Potential of cylinder deactivation to reduce fuel consumption at different engine loads

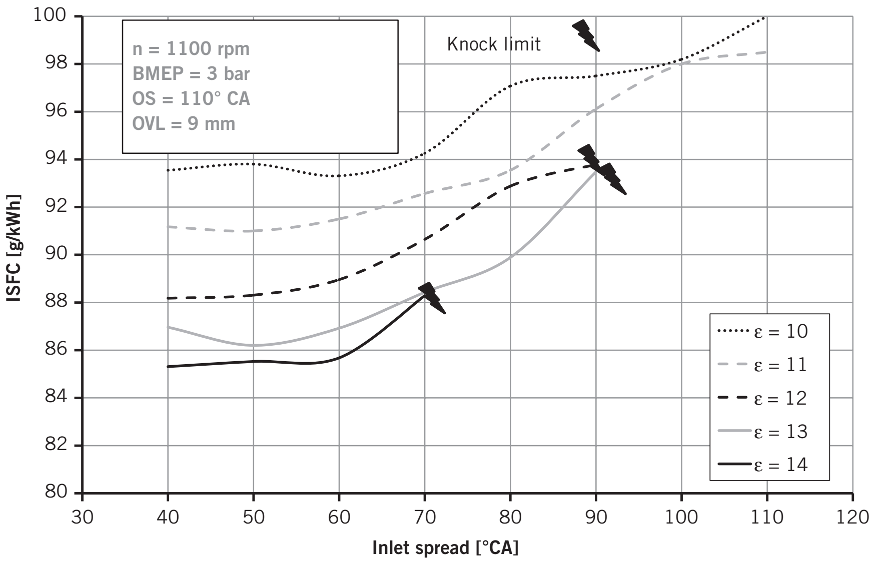

❽ Indicated fuel consumption with variable compression ratio

SUMMARY PART 1

This article demonstrates the availability of mechanical approaches for thermodynamical optimisation of gasoline engines. The individual techniques have to be evaluated with respect to reduction of fuel consumption, CO_2 emissions, costs and package. In general, the willingness of OEMs to examine new technologies and develop them further for mass production increases in the context of the enduring CO_2 discussion. A combination of several measures might be expedient as well. However, the potential to reduce fuel consumption has to be evaluated separately.

REFERENCES

[1] Otobe, Y.; Kawaguchi, H.; Ueshima, H.: Development of the High-Power, Low-Emission Engine for the Honda S2000. SAE Paper 2000-01-0670, 2000

[2] Grigo, M.; Wurms, R.; Budack, R.; Helbig, J.; Langa, Z.; Trost, W.: The New 2.0-litre TFSI Engine with Audi valvelift system. In: ATZextra "The New Audi Q5", 2008

[3] Eiser, A.; Fitzen, M.; Heiduk, T.; Mendle, J.: Zahlmann, S.; Bäumel, F.: 3.0 l TFSI – The New Top-of-the-Range V6-Engine from Audi. In: MTZ 70 (2009), No. 9

[4] Flierl, R.; Schmitt, S.; Kleinert, G.; Esch, H.J.; Dismon, H.: Univalve – A Fully Variable Mechanical Valve Lift System for Future Internal Combustion Engines. In: MTZ 72 (2011), No. 5

[5] Wurms, R.; Löbbert, P.; Dengler, S.; Budack, R.; Eiser, A.: Welche Ventiltriebsvariabilität ist sinnvoll? Conference Variable Valve Control, Haus der Technik, 2007, Essen

[6] Hannibal, W.; Flierl, R.; Schmitt, S.; Lauer, F.; Schopp, G.; Kleinert, G.: Einsatz teilvariabler und vollvariabler Ventilsteuerungen für unterschiedliche Motorkonzepte. Conference Ladungswechsel im Verbrennungsmotor, 2010, Stuttgart

[7] Schmitt, S.: Potentiale durch Ventiltriebsvariabilität auf der Auslassseite am drosselfrei betriebenen Ottomotor mit einstufiger Turboaufladung. To date unpublished doctoral thesis, 2011, Technical University of Kaiserslautern

[8] Lauer, F.: To date unpublished doctoral thesis, Technical University of Kaiserslautern

[9] Flierl, R.; Schmitt, S.; Wabbals, D.; Kleinert, R.: Fully Variable Valve Train and Variable Compression Ratio – First Measured Results. In: MTZ 70 (2009), No. 7/8

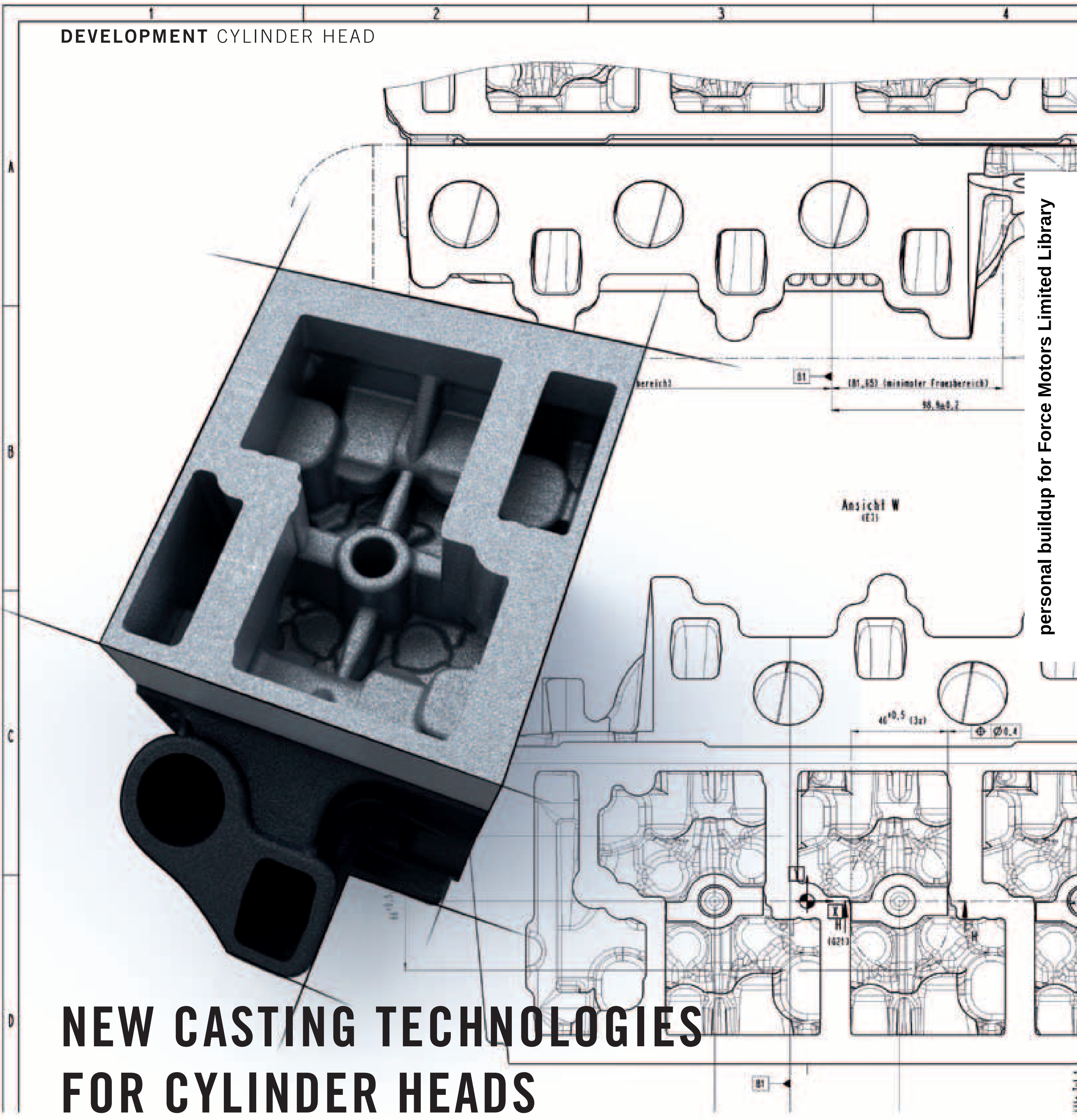

NEW CASTING TECHNOLOGIES FOR CYLINDER HEADS

The consistent pursuit of the downsizing idea leads especially in the development of modern drive assemblies to an increased specific power density and simultaneously to a reduced fuel consumption and lower pollutant emissions. But weight-reduced constructions of different engine components and their increased thermal and mechanical stress lead to constantly new challenges especially for the materials. The article from the Otto-von-Guericke-University Magdeburg provides a general overview of the current trend in both topics: the materials technology development and the manufacturing technology development of cylinder heads to improve their specific performance.

AUTHOR

DIPL.-WIRTSCH.-ING. STEFAN SCHARF
is Research Assistant and PHD Student at the Institute of Manufacturing Technology and Quality Management, Otto-von-Guericke-University Magdeburg (Germany).

PROBLEM DESCRIPTION

In the current discussion about future propulsion solutions for motor vehicles new problems lead to different approaches. The research priority is the continued development of internal combustion engines while reducing the total vehicle mass. This is mainly due to the statutory and socially requested reduction of the CO_2 level and the steadily increasing oil prices. With regard to the described problem, the idea of light weight constructions was highly provided, and more effort was put into the development of small-displacement engines in the recent past. Because of turbocharging, direct injection, and other technological developments, these small engines are nowadays able to retrieve almost the same performance as their bulky predecessor at a much lower level of fuel consumption. Thereby there is no loss regarding the driving comfort and driving pleasure. In the automotive world the entire vehicle-related arrangements for the targeted reduction of fuel consumption are known as downsizing. Due to the persecuted downsizing strategies the main influencing parameters to reduce fuel consumption can be influenced to achieve significant changes. Therefore they play a key role in the current development of modern vehicles. ❶ shows in a schematic overview the main parameters which influence the reduction of vehicle fuel consumption in total and their weighting.

Mechanical power
1 kW ~ 16 g CO_2/km

Weight
100 kg ~ 8.4 g CO_2/km

Air resistance (~ C_D*A)
0.1 m² ~ 3.4 g CO_2/km

Rolling resistance
1 ‰ ~ 1.9 g CO_2/km

Electrical consumer
1 A ~ 0.34 g CO_2/km

❶ Main influencing parameters to reduce the fuel consumption of the entire vehicle [1]

Significant potential to reduce the fuel consumption is a result of optimising the overall efficiency of the vehicle. This is achieved by a systematic reduction of the driving resistances, which includes a minimal roll resistance, a flow-optimised vehicle design and a reduced vehicle mass. Under the keyword power on demand the degree of engine efficiency of the drive source or the gear transmission are increased by general consumption lowering agreements or by shifting the engine operating points into more effective characteristic diagrams [2].

Consequently, the optimisation of the drive aggregates forms an essential developmental focus. Here, both the customer's demands regarding driving pleasure, comfort, purchase and operating costs, quality and reliability of the vehicles as well as the statutory provisions, such as the reduction of pollutant emissions, and resource conservation, delineate the tight constraints of the targeted development goals. Not at least also the feasibility of an effective and economical production decides of the acceptance by the customer and thus of the success of an engine. ❷ gives a summary of the general requirements of modern drive units.

In the development of modern aggregates, the desired goal of reduced fuel consumption is finally realised by increasing the specific utilisation of the engine. Such an aiming increase in power density in the aggregate can only be guaranteed by an increase in medium pressures. The consequences of this in turn are increased cylinder pressures and higher temperatures in the combustion engine. Regarding the combustion chamber thus much higher amounts of energy are to implement and to discharge and in fact of this also larger forces are to absorb [3].

DESIGN OF THE CYLINDER HEAD

The cylinder head has a significant impact on the operation of the engine behaviour in terms of power output, torque and exhaust emissions performance, fuel consumption and engine noise. The head is also exposed to high loads and represents the most challenging component of the engine regarding technical production aspects [4]. ❸ gives an informative over-

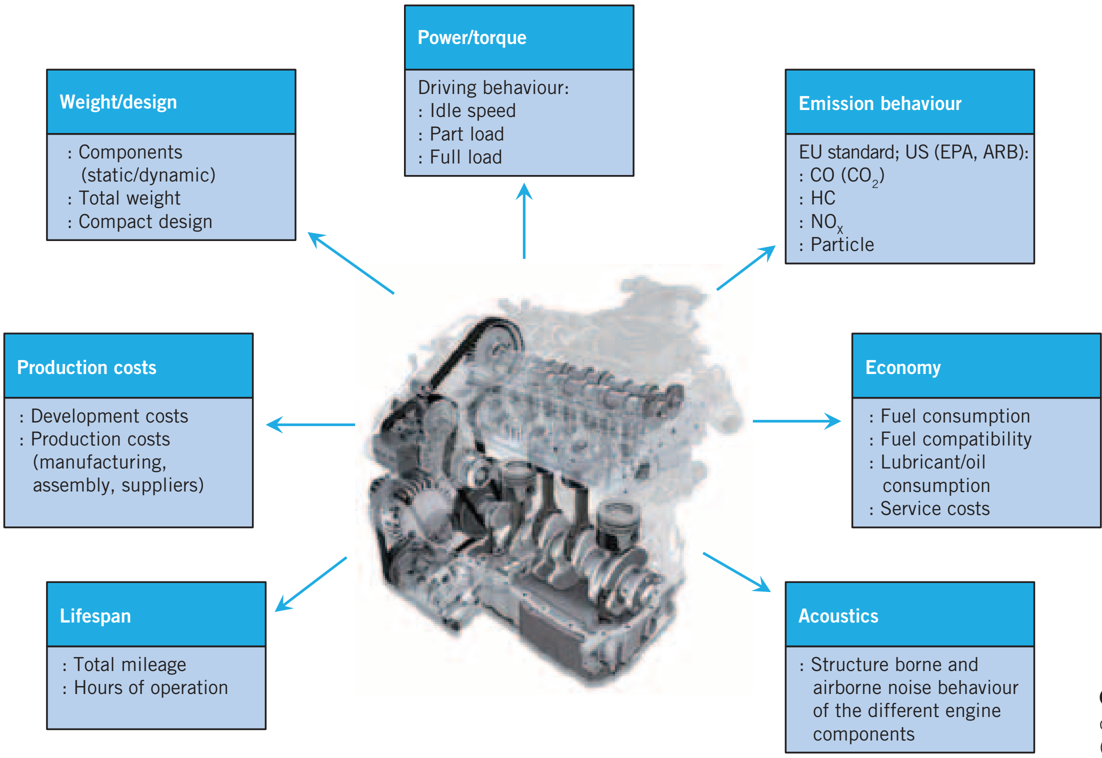

❷ Demands on modern drive aggregates [3] (source: VW)

view of the complexity thermo-mechanical stresses on the cylinder head, and over the latest design solutions to accommodate them.

The high (thermodynamic) alternating stress and the resulting component loads while the engine is running are occasionally taking the currently used materials to their breaking point. Especially the predicted peak pressure demands for future diesel engines, new design concepts for the cylinder head seem to be inevitable. As a result, a reinforced attempt is to develop alternative designs and manufacturing capabilities as well as the application of requirements-oriented new substitute materials.

DEVELOPED ALTERNATIVE SOLUTIONS

To negotiate the discrepancy between the absorption of growing component stresses and the continued pursuit of lightweight constructions, the idea to develop a cylinder head, which is manufactured according to the different stresses in the different parts from various materials which satisfy this requirements occurred at the Institute for Manufacturing Engineering and Quality Management of the Otto-von-Guericke-University Magdeburg in the context of various research projects for the Volkswagen AG. The observable trend toward an increasing functional integration and an increasing complexity of the components enhance partly the widely varying loads on the different areas of the cylinder head. That implies sophisticated demands to the materials.

On this account first an analysis of the cylinder head geometry and the determination and delimitation of the various component areas was carried out. Based on this the cylinder head was divided into different functional areas, which are shown in ❹.

In essence the component can be divided into the following functional areas: the

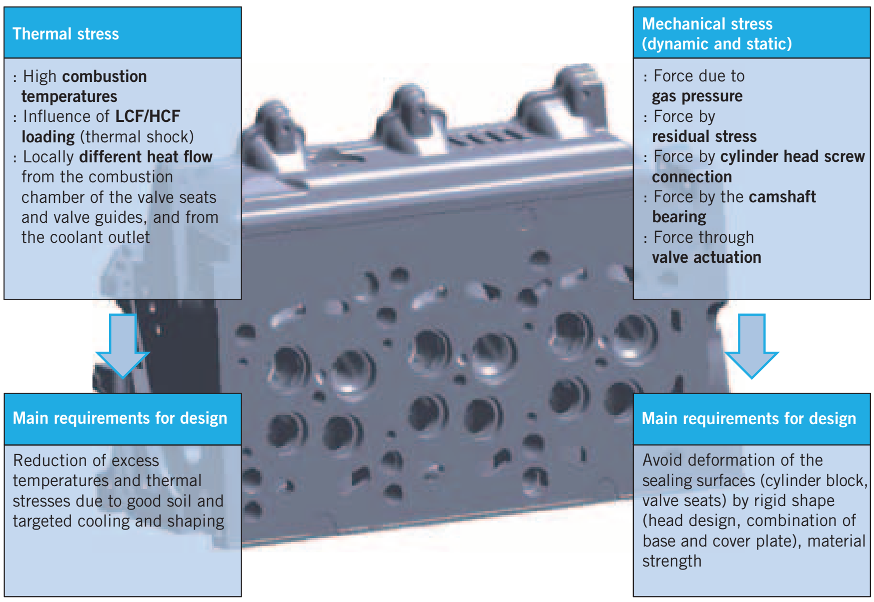

❸ Stresses and constructive solutions to the cylinder head [3] combustion chamber, the channels, and the camshaft bearings. Based on these considerations and taking into account the schematic correlations represented in ❺, different concept variants have been devised to realise the technical production of a cylinder head consisting of different materials which are firmly bonded or alternative positive connected.

These concept variants were divided for the purpose of a suitable classification in a variant scheme, ❻. Based on a mono head, that means starting from a cylinder head composed of one homogeneous material it is differenced after the number of the combined materials in the embodiments: homogeneous, double-layer and multilayer structure. Furthermore a distinction is made between the types of production-technics and the implementation of the material combinations in the variants: gradient casting, casting of functional elements as well as connecting different functional areas, which are producible from separate manufactured and combined layers. Based on these classifications different cylinder head types were defined, which are designated according to ❼ as mono head, funar head or mulay head.

The various embodiment variants for the production-related implementation of this cylinder head types are illustrated in a schematic overview in ❽. Therefore, those cylinder head designs in which the requirements can be fulfilled in the various functional areas with one alloy are grouped under the term mono head. These cylinder head types are currently used by default. Thereby, primarily hypoeutectic aluminium alloys are used. For the production of these types the processes of gravity die casting – either static or dynamic – (option 1), the casting in the lost foam method (option 2) and (in the passenger car sector only used occasionally) the casting of cast iron in lost forms (option 3) are applied.

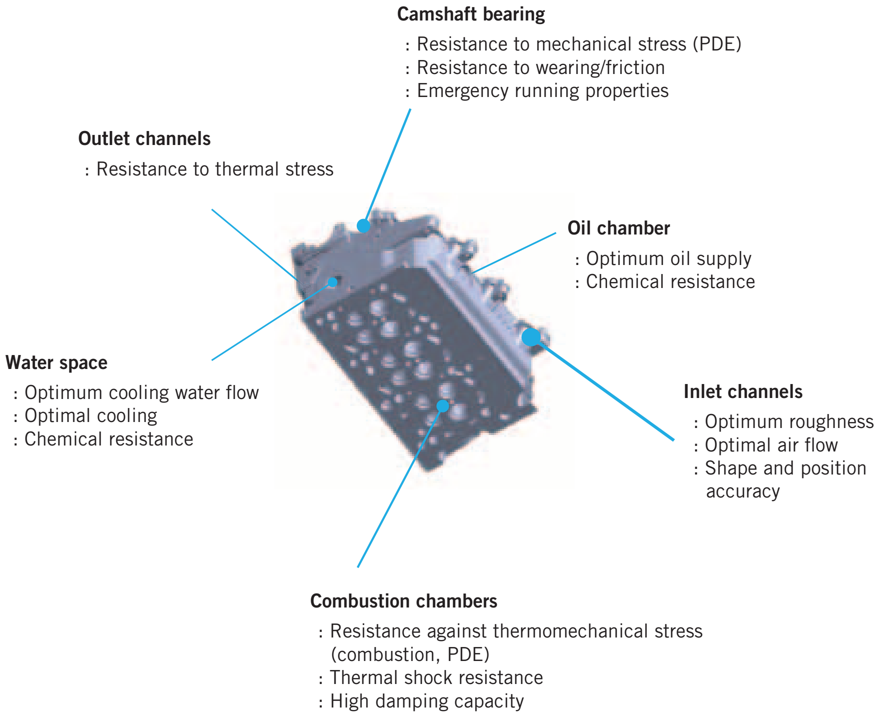

❹ Illustration of the various functional areas of a cylinder head [5]

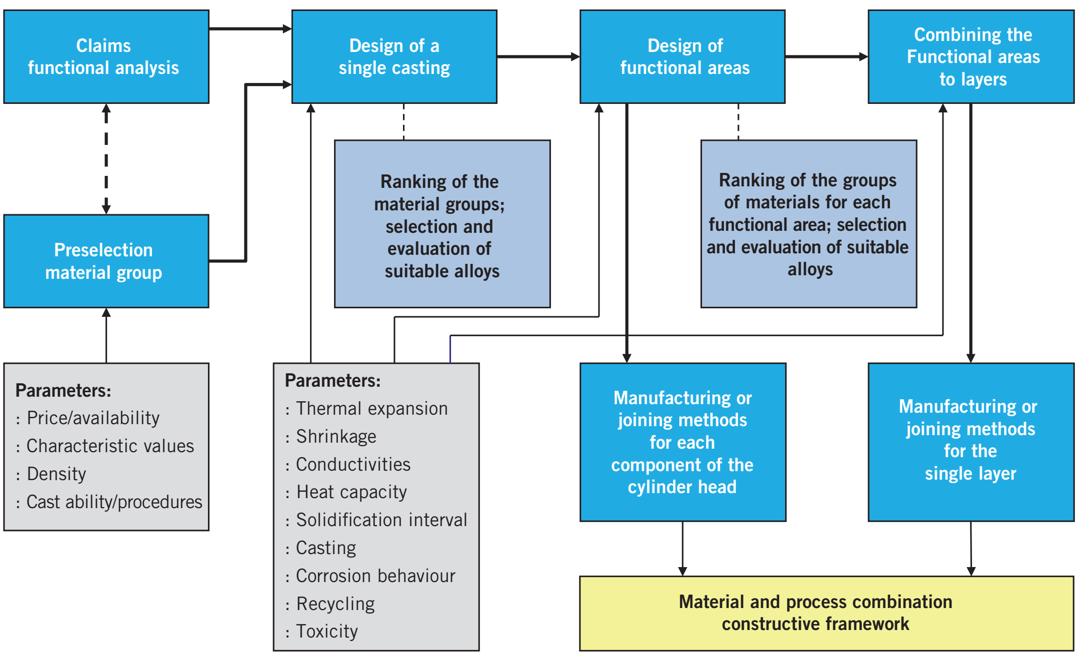

❺ Schematic procedure for the derivation of appropriate design variants [5]

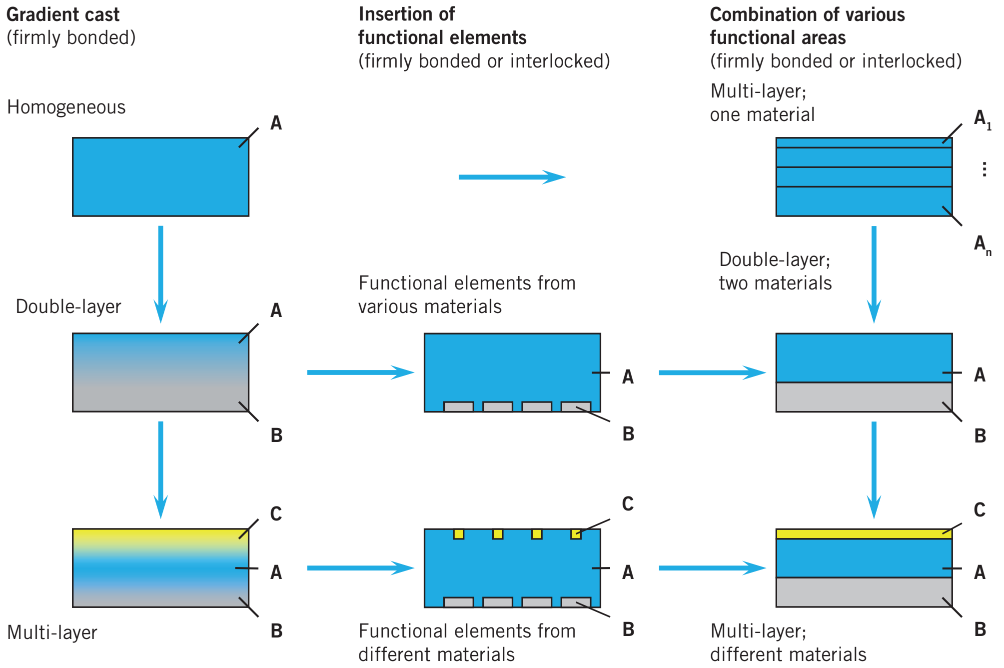

❻ Schematic overview of the possible partition types [6]

For cylinder head concepts, where the component loads are absorbed by functionally distributed different alloys or even different materials, the terms funar head and mulay head have been introduced. The term funar head (derived from functional area) represents the implementation of functional elements, which act only locally reinforcing in certain areas of the cylinder head. Mulay head (based on the term multi-layer) are those cylinder head concepts, in which complete functional areas can be produced in the form of single layers made of different alloys or materials. The head types which are summarised under the designation funar head can be differentiate again into three categories: the execution of an aluminium cylinder head with a cast-iron-based combustion chamber and/or cam bearing inserts (option 4), the execution of these operations from aluminium-bronze alloys in the combustion chamber area or brass inserts in the camshaft range (option 5) and the casting of sheet metal structures in the channel region (option 6).

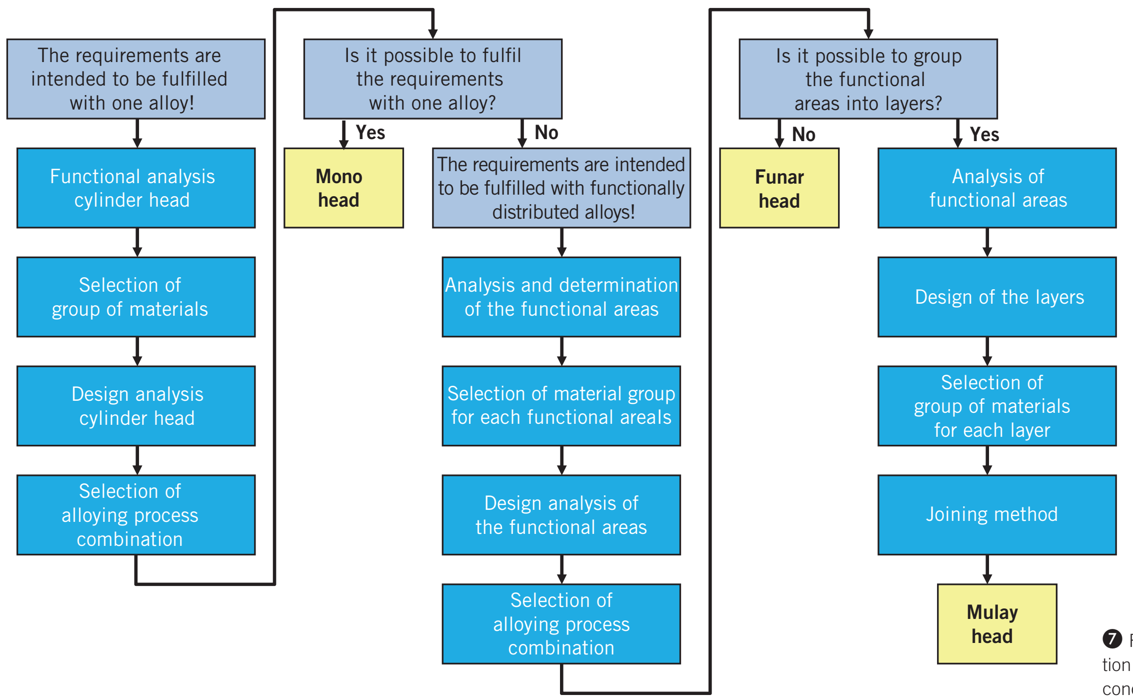

❼ Flow chart for classification of the cylinder head concepts [5]

In contrast to this, the mulay head variants consist of a subdivision of the cylinder head in different layers regarding the design and manufacturing. These layers can be manufactured by the combination of different casting processes with the goal of using the advantages of each technique and the process typical microstructures. For example the high stressed combustion chamber layer could be manufactured via gravity die casting while the rest of the head is casted in the high pressure die casting (option 5). Furthermore the different cylinder head areas can be produced with different aluminium alloys in the gradient casting (option 8). Finally there is the possibility to combine separate produced layers with combined functional areas of different materials (option 9).

HOMOGENEOUS CYLINDER HEAD

The concept version of a homogeneous cylinder head (mono head) containing a hypoeutectic aluminium alloy represents the current state of the art. While in the past the previously casted iron materials were substituted by aluminium based alloys to realise the idea of lightweight, the steadily increasing component stresses require continuously innovative technical enhancements. This include extensive developments due to the used alloys, new research results in the field of heat treatment and inter alia highly complex design features on the component cylinder head. Due to process developments and the deployment of new casting technologies like the low pressure casting or dynamic casting methods such as the Rotacast or the NDCS enabled to fulfil the new component requirements and the production of high strength components at acceptable costs. To absorb the expected operating loads of future engine generations, the possibilities of homogeneous aluminium based head concepts for further performance improvements seem utilised among experts. Because of this the development of alternative materials and production facilities are two of the main current interests in science and research [7].

According to the demands of increased component strength, a practical suitability for series production and not at least on

Mono head

The casting is designed for the maximum stress of a specific material

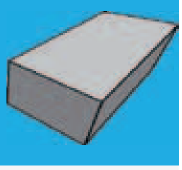

Material:
: High-strength aluminium alloys
: Cast iron materials

Process:
: Die casting
: Lost foam

Variations:
: *Option 1*
High-strength Al alloys/die casting
: *Option 2*
High-strength Al alloys/lost foam
: *Option 3*
GJL/GJV

Funar head

Functional areas are identified and the respective appropriate materials are selected

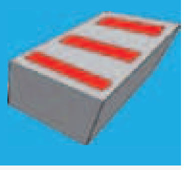

Residual – cylinder head:
: Aluminium/magnesium

Combustion chambers:
: High-strength Al alloys
: Nodular graphite cast iron
: Steel/cobalt/nickel
: Aluminium-bronzes

Camshaft bearings:
: High-strength Al alloys
: Cast iron materials
: Brass

Joining methods:
: Moulded
: Mounted
: Laser welded
: Moulding of prefabricated channelstructures

Variations:

: *Option 4*

Combustion chambers:	GJL/GJV
Camshaft bearings:	GJL/GJV
Residual cylinder head:	Al alloy

: *Option 5*

Combustion chambers:	Al-bronze
Camshaft bearings:	Brass
Residual cylinder head:	Al alloys

: *Option 6*

Combustion chambers:	Al-bronze
Camshaft bearings:	Brass
Channels:	Al/steel sheet
Residual cylinder head:	Al alloys

Mulay head

Functional areas are grouped into separate producible layers

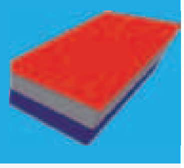

Construction:
: Different aluminium alloys in gradient casting
: Layered structure and subsequent assembly of the individual "plates"
: Functional areas are manufactured separately and moulded firmly bonded or interlocked

Joining method:
: Gradient casting
: Moulded
: Mounted
: Glued
: Laser welded

Variations:

: *Option 7*

Combustion chamber layer: (die casting/assembly)	Al alloys
Residual cylinder head: (high pressure die casting/squeeze casting)	Al alloys

: *Option 8*

Combustion chamber layer:	Al layer
Residual cylinder head: (gradient casting)	Al alloys

: *Option 9*

Combustion chamber layer: (lost form)	GJL/GJV
Channels:	Al/steel-sheet
Residual cylinder heads:	Al alloys

❽ Various embodiment variants of the cylinder head concepts [5] the basis of new possibilities to reduce the wall thickness also a return to cast iron materials is drawn into consideration. Corresponding to the design variants which are shown in ⑧, the mono head concept is basically divided into two material categories, high strength aluminium alloys and cast iron materials.

Finally considering the thermodynamic behaviour, the weight disadvantage of cast iron in comparison to aluminium alloys must balance the higher strength properties. To overcome this discrepancy and because of the fact that the increased strength properties are required only in specific, locally defined areas of the cylinder head, the concept solutions in which aluminium is replaced by cast-iron-based materials only in the highly stressed component areas seem to be a purposeful solution [8].

CYLINDER HEAD WITH FUNCTIONAL CAST-IN ELEMENTS

Such a hybrid concept solution is the cast-in of functional elements (funar head). According to this approach structurally reinforcing inserts of high strength materials are cast into the base material. This variant is already applied in the series production of various other engine components like the cylinder crankcase. So for example reinforcements for the bearing block or special cylinder liners are produced in iron materials and cast into the existing basic structure comprise of an aluminium alloy. Alternatively complex scaffolds are produced as functional elements like the magnesium-aluminium composite crankcase from the BMW AG. The outcome from recent investigations for the production of funar cylinder heads is so far not the desired result of both in the context described topics of the various research projects at the Institute of Manufacturing Technology and Quality Management of the Otto-von-Guericke-University and according to the published research results.

GRADIENT-CAST

Also the gradient casting (mulay head) was investigated extensively at the University of Magdeburg. These works were also conducted in the context of a research project with the Volkswagen AG and the former Rautenbach Wernigerode GmbH (now Nemak Wernigerode GmbH). For this project two requirement-oriented aluminium alloys were casted by a controlled mold filling in accordance with the local different mechanical and thermal stresses of a cylinder head. The alloys have been poured in a special way, so that a smooth transitional layer with a defined width could be produced gradually continuous from one to the other alloy [9-11]. A comparison between a conventional alloy- or material boundary and a gradient material transition is shown in ❾ [12].

Although the works on the gradient casting finally led to readiness for series production and the produced cylinder heads were installed and tested in experimental vehicles, this production variant is (based on the present knowledge) not being applied at present.

HETEROGENEOUS HYBRID CONSTRUCTION

Another way to absorb the different loads in the cylinder head is according to the presented option 9 the idea of a hybrid composite construction (mulay head), where the lower cylinder head area (which is exposed to high combustion pressures and temperatures) is manufactured from cast iron based materials.

For the scientific investigation of this concept version, the Institute of Manufacturing Technology and Quality Management of the Otto-von-Guericke-University has been commissioned to conduct a feasibility analysis of producing a hybrid cylinder head from a cast iron material and an aluminium alloy by the Volkswagen AG. To execute and investigate this innovative assignment competently and appropriately, a joint research project with well-known industry partners was initiated. This includes beside the University of Magdeburg the IAV GmbH, the Martinrea Honsel GmbH and the Eisenwerk Brühl GmbH. To investigate the design and manufacturing challenges of this hybrid construction solution in detail and to develop a suitable composite material bond initially a demonstrator was produces which is similar to a cylinder head. Particular emphasis was placed on a strict separation of media-carrying functional groups to avoid any leaks in the transition areas and to ensure a corrosion-resistant design of the coolant and the combustion gas bearing areas. As result such a hybrid demonstrator was designed and manufactured. This demonstrator has in comparison to a pure aluminium construction a higher component weight of approximately 50 % but it also withstands much

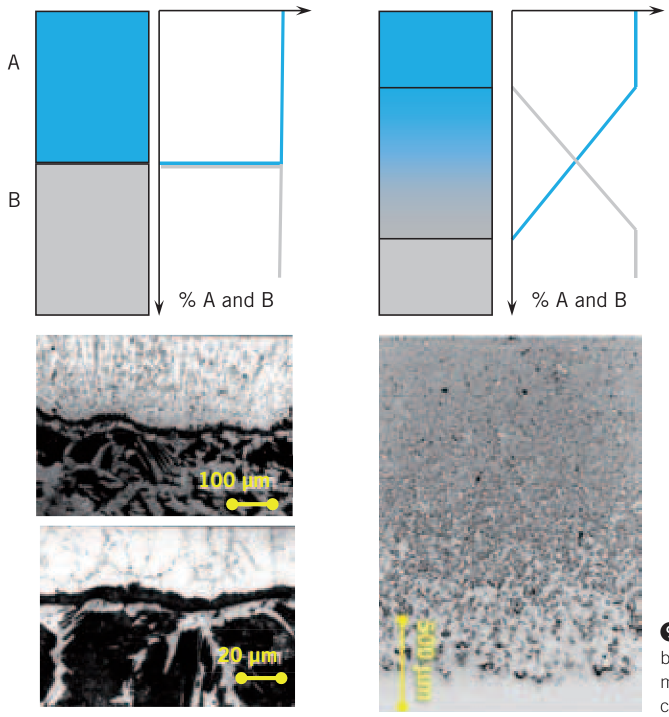

❾ Comparison between composite materials and gradient casting [5] higher loads. In comparison to pure cast iron design, the weight of the hybrid demonstrator is only about 55 %.

Due to the increased strength properties of the cast iron material a heterogeneous designed mulay head could be loaded much higher than previously known units. Via a further increase of the specific power density at the entire engine, the downsizing idea could be systematically continued. Furthermore such a hybrid cylinder head design allows occasionally also from the production-technical point of view a high saving potential. Because of the application of an iron-based cast material to absorb the critical loads, the complex and cost-intensive efforts, to form a particularly fine microstructure in the aluminium cast (restrictions by dendrite arm spacing), can be eliminated. As a consequence there are a multiple advantages for the production of the component, which can be summarised as following:

- no mandatory binding to complex die casting methods with cooling of the ground plate (applicability of well automated and cost effective casting)
- simplification of complex melt treatments
- opportunity to use also secondary aluminium
- elimination of heat treatment.

It can be ascertained that this heterogeneous hybrid construction represents a very interesting approach which includes a high potential for further efficiency increases of advanced technologies for driving units. Regarding of the existing confidentiality, the detailed scientific knowledge of the production engineering and of the conducted investigations can only be published in a later stage.

CONCLUSIONS

In summary, the various presented design variants illustrate that the imposed restrictions on the targeted reduction of fuel consumption and pollutant emissions act as a key driver of continuous development in advanced materials and manufacturing development. That emphasizes again the importance of the automotive industry as a motor in the development of novel materials, processes and technologies for various application areas of the modern society.

REFERENCES

[1] Lösche-ter Horst, T.: Effizienzsteigerung moderner Aggregate durch weitere Reibungsreduzierung. ATZ/MTZ Conference Reibungsminimierung im Antriebsstrang, Esslingen, 2009
[2] Golloch, R.: Downsizing bei Verbrennungsmotoren. Ein wirkungsvolles Konzept zur Kraftstoffverbrauchssenkung. Berlin/Heidelberg/New York: Springer, 2005
[3] Pischinger, S.: Verbrennungsmotoren. Aachen, RWTH, lecture notes 26th edition, 2007
[4] v. Basshuysen, R.: Handbuch Verbrennungsmotor. Grundlagen, Komponenten, Systeme, Perspektiven. Wiesbaden: Vieweg + Teubner, 2010
[5] Behm, I.; Sobczyk, M.: Internal information, Otto-von-Guericke-Universität Magdeburg, Institut für Fertigungstechnik und Qualitätssicherung, 2001
[6] Knirsch, S.; Ambos, E.; Todte, M.: Werkstoff- und Verfahrensentwicklung für Zylinderköpfe von hochbelasteten Verbrennungsmotoren. In: MTZ 65 (2004), No. 4, pp. 292–297
[7] Sorger, H.; Zieher, F.; Sauerwein, U.; Schöffmann, W.: Hoch belastete Zylinderköpfe für Otto- und Dieselmotoren – Trends und Potenziale. In: MTZ 69 (2008), No. 2
[8] Hamm, T.; Ecker, H. J.; Rebbert, M.; Grafen, M.: Zylinderkopfkonzepte für hohe Spitzendrücke. 16th Aachen Colloquium Automobile and Engine Technology, 2007
[9] Taran, V.: Entwicklung einer Technologie zur Fertigung eines Aluminium-Zylinderkopfes aus Gradientenguß. Dissertation, Otto-von-Guericke-Universität Magdeburg, 2001
[10] Bähr, R.: Gradientenguss fur Motorbauteile. In: Gießereiforschung 55 (2003) No. 1, pp 1-4
[11] Bähr, R.: Neue Erkenntnisse zum Gradientenguss. VDI-Berichte No. 1718, pp. 83–92
[12] Bähr, R., Behm, I.: Internal information, Otto-von-Guericke-Universität Magdeburg, Institut für Fertigungstechnik und Qualitätssicherung, 2007

FRICTION IN HIGHLY LOADED JOURNAL BEARINGS

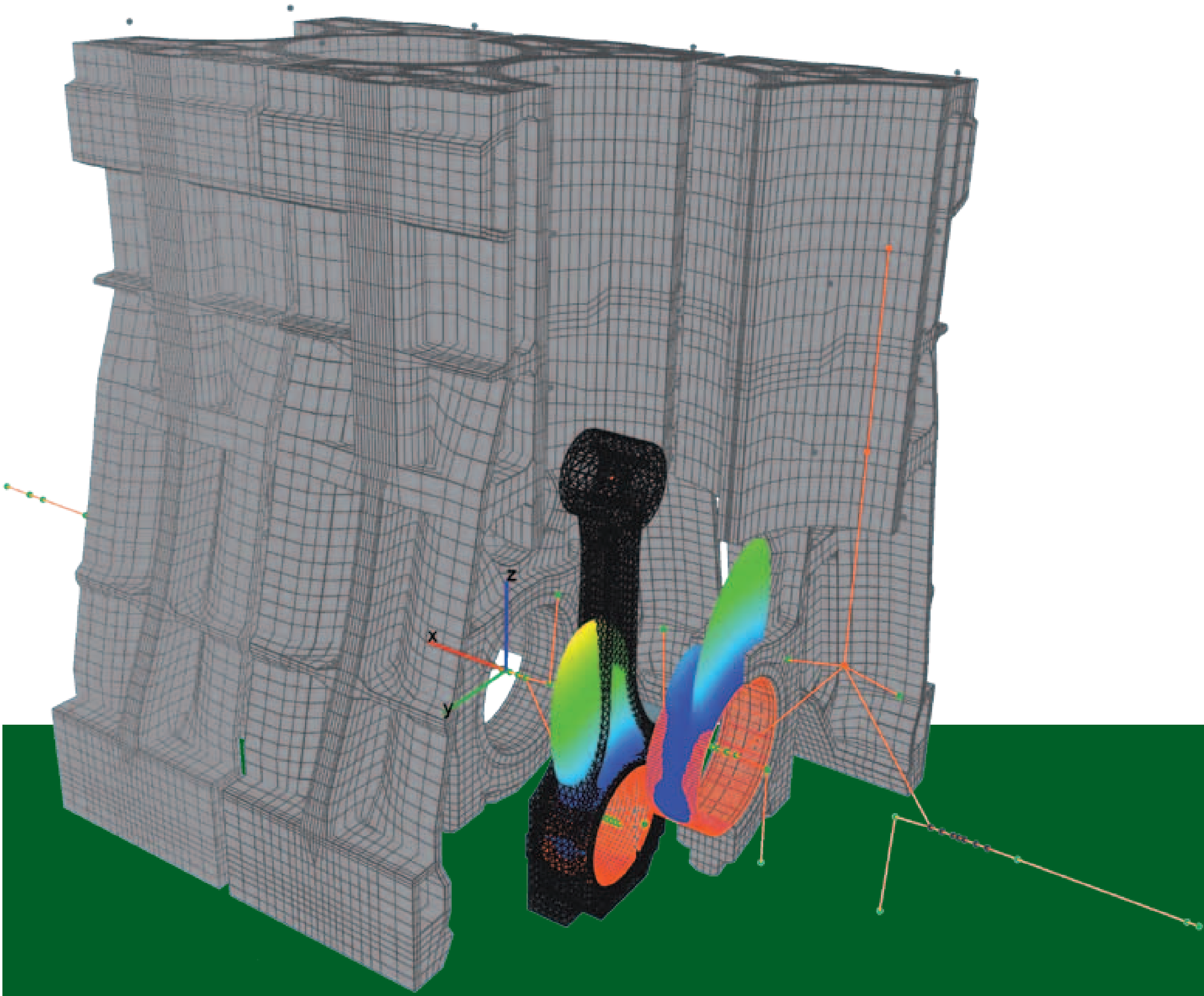

As part of a joint project with Miba Gleitlager and OMV Refining & Marketing, the Virtual Vehicle Competence Centre developed a validated simulation method for an exact and reliable prognosis of the friction power losses in radial journal bearings, which is applicable over an extended area of operating conditions far into mixed lubrication.

AUTHORS

DI CHRISTOPH PRIESTNER
is Leader of the Tribology Group at the AreaC of the Virtual Vehicle Competence Center in Graz (Austria).

DR. HANNES ALLMAIER
is Lead Engineer and working on Model Development and Methodology at the AreaC of the Virtual Vehicle Competence Center in Graz (Austria).

MAG. DI. FRANZ REICH
is Head of the AreaC NVH and Friction of the Virtual Vehicle Competence Center in Graz (Austria).

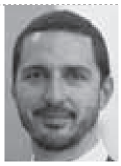

DI CHRISTIAN FORSTNER
is Head of the Application Engineering Department of the Miba Gleitlager GmbH in Laakirchen (Austria).

DR. FRANZ NOVOTNY-FARKAS
is Head of the Research & Development Department at the Competence Center Lubricants of the OMV Refining & Marketing GmbH in Wien (Austria).

MOTIVATION

Innovative engine concepts such as downsizing and ever increasing peak cylinder pressures lead to rising operational demands of the crankshaft main and big end journal bearings. Simultaneously low viscosity lubricants are used to reduce the friction losses in the engine and thereby optimise the specific fuel consumption of the engine to. Despite of all these measures, bearing reliability shall not be affected through occurring mixed lubrication.

The performance of the new method described below is validated through a detailed comparison with large measurement data taken from a comprehensive test program under application of various oils, loads and journal speeds. By means of the presented simulation method, the potential for friction reduction in the area of journal bearings is illustrated through a modern four-cylinder passenger car diesel engine.

The necessity to construct engines which are more efficient results in versatile complex operating conditions for the heavily stressed crankshaft main and big end bearings of modern engine conceptions. Both, increasing peak cylinder pressure and start-stop systems or demand-oriented oil supply units, lead to strained conditions in various ways and to fewer load reserves in these journal bearings. Since, loads will be further increasing in the future and meanwhile, development time will be shortened, simulation methods become increasingly necessary. Such a method assists in the preliminary design stages to dimension the highly stressed journal bearings and also assists in identifying potential issues with the bearing reliability during early stages of the design. As the journal bearings of the crank train are next to the piston assembly the other major contribution to friction in an engine, the potential for friction reduction is discussed after a short presentation of the simulation method.

SIMULATION METHOD

The origin of the EHD method is an elastic multi body systems simulation, which is employed for the calculation of the oilfilm in reference to Patir and Cheng's extended Reynolds equations, Eq. 1,

EQ. 1

$$-\frac{\partial}{\partial x}\left(\theta\phi_x \frac{h^3}{12\eta_p}\frac{\partial_p}{\partial x}\right) - \frac{\partial}{\partial z}\left(\theta\phi_z \frac{h^3}{12\eta_p}\frac{\partial p}{\partial z}\right) + \frac{\partial}{\partial x}\left(\theta\,(\bar{h} + \sigma_s\phi_s)\,\frac{U}{2}\right) + \frac{\partial}{\partial t}\,(\theta\,\bar{h}) = 0$$

whereas the pressure and shear flow factors (ϕ_x, ϕ_z, ϕ_s) were suitably chosen.

The realistic description of the lubricant is paramount, specifically the increase of the viscosity under pressure (η_p), as illustrated in ❶.

The metal-metal contact that appears in mixed lubrication is calculated by means of the contact model of Greenwood and Tripp,

EQ. 2

$$p_a = KE^*\,4.4\,10^{-5}\,(4 - H_s)^{6.8}$$

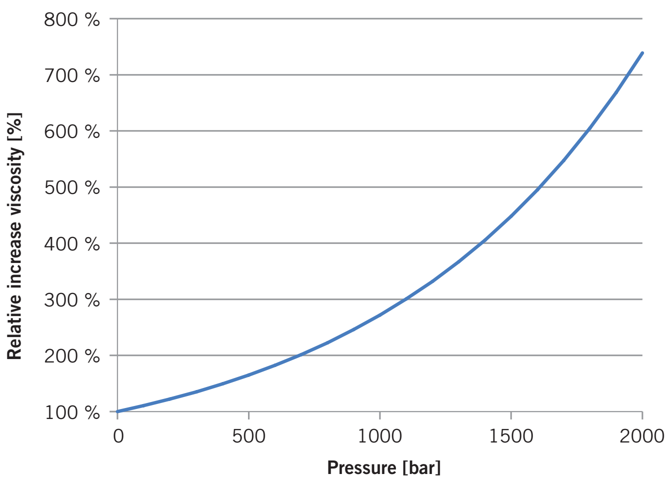

❶ Exemplary illustration of the pressure-dependent viscosity increase relative to the viscosity at 0 bar, which is defined as a 100 %

in which the data needed for this model was calculated suitably from the measured surface roughness of the used bearing shells.

Furthermore, it is crucial to depict the actual contour of the bearing shell in the simulation. For this purpose, the wear depth of the bearing shells was measured after respective test runs and employed as surface profiles for the simulation.

Moreover, to measure the frictions losses for the test runs which were conducted, the development of a method became necessary to map the numerous measured temperatures on a constant oil-temperature suitable for the simulation. The method is illustrated in detail in [1].

VALIDATION

The journal bearing testing rig LP06 of the Miba Gleitlager GmbH was used to calculate the friction power losses in the journal bearings. As illustrated in ❷, the test-rig consists of an electric drive with journal, torque sensor, two journal bearings as support and the actual test bearing which is hydraulically loaded with dynamic loads up to 193 kN (corresponds to a specific bearing load of 75 MPa). In the following, the validation was conducted for single grade lubricants of the viscosity grades SAE40/SAE30/SAE20/SAE10 (rheological data in ❸), as well as for bearing dimensions common for heavy duty vehicles (76 mm diameter and 34 mm width). An adaptation of the simulation model is effortlessly applicable for passenger cars and their common multi grade lubricants if the shear dependency of the lubricant viscosity is specified.

The simulation results are juxtaposed for direct comparison with the measurement data from the test-rig in ❹. As shown, the results cover a large range of operating conditions from pure hydrodynamic lubrication for high journal speeds and low loads when lubricating with high viscosity oils, to emergent mixed lubrication for low speeds and high loads when lubricating with low viscosity oils.

As demonstrated by the illustration, the congruence between simulation and measurement, both for the various revolutions per minute and loads is excellent and ranges within the measurement accuracy of the test-rig, with a single exception that is, however, still close to the error bar.

Especially in order to analyse the occurring metal-metal contact in the mixed lubrication, a bearing durability test was conducted on the test-rig through which, under even more severe conditions, the emerging metal-metal contact was measured by contact voltage measurements between journal and test bearing. This test was also calculated with the simulation method presented here and the metal-metal contact predicted through the simulation is juxtaposed to the contact voltage measurement in ❺. As shown in the figure, metal-metal contact occurs throughout significant parts of the dynamic load which is also closely predicted by the simulation.

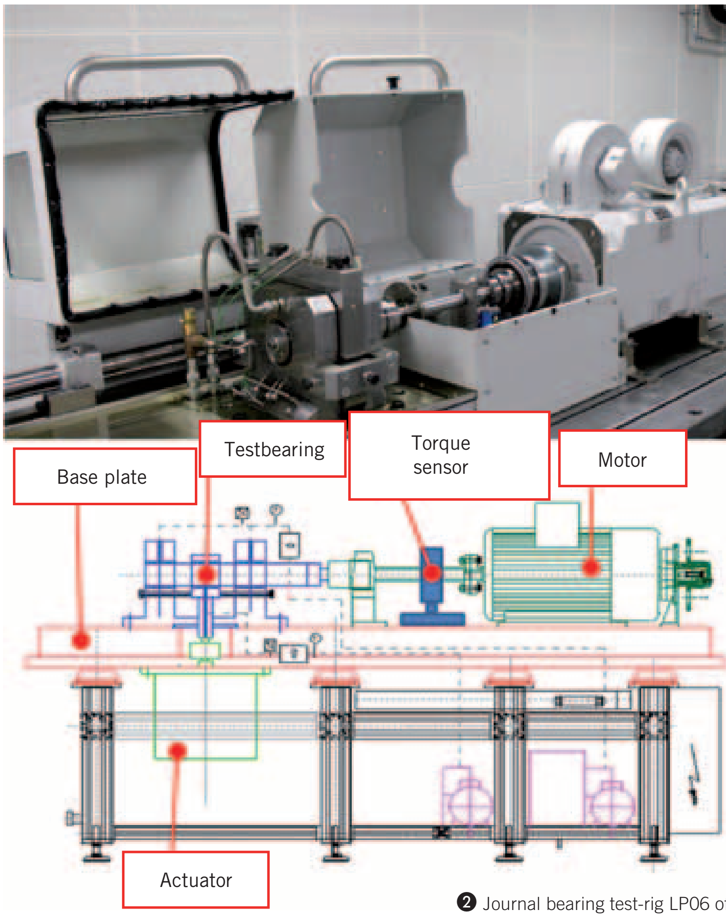

❷ Journal bearing test-rig LP06 of Miba Gleitlager

DESIGNATION	SAE10	SAE20	SAE30	SAE40
V_{40} [mPas]	21.4	50.1	78.8	121.7
V_{100} [mPas]	4.1	6.8	9.0	11.9
DENSITY [kg/m³]	835.5	862.5	869.2	874.3

❸ Rheological data of the lubricants

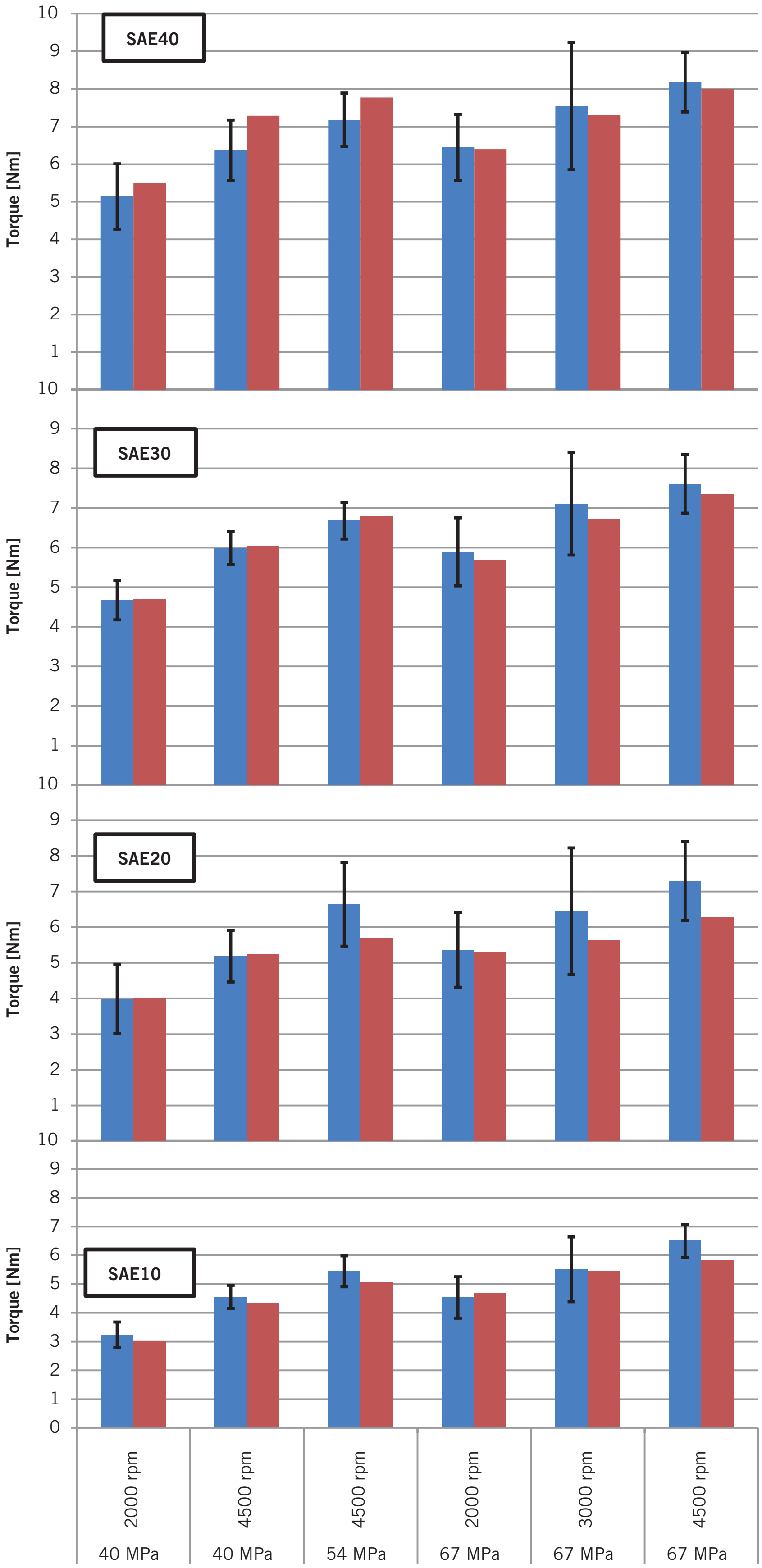

❹ Comparison of the friction torque, measured on the test-rig, conjointly with the measurement precision (illustrated in blue with black error bars) with the results of the simulation (illustrated in red) for the various number of shaft speeds (2000/3000/4500 rpm) and different loads (40/54/67 MPa)

Thus, a simulation method becomes available which is validated in many aspects and consequently allows for an analysis of various means of friction reduction in passenger car engines for efficiency.

FRICTION OPTIMISED JOURNAL BEARING DIMENSIONING FOR A PASSENGER CAR ENGINE

In the following, the potential for friction reduction in the journal bearings of the crank train shall be analysed for a modern four-cylinder passenger car turbodiesel engine lubricated with common multi grade oils. In particular, Styrene-Isoprene-Copolymer (SICP)-additive enhanced oils are considered in the following (in terms of shear rate dependency of the lubricant). For all variants, the friction will be calculated as sum of all five crankshaft main bearings and four big end bearings at full-load operation with a peak cylinder pressure of 190 bar, which leads to specific bearing loads of up to about 50 MPa for the main bearings and to about 90 MPa for the big end bearings. Further, the dynamic oil supply for the big end bearings is realistically represented in the simulation as oil supply network.

In the following basic example, easily modifiable parameters such as bearing shell width and viscosity grade (SAE-class) of the engine oil are focused on. The savings potential derived from the reduction of the bearing shell width is set with the reduction of the oil-filled volume and the use of low viscosity oils directly influences the viscosity losses. Both measures reduce the load capacity of the bearings and therefore it is crucial to identify occurring mixed lubrication to find a low friction solution which does not impair the bearing lifetime through emerging mixed lubrication.

To illustrate the influence of the bearing shell width on the friction losses, widths of 21 mm and 16 mm are studied in addition to the original width of 18 mm. Further, the original lubricant-grade 10W40 is compared to 0W30 and for a specific case to 0W20. Two different oil temperatures are considered in the simulation because in everyday life not only warm engine conditions exist but also low oil temperatures occur specifically with low exterior temperatures or for short driving dis-

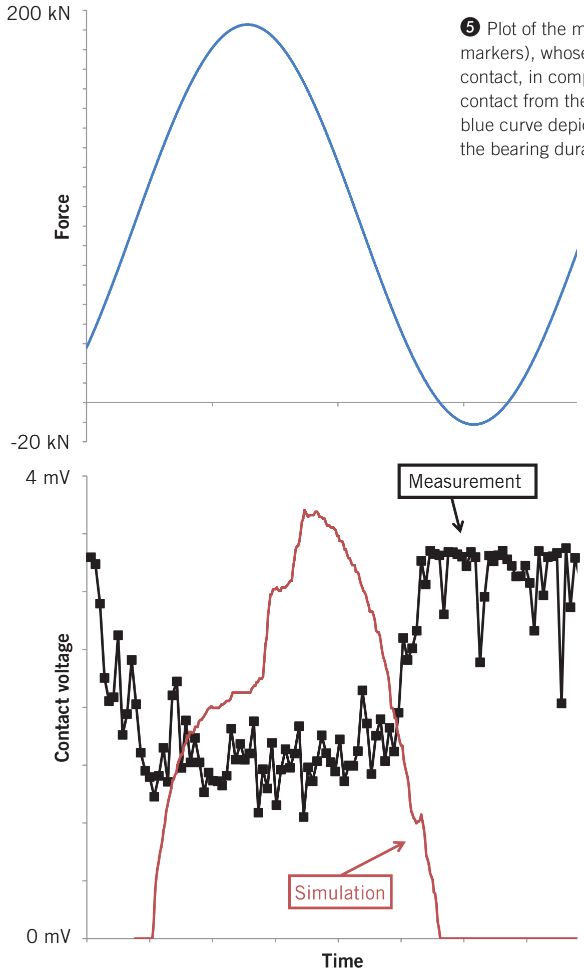

❺ Plot of the measured contact voltage (black markers), whose decrease signals a metal-metal contact, in comparison to the predicted metal-metal contact from the simulation (red line); on top the blue curve depicts the applied load as reference for the bearing durability test

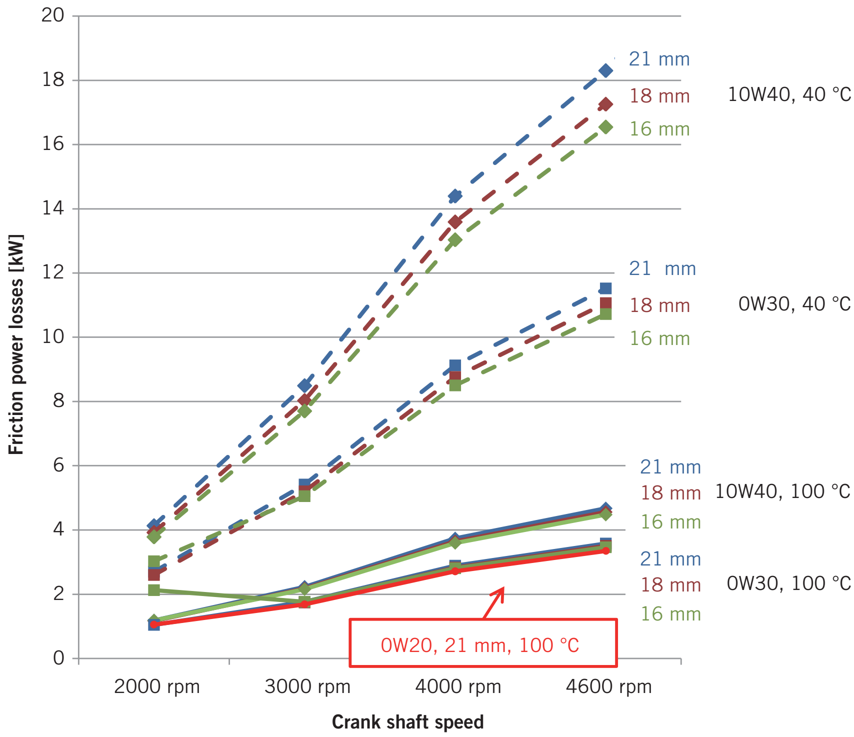

❻ Friction power losses in the journal bearings at various speeds for different bearing shell widths, lubricant viscosity grades and operating temperatures

tances. For the warm engine operation 100 °C and for the cool operation 40 °C oil temperature is considered.

❻ shows the summary of all results evaluated through the total friction power losses for all journal bearings at different speeds.

Most notable from the results is that the oil temperature impacts the friction performance most intensely which is taken advantage of by many modern engines through a reduction of the oil volume in the oil sump and the related quicker warming-up of the engine. In particular, the friction power losses are cut in half throughout the entire speed range by increasing the lubricant temperature from 40 to 100 °C.

Furthermore, it is shown that the different oil viscosities have a much stronger effect than the changes in bearing width. Referring to the example a savings potential is found to be in average 35 % for the cold and still 20 % for the hot case through changing from 10W40 to 0W30. In contrast, using more narrow bearings leads to a reduction of the losses by 9 % for the cold case and at high speeds, but yields only a reduction of maximum 3 % of the total journal bearing losses for the studied hot lubricant temperature. This minimal impact can be employed to use even lower viscosity oil for the engine and – while the load carrying capacity by utilising wider bearings needs to be restored for this lubricant – a net reduction of friction power losses can be achieved.

⑥ also shows how the presented method assists in identifying potential issues with mixed lubrication: for the case of a 16 mm wide bearing and lubrication with 0W30 there occurs for a lubricant temperature of 100 °C already significant metal-metal contact at 2000 rpm which leads to a significant rise in friction for this engine and potentially to problems in the operating reliability. However, with an enlarged bearing width even lower viscosity oil can be used; for the case presented the optimum is a low viscosity 0W20 oil combined with a broader bearing shell, in this case 21 mm. Thereby, in comparison to the original configuration with 18 mm bearings and 10W40 oil, the journal bearing losses can be reduced by 10 % at 2000 rpm and by approximately 30 % at 4600 rpm despite the significantly wider bearing shells.

CONCLUSION

The results show that small changes in the bearing geometry bear no significant impact on the friction losses in the journal bearings. However, the use of a low viscosity lubricant holds obvious advantages in regards to a reduction of these losses, despite the need of wider bearings for the maintenance of the bearing load capacity. In the reviewed example this combination of, ideally, low viscosity lubricants with wider bearings for the maintenance of the load capacity revealed itself as optimal and proves approximately 10 to 30 % decreased losses in comparison to the initial situation. Alternatively, if more complex in design, the increase in size of the journal bearing diameter and the therefore necessary larger journal diameter brings advantages also in regards to the NVH performance due to the increased stiffness of the crankshaft. Further measures for friction reduction like a load dependant oil supply could potentially also attain significant savings and be analysed through the presented model.

While this basic example of friction reduction in engines displays the efficiency of various measures, it is important to emphasise that the choice of the optimum lubricant affects the whole engine and the other major source of mechanical losses, namely the piston assembly, challenges with (partly) opposing requirements to the lubricant. In this sense, the optimum choice of the lubricant in terms of friction reduction shall only be taken under consideration of the complete system.

REFERENCE

[1] Allmaier, H.; Priestner, C.; Six, C.; Priebsch, H.H.; Forstner, C; Novotny-Farkas, F.: Predicting friction reliably and accurately in journal bearings – a systematic validation of simulation results with experimental measurements. In: Tribology International 44 (2011), pp. 1151 – 1160

THANKS

The authors acknowledge the financial support of the Comet K2 - Competence Centers for Excellent Technologies Program of the Austrian Federal Ministry for Transport, Innovation and Technology (BMVIT), the Austrian Federal Ministry of Economy, Family and Youth (BMWFJ), the Austrian Research Promotion Agency (FFG), the Province of Styria and the Styrian Business Promotion Agency (SFG).

OPPOSED-PISTON OPPOSED-CYLINDER ENGINE FOR HEAVY-DUTY TRUCKS

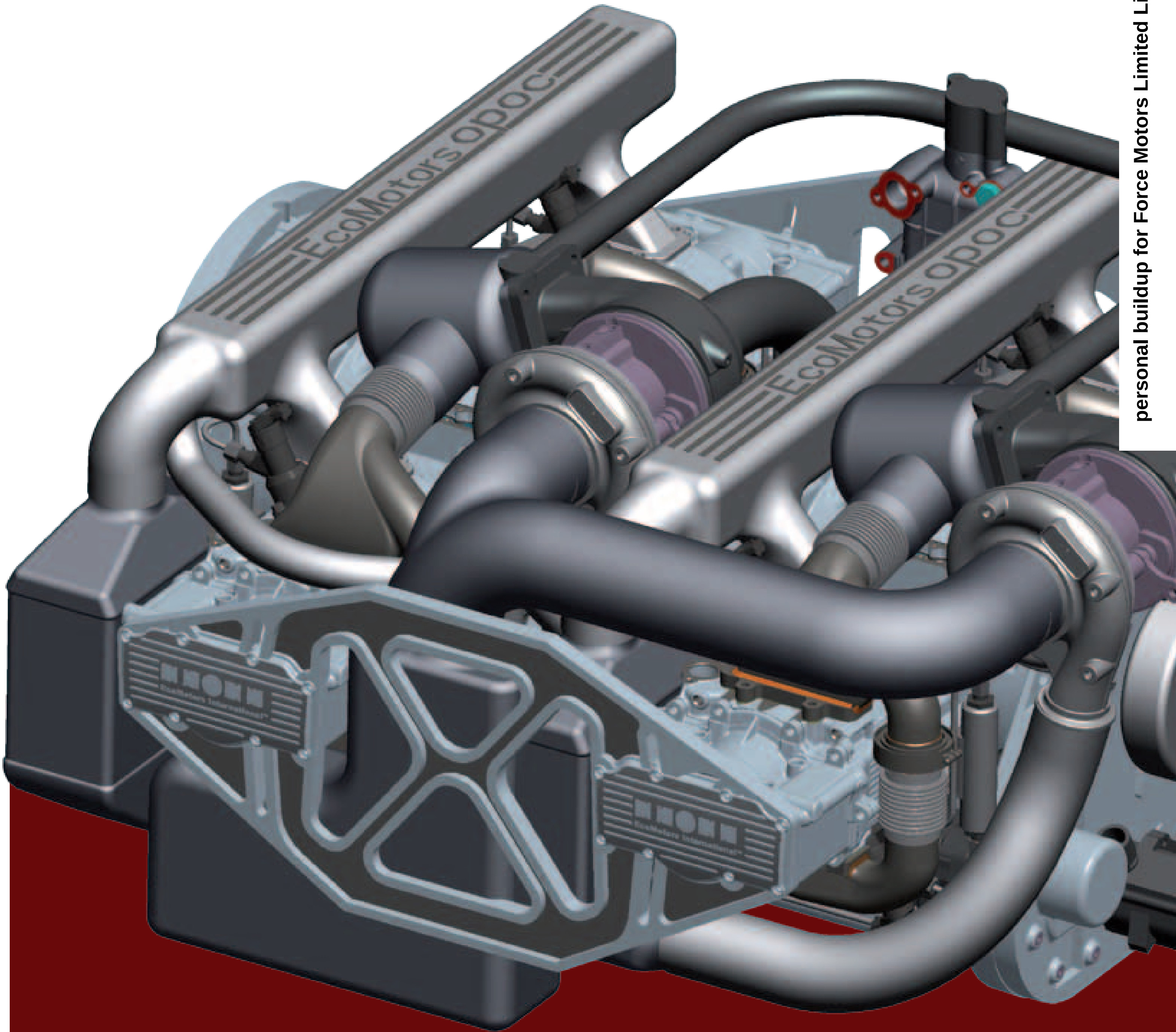

With its opposed-piston opposed-cylinder engine, EcoMotors is for the first time combining the advantages of the two-stroke principle – especially with regard to its compact design and its cost benefits – with compliance with future exhaust emissions standards. The design is based on independently operating two-cylinder modules that can be coupled together depending on the load to produce a four-cylinder unit with a power output of 360 kW.

AUTHORS

PROF. DR.-ING. PETER HOFBAUER
is Founder and Chief Technical Officer of EcoMotors International in Allen Park, Michigan (USA).

DR. DIANA D. BREHOB
is Chief IP Counsel at EcoMotors International in Allen Park, Michigan (USA).

THE CONCEPT

EcoMotors has been developing an opposed-piston opposed-cylinder engine for heavy-duty commercial trucks since 2008, ❶, [1-5]. The main development objective is to meet EPA mandated 2010 emissions and beyond. Although the engine is not yet production ready, tests conducted by independent, external engineering contractors show low fuel consumption and emissions, indicating that target levels are already achievable with a SCR (Selective Catalytic Reduction). The goal of ongoing development, however, is to meet the EPA standards of 0.2 g/kWh NO_x without SCR. According to a consultant's production plan, investment and production costs will be lower than for a conventional engine.

The new engine, called "OPOC" (for opposed pistons opposed cylinder", has only one central crankshaft located between opposed cylinders in which a pair of opposed pistons are working. It consists of two identical modules, ❷, each with two cylinders. One module has a power output of 180 kW. Two modules with a rated output of 360 kW are coupled by an electronically controlled clutch (ECC). To create a fully balanced crank train and also enable asymmetrical port timing for the direct gas exchange, the intake and exhaust pistons are asymmetrically arranged.

The inner pistons are coupled to the crankshaft with conventional pushrods, while the outer pistons are coupled to the crankshaft by a pair of pullrods. Because the pullrods are in tension over almost all conditions, they can be very slender without buckling concerns. The pullrods extend beyond the piston skirt and couple with the piston via a bridge. The bridge has flat bearing surfaces contained between and riding upon bronze-based linear bearings affixed to the block.

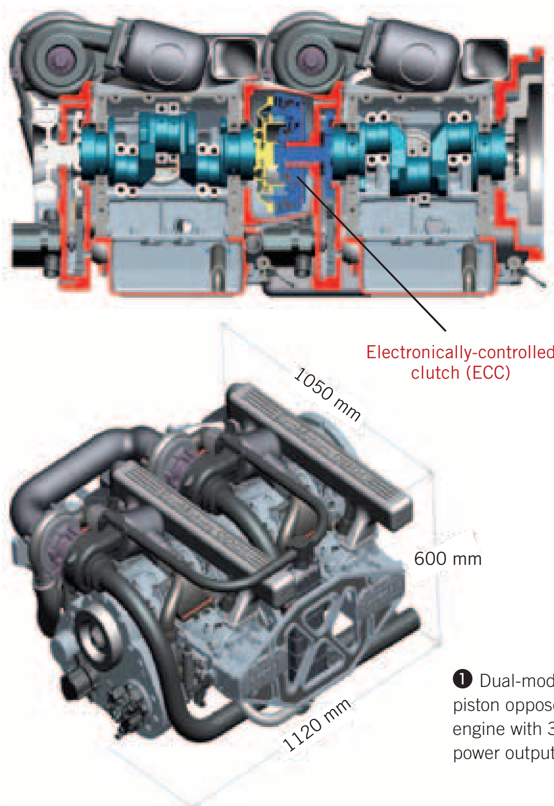

❶ Dual-module opposed-piston opposed-cylinder engine with 360 kW nominal power output

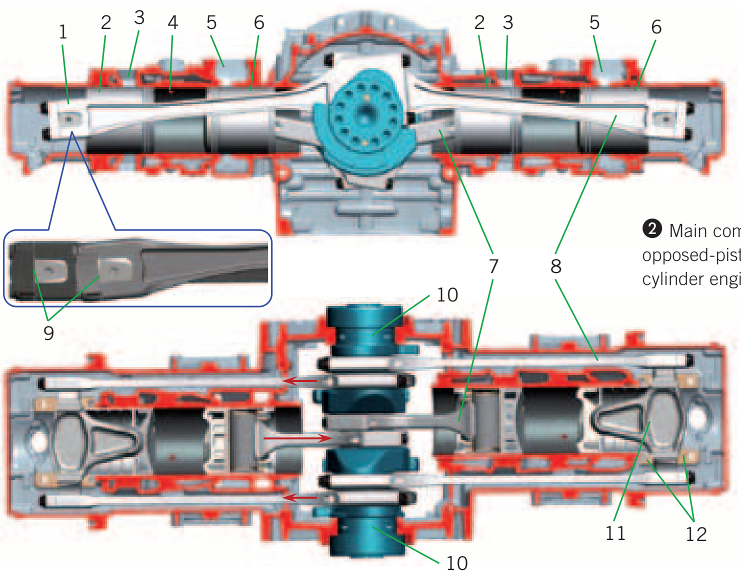

❷ Main components of the opposed-piston opposed-cylinder engine

1 – Rocking joint
2 – Exhaust piston
3 – Exhaust port
4 – Injector port
5 – Intake port
6 – Intake piston
7 – Pushrod
8 – Pullrod
9 – Rocking bearing
10 – Main bearing
11 – Guided bridge
12 – Linear bearing

DIMENSIONS	UNIT	
BORE	mm	100
STROKE, INNER PISTON	mm	90
STROKE, OUTER PISTON	mm	70
PHASE ANGLE	°	21
EFFECTIVE EXPANSION STROKE	mm	102.9
EFFECTIVE COMPRESSION STROKE	mm	91.6
NUMBER OF CYLINDERS		4
TOTAL DISPLACEMENT	l	5
TOTAL EFFECTIVE DISPLACEMENT	l	2.88
ENGINE HEIGHT	mm	600
ENGINE LENGTH	mm	1120
ENGINE WIDTH	mm	1050

MEASURED RESULTS AND GOALS		DYNAMOMETER	GOALS	
		NOV. 2011	SOP[1]	POTENTIAL[2]
RATED POWER	kW	450	360	450
@ ENGINE SPEED	rpm	3500	3200	3200
MAX. TORQUE	Nm	1600	1250	1600
@ ENGINE SPEED	rpm	2100	2200	2100
ENGINE WEIGHT[3]	kg	612	480	400
NO_x EMISSIONS[4]	g/kWh	3.25	1.0	0.2
SOOT EMISSIONS[4]	FSN	1.25	0.6	0.3
BEST BSFC	g/kWh	204	190	180

1 – Start of Production (engine out emissions)
2 – No SCR, optimised use of EGR
3 – Weight includes compacted graphite iron (CGI) crankcase and cylinder block, electronically-controlled clutch, the electronically-controlled turbochargers, and power control units
4 – Weighted number from the 13-mode test shown in ④

❸ Main engine parameters and test results

Due to the crankshaft having split journals offset by 21° CA, the exhaust piston precedes the intake piston in travel to the extreme limits. The exhausts ports open prior to the intake ports opening. This creates a blow down to the turbine of the electronically controlled turbocharger (ECT). The exhaust ports close prior to the intake ports closing, which enables boosting without losing air through the exhaust ports.

A great advantage of the new architecture over prior opposed-piston (OP) engines, for example the Junkers engine, is the single crankshaft which operates two cylinders. Prior OP engines needed two crankshafts for only one cylinder. These crankshafts have to be coupled with a heavy gear train. Main bearing forces of the new engine are less than one tenth of conventional diesel or OP engines of comparable performance [2], which required a main bearing for each cylinder. As the forces from the two pistons act in opposite directions, the resultant force is almost zero. Thus, the entire engine needs only two main bearings with almost no load, which can be smaller in diameter, thereby reducing engine friction.

❸ shows the parameters and targets for a truck engine on which the new application is based. A moderate rated engine speed and mean piston speed have been chosen for initial production.

OP engines can be operated as two-stroke engines at almost twice the engine speed as a conventional engine of the same total stroke. The direct gas exchange of the engine delivers an expansion stroke every revolution in each cylinder, providing a thermodynamic cycle frequency and thereby the power density almost four times that of a conventional engine. Because there are almost no forces on the main bearings, the crankcase can be very lightweight compared to prior OP engines.

Despite the intake and exhaust crank throws being offset by 21° CA, each engine module can be fully balanced. This is not possible with former OP engines. The reciprocating mass of the inner pistons, which includes translatory components of the connecting rods, is less than the reciprocating mass of the outer pistons, partially due to the long pullrods and the bridges associated with the outer pistons. The OPOC module is fully balanced by ensuring $r1*m1 = r2*m2$, where $r1 =$ 45 mm and $r2 =$ 35 mm are the inner and outer throws,

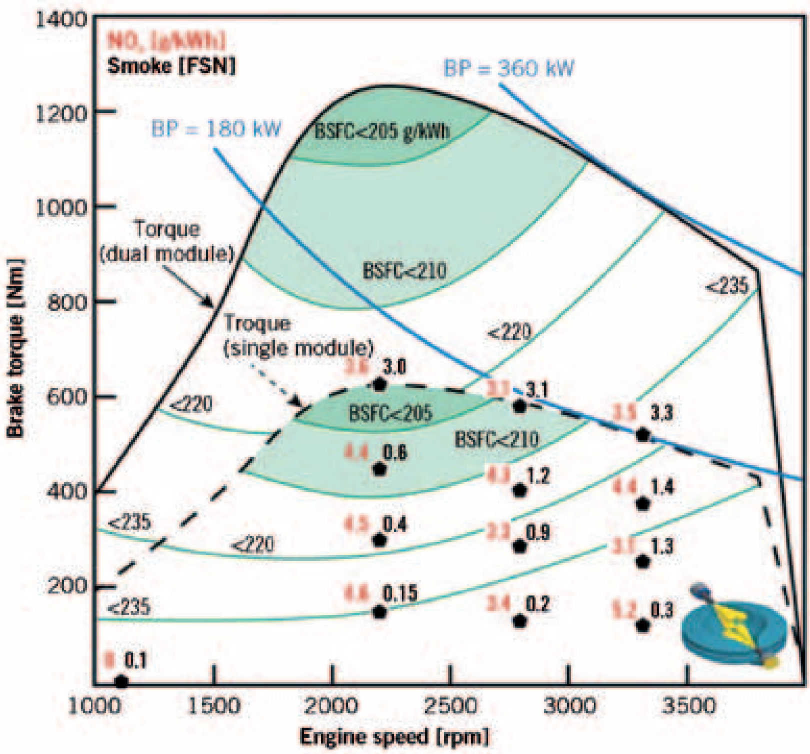

❹ Engine-out emissions of NO_x, soot and fuel consumption (measured)

respectively, and *m1* and *m2* are the corresponding, adjusted reciprocating masses.

Because the side forces created by the outer conrods are very small, the outer piston bridge is guided with crosshead-type linear bearings. This eliminates the side forces from acting on the piston skirt.

A classic problem in two-stroke engines is friction at the piston pin because the forces always acting in the same direction prevent oil from entering between the bearing surface and the pin. In the rocking joint, ②, there is no relative motion between the rocking surfaces, thereby eliminating friction. If the radius of curvature is selected to ensure that the pressure at the contact point is less than the Hertzian pressure, wear is prevented.

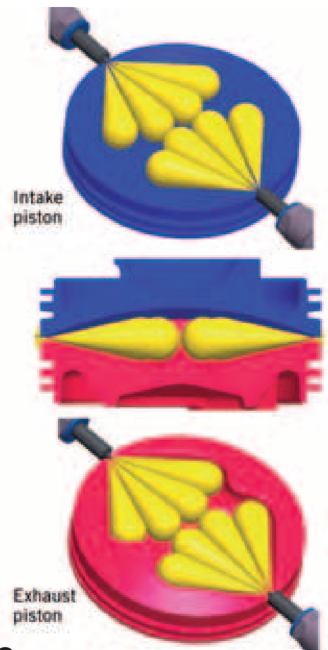

❺ Butterfly combustion chamber

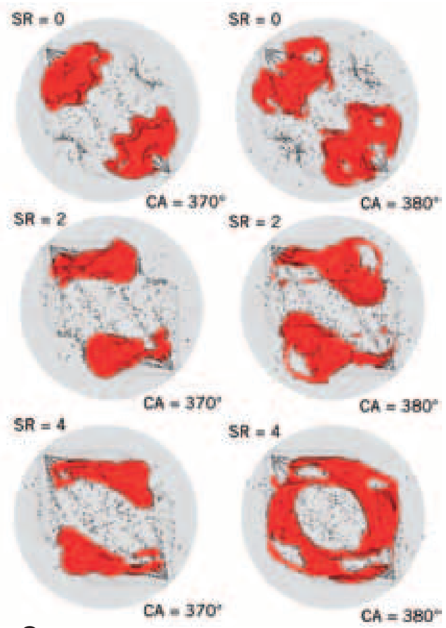

❻ Simulation of flame propagation

EMISSIONS, FUEL ECONOMY AND POWER

Results from a 180 kW module in the 13-mode US test are shown in ❹ under the dashed torque curve. Due to the coupling of two modules, two low BSFC sweet spots are available, which, when combined, cover about 60 % of the torque range under the dual-module curve at 2200 rpm. Flexibility in using one or two modules presents great opportunity for fuel economy improvement.

The concept offers additional potential to reduce fuel consumption:

: reducing friction even further to the level of the architecture's potential (about half that of a conventional engine)
: increasing the compression ratio to exploit the lower inherent friction of the engine
: accelerating the heat release (high peak pressures are possible)
: improving the direct gas exchange by tuning the gas dynamics with the result of lower electrical power consumption for the ECT in critical regions of the engine map and higher waste heat recovery with the ECT in other regions of the engine map.

Initial weighted, 13-mode emission results indicate that EPA standards can be met with a simplified, cost-effective SCR system. The goal is to avoid SCR by refinement of the combustion system and, for example, by judicious use of EGR.

COMBUSTION SIMULATION

Combustion system design and optimisation were conducted using the 3D CFD code "KIVA-3V" [6, 7]. Physics-based submodels were developed to improve numerical coupling of the liquid and gas phases, spray atomisation and spray vaporisation, as well as to account for liquid distortion during travel. The dynamic mesh algorithm was modified to handle movement of both intake and exhaust pistons.

The combustion simulation includes the cylinder and intake and exhaust geometry, so that the gas scavenging process determines the in-cylinder swirl and residual

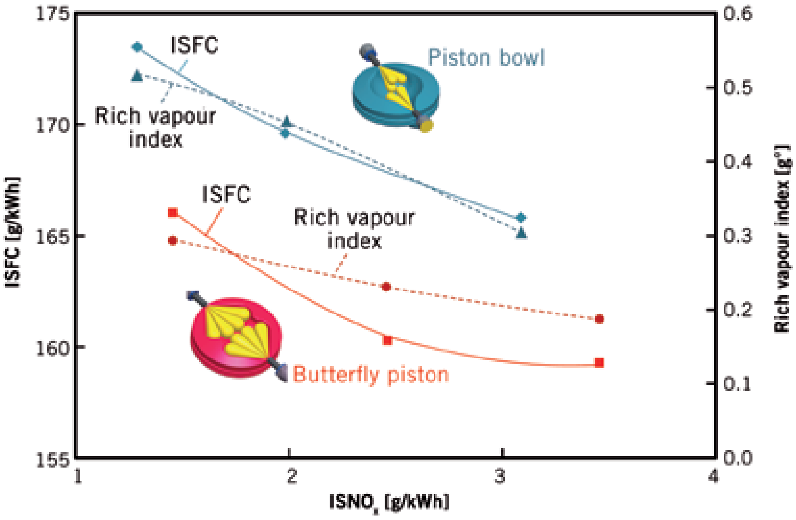

❼ Comparison of a piston-bowl and butterfly combustion chamber

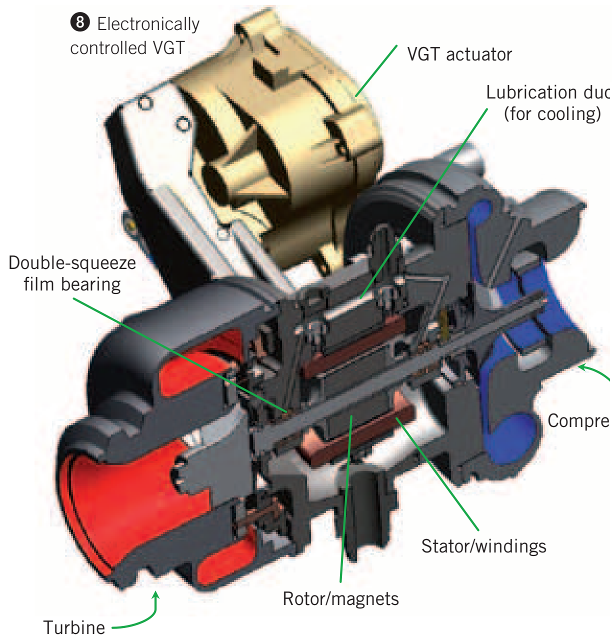

❽ Electronically controlled VGT

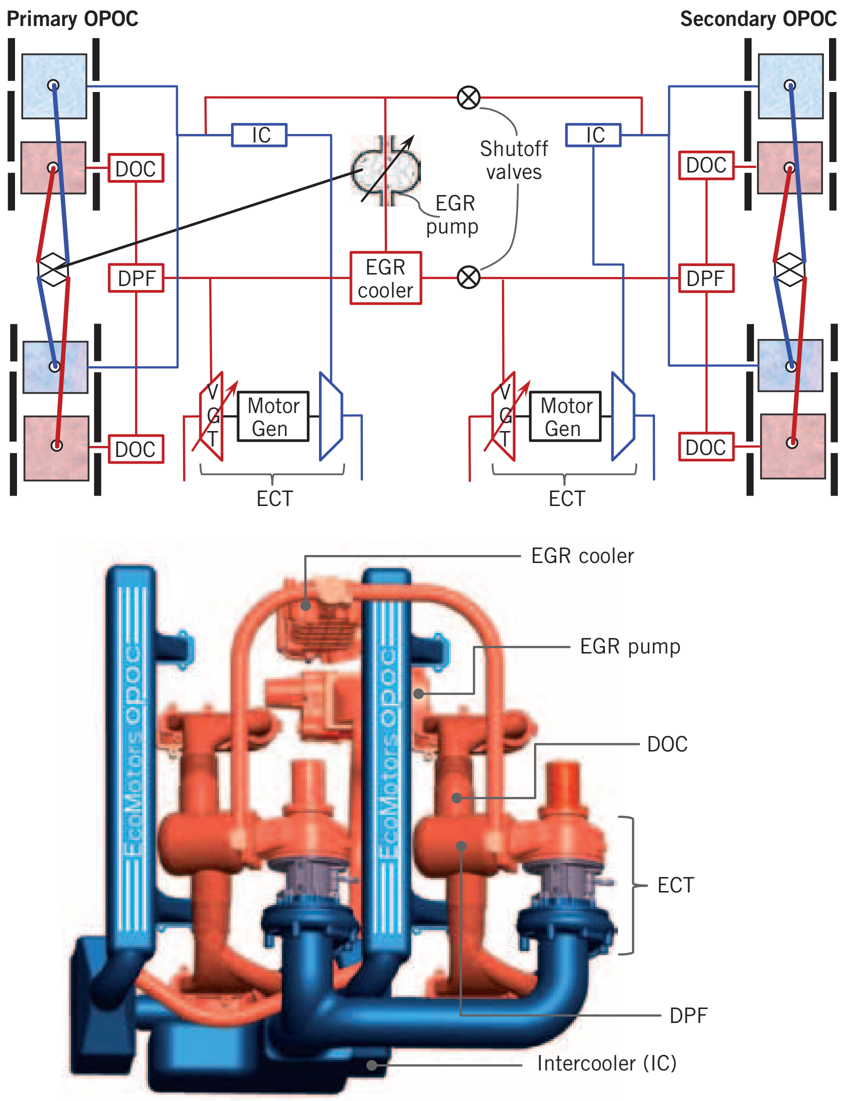

❾ The gas exchange system is said to achieve NO_x emissions of below 0.2 g/kWh

distribution. ISFC is calculated based on simulated in-cylinder pressure and injected fuel amount.

NO_x is based on an extended reaction-kinetic set of Zeldovich differential equations. Rich vapour index is used in the present work as a proxy for soot, as there are insufficient soot data to validate the soot model.

Opposed-piston engines use side-mounted injectors. Side injection presents challenges and promising opportunities in mixing and air utilisation, which affect combustion efficiency and emissions.

A new piston design, shown in ❺, has a large squish area and two fan-shaped bowls in the pistons that together form a butterfly shape. The two protuberances that extend inwardly into the combustion chamber at about 90° offset from the injectors act to disrupt the swirl flow and push the combusting gases into the centre of the cylinder.

❻ shows the simulated flame development for the chamber at swirl ratios (SR) of 0, 2 and 4. With no swirl, the combusting plumes do not progress from the initial region of ignition near the injector through the chamber sufficiently by CA = 380°. At SR = 4, the combusting plumes overlap to encircle the chamber by CA = 380°. But, SR = 4 is clearly too high as a large volume of gases in the centre are untouched by the combusting plume. SR = 2, in contrast, provides displacement of the combusting plume from the injectors. And, interaction of the plume with the protuberance pushes the plume toward the centre of the chamber.

Simulated performance comparisons of two piston/injector designs with optimised swirl are plotted in ❼. ISFC and rich vapour index are plotted as a function of $ISNO_x$ resulting from injection timing sweeps.

SCAVENGING

Non-crankcase scavenged two-stroke engines present scavenging challenges, such as providing sufficient start-up boost and operating boost by a single system. In the new engine concept, at low enthalpy conditions, such as at start, the electric machine of the ECT supplements exhaust enthalpy to drive the compressor. As exhaust energy increases, the turbine contributes more to drive the compressor. In lieu of a wastegate, the electric machine acts as a generator by loading the shaft and applies power to the crankshaft or battery through a bi-directional alternator. A Variable Geometry Turbine (VGT) increases the effective range of the ECT to allow the ECT to operate more efficiently.

The ECT, ❽, is a mechatronic-compound machine with a redesigned centre bearing housing encapsulating an electric machine mounted directly on the shaft between the compressor and turbine sections of a turbocharger. The electric machine in the ECT is a motor/generator that can add/subtract torque to/from the turbocharger shaft to supplement/absorb exhaust enthalpy. To create the increased boost, the overwhelming majority of the desired energy is absorbed from the exhaust and not provided by the electric motor. Therefore, a 5 kW motor/generator is sufficient for the 180 kW engine module for an unlimited duration.

The shaft bearing system uses turbocharger double-squeeze film bearings on either side of the electric machine and a thrust bearing to support radial and axial loads. The specialised cooling system ensures adequate heat rejection of the stator assembly over the entire operating range and reduces localised hot spots to avoid oil coking and varnish build-up. A majority of the ECT is comprised of conventional turbocharger parts including VGTs, but with a longer shaft to accommodate the new centre housing with the electric machine.

As the effectiveness of the turbine relates to the pressure ratio (PR) across the turbine, decreasing downstream restriction has a greater effect on PR than upstream restriction. It has been simulated and validated that placing the Diesel Oxidation Catalyst (DOC) and Diesel Particulate Filter (DPF), ❾, upstream of the turbine is highly effective because the PR is improved and catalytic reactions increase exhaust enthalpy. Potential for catalyst substrate flaking off and passing through the turbine is largely mitigated by advancements in metal substrates. Modern exhaust aftertreatment systems can tolerate temperature 950 °C and below.

Two-stroke scavenging relies on a higher intake pressure than exhaust. A small positive-displacement blower drives EGR to meet NO_x requirements. A high-pressure loop EGR system is used to reduce the EGR pumping losses and to prevent corrosion-inducing compounds from passing through the compressor. A shared EGR system addressing component redundancy drives up to 50 % EGR to a single engine or 25 % EGR during tandem operation.

The scavenging simulation, ❿, shows some backflow from the cylinder into the intake belt at intake port opening (145° CA). Such backflow could be overcome by re-

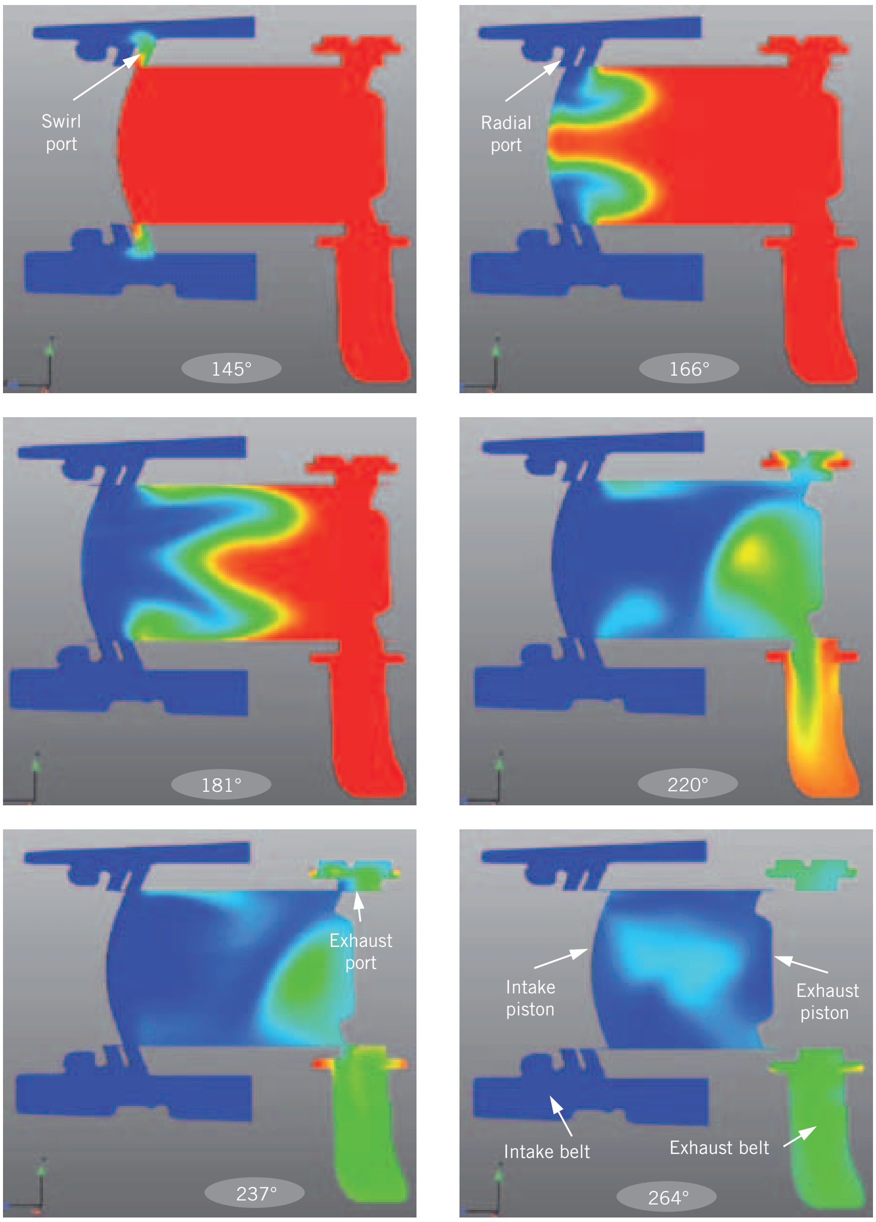

❿ Gas exchange simulation

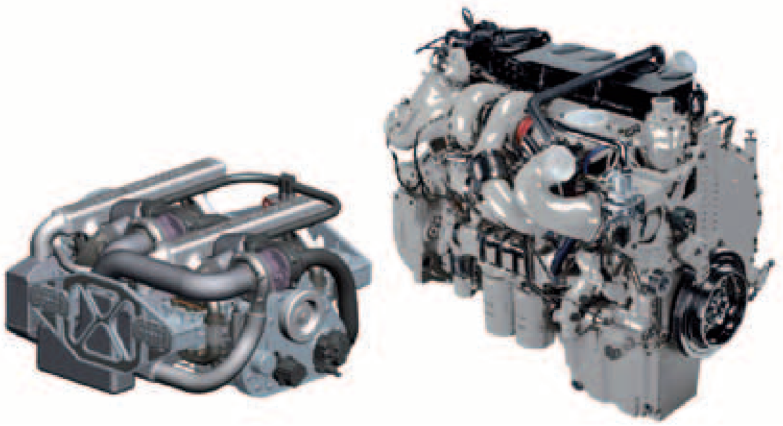

	TORQUE		ADVANTAGES OF OPPOSED-PISTON OPPOSED-CYLINDER ENGINE VS. INLINE ENGINE
	50 %	100 %	
PISTON RINGS	6.6 %	3.1 %	Smaller bore diameter (100 vs. 126 mm); lower bore distortion; lower piston speed
PISTON SKIRTS	1.1 %	0.7 %	Lower side forces
PISTON PINS	-0.4 %	-0.7 %	
MAIN BEARINGS	2.4 %	2.6 %	2 bearings (50 % torque) or 4 bearings (100 % torque) vs. 7; very low forces
JOURNAL BEARINGS	-0.7 %	-1.8 %	
VALVETRAIN	1.6 %	1.3 %	No valvetrain
TOTAL	10.6 %	5.2 %	

⓫ Influence of friction on fuel consumption

ducing port height, but would negatively impact air delivery at high speed. Intake swirl ports impart a tangential angle to the incoming flow to promote swirl. The centrifugal force of the swirl flow displaces combusted gases at the periphery of the chamber (166° CA). Incoming flow also has a component directed along the intake bowl that displaces combustion gases at the centre of the chamber (181° CA). This component of flow has little effect at 166° CA, but strongly impacts the flow by 181° CA. The goal is to optimise the green mixed area between the fresh and exhaust gas as a flat, narrow zone perpendicular to the axis of the liner. Some leakage of fresh charge is seen at snapshots 220° CA and 237° CA. At port closure, 264° CA, some residuals (shown in green) localised in the centre of the chamber are trapped and some fresh air has short circuited the cylinder as evidenced by green in the exhaust belt.

Finding the optimal balance between trapping and scavenging is crucial. An ECT is mandatory to achieve a suitable balance by controlling pressure differential between the intake and exhaust to provide trapping and scavenging efficiencies that approach four-stroke operation.

MODULARITY

The ECC is key to a true modular displacement powertrain. The ECC couples two engine modules to provide torque on demand and cycle fuel economy gains near 30 %. Friction and losses associated with gas exchange are eliminated in a shutoff module at part load. As the single module has fully balanced mass forces, two engines can be coupled in less space than a conventional engine of the same power output.

The ECC has an electronically-controlled friction element to selectively couple one or both modules to the output shaft. The friction element allows "bump-starting" of the non-operating engine to obviate a second starter motor.

The ECC also has a two-position, lockup element to generate a phase angle of 90° between the two modules. This coupling is possible in two opposing positions (in each slip rotation). This produces an even firing order as in a V8.

A bespoke control system manages the ECC and specialised control algorithms dictate operating modes for maximum fuel economy without sacrificing performance or comfort.

CONCLUSION

Initial dynamometer results from a prototype opposed-piston opposed-cylinder engine confirm the engine's expected high power density and low BSFC.

The analysis in ⓫ shows a 10.6 % improvement in fuel consumption due to the reduction in friction alone, compared to a six-cylinder inline engine with the same power output, both measured at 50 % of maximum torque. At maximum torque, the fuel consumption benefit is 5.2 % due to friction reduction alone.

Emissions from an unoptimised combustion system are sufficient to meet applicable emission standards with SCR with the promise to do so without SCR with further development.

REFERENCES

[1] Hofbauer, P.: Internal Combustion Engine with a Single Crankshaft and Having Opposed Cylinders with Opposed Pistons. U.S. Patent 6,170,443, 2001
[2] Hofbauer, P.: Opposed Piston Opposed Cylinder (opoc) Engine for Military Ground Vehicles. In: SAE 2005-04-11-0278, 2005
[3] Peng, L.; Tusinean, A.; Hofbauer, P.; Deylami, K.: Development of a Compact and Efficient Truck APU. In: SAE 2005-01-0653, 2005
[4] Franke, M.; Huang, H.; Liu, J.P.; Adomeit, P.: Opposed Piston Opposed Cylinder (opoc) 450 hp Engine: Performance Development by CAE Simulations and Testing. In: SAE 2006-01-0277, 2006
[5] Tusinean, A.; Huang, H.; Liu, J.P; Kalkstein, J.; Röver, W.; Zhong, L.: Opposed Piston Opposed Cylinder (opoc) 5/10 kW Heavy Fuel Engine for UAVs and APUs. In: SAE 2006-01-0278, 2006
[6] Amsden, A.A.: KIVA-3V, A Block-Structured KIVA Program with Vertical or Canted Valves. In: Los Alamos National Laboratory Report LA-13313-MS, 1997
[7] Amsden, A.A.: KIVA-3V, Release 2: Improvement to KIVA-3V. In: Los Alamos Laboratory Report LA-13608-MS, 1999

THANKS

The authors would like to thank the following EcoMotors employees who contributed to this article: Adrian Tusinean, Tyler Garrard, Yue-Xin Huang, Philipp Seyfried, Huixian Shen, Chou Lee.

PEER REVIEW

PEER REVIEW PROCESS FOR RESEARCH ARTICLES IN ATZ, MTZ AND ATZ ELEKTRONIK

STEERING COMMITTEE

Prof. Dr.-Ing. Lutz Eckstein	RWTH Aachen University	Institut für Kraftfahrzeuge Aachen
Prof. Dipl.-Des. Wolfgang Kraus	HAW Hamburg	Department Fahrzeugtechnik und Flugzeugbau
Prof. Dr.-Ing. Ferit Küçükay	Technische Universität Braunschweig	Institut für Fahrzeugtechnik
Prof. Dr.-Ing. Stefan Pischinger	RWTH Aachen University	Lehrstuhl für Verbrennungskraftmaschinen
Prof. Dr.-Ing. Hans-Christian Reuss	Universität Stuttgart	Institut für Verbrennungs-motoren und Kraftfahrwesen
Prof. Dr.-Ing. Ulrich Spicher	Universität Karlsruhe	Institut für Kolbenmaschinen
Prof. Dr.-Ing. Hans Zellbeck	Technische Universität Dresden	Lehrstuhl für Verbrennungsmotoren

ADVISORY BOARD

Prof. Dr.-Ing. Klaus Augsburg
Prof. Dr.-Ing. Bernard Bäker
Prof. Dr.-Ing. Michael Bargende
Prof. Dipl.-Ing. Dr. techn. Christian Beidl
Dr.-Ing. Christoph Bollig
Prof. Dr. sc. techn. Konstantinos Boulouchos
Prof. Dr. Dr. h.c. Manfred Broy
Prof. Dr.-Ing. Ralph Bruder
Dr. Gerhard Bruner
Prof. Dr. rer. nat. Heiner Bubb
Prof. Dr. rer. nat. habil. Olaf Deutschmann
Dr. techn. Arno Eichberger
Prof. Dr. techn. Helmut Eichlseder
Prof. Dr. Wilfried Eichlseder
Dr.-Ing. Gerald Eifler
Prof. Dr.-Ing. Wolfgang Eifler
Prof. Dr. rer. nat. Frank Gauterin
Prof. Dr. techn. Bernhard Geringer
Prof. Dr.-Ing. Uwe Grebe
Dr. mont. Christoph Guster
Prof. Dr.-Ing. Holger Hanselka
Prof. Dr.-Ing. Horst Harndorf
Prof. Dr. techn. Wolfgang Hirschberg
Univ.-Doz. Dr. techn. Peter Hofmann
Prof. Dr.-Ing. Bernd-Robert Höhn
Prof. Dr. rer. nat. Peter Holstein
Dr. techn. Heidelinde Holzer
Prof. Dr.-Ing. habil. Werner Hufenbach
Prof. Dr.-Ing. Armin Huß
Prof. Dr.- Ing. Roland Kasper
Prof. Dr.-Ing. Tran Quoc Khanh
Dr. Philip Köhn
Prof. Dr.-Ing. Ulrich Konigorski
Dr. Oliver Kröcher
Prof. Dr.-Ing. Peter Krug
Dr. Christian Krüger
Univ.-Ass. Dr. techn. Thomas Lauer
Prof. Dr. rer. nat. Uli Lemmer
Dr. Malte Lewerenz
Prof. Dr.-Ing. Markus Lienkamp
Prof. Dr. rer. nat. habil. Ulrich Maas
Prof. Dr.-Ing. Markus Maurer
Prof. Dr.-Ing. Martin Meywerk
Prof. Dr.-Ing. Klaus D. Müller-Glaser
Dr. techn. Reinhard Mundl
Prof. Dr. rer. nat. Cornelius Neumann
Prof. Dr.-Ing. Peter Pelz
Prof. Dr. techn. Ernst Pucher
Dr. Jochen Rauh
Prof. Dr.-Ing. Konrad Reif
Prof. Dr.-Ing. Stephan Rinderknecht
Dr.-Ing. Swen Schaub
Prof. Dr. sc. nat. Christoph Schierz
Prof. Dr. rer.-nat. Christof Schulz
Prof. Dr. rer. nat. Andy Schürr
Prof. Dr.-Ing. Ulrich Seiffert
Prof. Dr.-Ing. Hermann J. Stadtfeld
Prof. Dr. techn. Hermann Steffan
Prof. Dr.-Ing. Wolfgang Steiger
Prof. Dr.-Ing. Peter Steinberg
Prof. Dr.-Ing. Christoph Stiller
Dr.-Ing. Peter Stommel
Dr.-Ing. Ralph Sundermeier
Prof. Dr.-Ing. Wolfgang Thiemann
Prof. Dr.-Ing. Helmut Tschöke
Dr.-Ing. Pim van der Jagt
Prof. Dr.-Ing. Georg Wachtmeister
Prof. Dr.-Ing. Jochen Wiedemann
Prof. Dr. techn. Andreas Wimmer
Prof Dr. rer. nat. Hermann Winner
Prof. Dr. med. habil. Hartmut Witte

Scientific articles of universities in ATZ Automobiltechnische Zeitschrift, MTZ Motortechnische Zeitschrift and ATZelektronik are subject to a proofing method, the so-called peer review process. Articles accepted by the editors are reviewed by experts from research and industry before publication. For the reader, the peer review process further enhances the quality of the magazines' content on a national and international level. For authors in the institutes, it provides a scientifically recognised publication platform.

In the Peer Review Process, once the editors has received an article, it is reviewed by two experts from the Advisory Board. If these experts do not reach a unanimous agreement, a member of the Steering Committee acts as an arbitrator. Following the experts' recommended corrections and subsequent editing by the author, the article is accepted.

In 2008, the peer review process utilized by ATZ and MTZ was presented by the WKM (Wissenschaftliche Gesellschaft für Kraftfahrzeug- und Motorentechnik e. V./ German Professional Association for Automotive and Motor Engineering) to the DFG (Deutsche Forschungsgemeinschaft/German Research Foundation) for official recognition. ATZelektronik participates in the Peer Review since 2011.

AUTHORS

DR. DIPL.-PHYS. CHRISTIAN GRÜNZWEIG
is Project Manager for Industrial Applications of the Neutron Imaging and Activation Group at the Paul Scherrer Institute (PSI) in Villigen (Switzerland).

DR. DIPL.-FORSTWIRT DAVID MANNES
is Member of the Neutron Imaging and Activation Group at the PSI in Villigen (Switzerland).

DR. DIPL.-ING. ANDERS KAESTNER
is Beam Line Scientist of the Neutron Imaging und Activation Group at the PSI in Villigen (Switzerland).

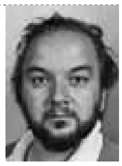

DR. DIPL.-CHEM. MATTHIAS VOGT
is Post-Doc in the Department of Chemistry and Applied Bioscience at ETH Zurich (Switzerland).

VISUALISING THE SOOT AND ASH DISTRIBUTION IN DIESEL PARTICULATE FILTERS USING NEUTRON IMAGING

Neutron tomography is presently the only possibility to obtain information about the three-dimensional distribution of soot and ash in a filter monolith. The estimation of the soot distribution in a diesel particulate filter with neutron imaging is possible because neutrons are highly sensitive to the element hydrogen, which is content of soot. In order to increase the soot contrast and hence increase the probability of soot detection, the Paul Scherrer Institute in collaboration with the ETH Zurich have developed a gadolinium additive that can be directly added to the diesel fuel.

THE SEAL OF APPROVAL FOR SCIENTIFIC ARTICLES IN MTZ.
MTZ
PEER REVIEW
RECEIVED 2011-08-25
REVIEWED 2011-10-24
ACCEPTED 2011-12-12
REVIEWED BY EXPERTS FROM RESEARCH AND INDUSTRY.

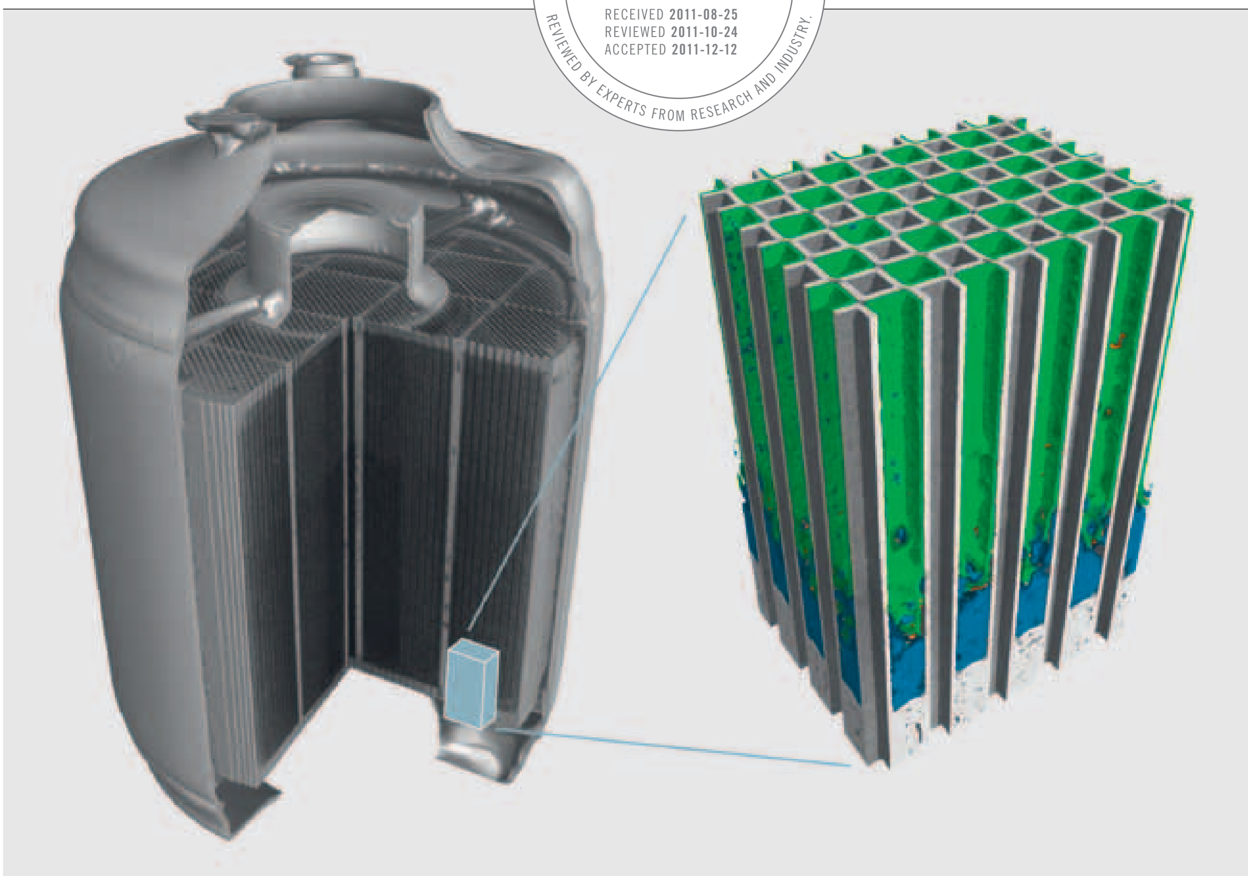

1 INTRODUCTION

Even though diesel particulate filters (DPF) are commonly used, it is still difficult to measure the soot distribution within the filter. Presently, the total amount of soot and ash is only measured by means of simple weighing. X-ray imaging is a conventional non-destructive imaging method mainly used to obtain volumetric information concerning the ash distribution in the filter. The soot distribution can hardly be measured using this method, especially in canned DPFs [1].

The localisation and quantification of soot in DPF is of great interest mainly because of two reasons: Firstly, for answering questions regarding the design and optimisation of filters and flow geometries. Secondly, it can provide experimental proofs regarding the soot deposits and the possibility to validate theoretical simulation. It can therefore serve as a base for the design of new models that describes the loading processes of DPFs.

In this article we present a non-destructive imaging method as an alternative to the X-ray technology. Using neutrons instead of X-ray allows the successful investigation of the soot and ash distributions in DPFs. Herein we discuss our recent results from neutron tomography measurements of a canned diesel particulate filter. The monolith is manufactured from silicon-carbide (diameter of 144 mm (5.66 "); height of 130 mm). The upper third of the monolith, close to the gas inlet, is covered with a catalytic coating. The filter was loaded and regenerated two times, prior the final loading phase. Eventually 32 g soot was deposited in the filter during the last loading.

The soot and the ash in the filter were chemically analysed to determine their elemental composition. Therefore a small amount of soot and ash were recovered from the filter. According to the analysis the soot contained 7.6 % hydrogen. The main components of the ash were calcium (37 %), zinc (19 %), sulfur (15 %), phosphor (8 %), and copper (2 %).

2 NEUTRON IMAGING

2.1 NEUTRON INTERACTION WITH THE DPF COMPONENTS

Unlike X-rays, neutrons are electrically neutral and hence do not interact with the electrons that surround the nucleus. Neutrons only interact with the nucleus; the nature of this interaction can be very different depending on the specific chemical element and the energy of the neutron. Hence, for neutron beams the attenuation is not increasing with an increase in atomic weight, as for X-rays, but is rather element specific. Therefore neutron imaging depicts an excellent complementary or alternative technology to conventional X-ray imaging.

The attenuation of neutrons in matter can be approximately described by Lambert-Beer's law. With the sample composition known from chemical analysis and the material density, it is possible to compute the expected attenuation coefficient of the sample. ❶ shows the comparison of the theoretically expected contrasts for X-ray and for neutrons of the relevant components of the DPF (monolith, ash, and soot) .The calculation employed the element specific parameters for soot and ash derived from the chemical analysis. Because there is no exact information about the density and porosity of soot and ash, this information was neglected and their densities were assumed to be 1 g/cm^3. Therefore, ① depicts the relative attenuation coefficients, Σ_{rel}, arising from the microscopic cross sections weighted by the relative percentage of occurrence of each chemical element. The attenuation coefficient of the steel can is 1.2/cm for neutrons, and 1.6/cm for X-ray.

2.2 NEUTRON TOMOGRAPHY

Tomographic investigations allow acquiring information non-destructively about the material composition and distribution, as well as the inner structure of samples [3]. Further, the tomography (3D) provides a significant advantage over the radiography (2D); namely each voxel (3D pixel) contains information of the local attenuation coefficient. In addition to the structural data it

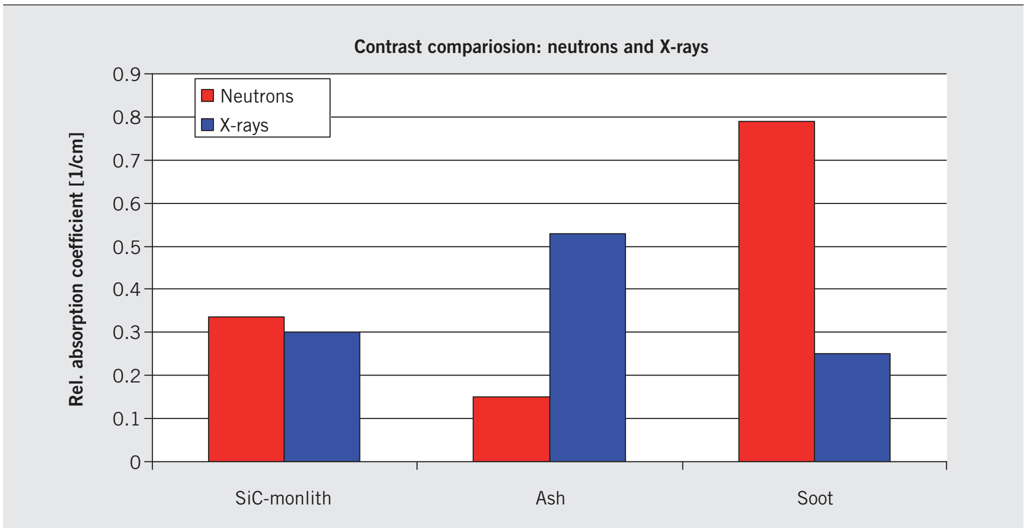

❶ Comparison of the theoretically expected attenuation coefficients of the diesel particulate filter components using neutrons (25 meV) and X-rays (120 keV); the influence of the particle density and porosity are not considered; the different materials such as monolith, ash and soot for neutrons are distinguishable; soot provides the strongest contrast; the absorption behaviour of soot and ash for both types of radiation is diametrical

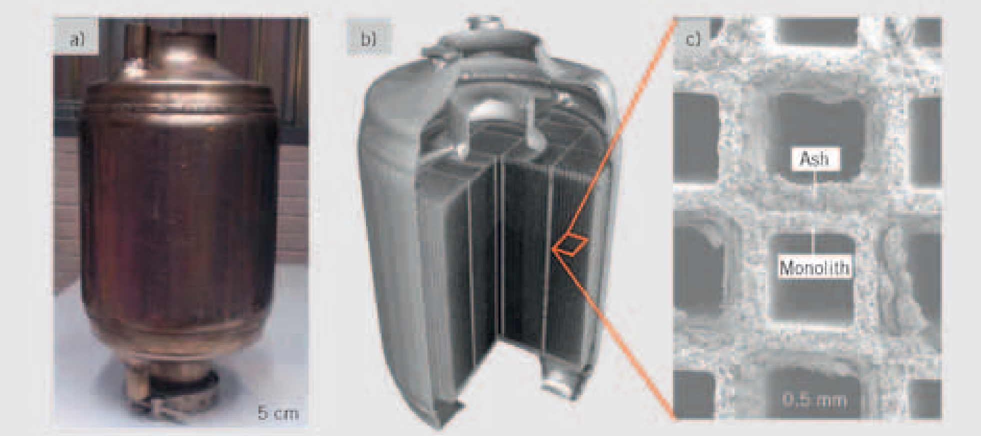

❷ (a) Photograph of the canned DPF; (b) neutron tomography data: the steel jacket is no barrier for neutrons and allows an insight into the loaded monolith; the additional coverage mounted at the inlet side, which protects the central area of the monolith during loading, can be seen; (c) scanning electron micrograph showing the soot layer with a thickness of 250 microns at the filter wall

is therefore possible to locally quantify the sample materials within the limit of the pixel/voxel resolution.

Currently there are 15 equivalent neutron imaging facilities worldwide. Switzerland possesses two of such facilities at the Paul Scherrer Institute: one beam line provides thermal neutrons, Neutra [4], and the other a cold neutron beam, Icon [5]. On both facilities, three different imaging setups for tomographic investigations are available: (i) maxi setup, (ii) midi setup, and (iii) micro setup. The setups differ in the size of the field of view (300 × 300, 150 × 150, and 27 × 27 mm^2) and the resulting pixel resolution 150, 75, and 13.5 µm/px.

3 EXPERIMENTAL RESULTS

3.1 MAXI SETUP

The measurement of the entire canned DPF contains spatially resolved information on the local level of the deposits in the monolith. The overview neutron tomography (NT), with a resolution of 150 µm/px, is shown in ❷. In ② (a) a photo of the DPF can be seen. ② (b) shows a three-dimensional volumetric view of the DPF. One can clearly distinguish the monolith with its individual segments and the filter channels. The special feature of this DPF is the additional mounting of an inlet-sided centric masking, which was installed before the last loading phase. This coverage is blocking partially the exhaust flow onto the monolith. The diameter of the mounting was chosen such that the central segment is completely protected and its surrounding segments were only partially loaded. The outer segments were exposed to the full exhaust stream. For the NT measurement 625 projections over an angular range of 360° were taken with an exposure time of 20 s per projection. ② (c) shows a scanning electron micrograph of a part of an outer segment. The soot layer with a thickness of 250 microns on the filter wall is clearly recognizable.

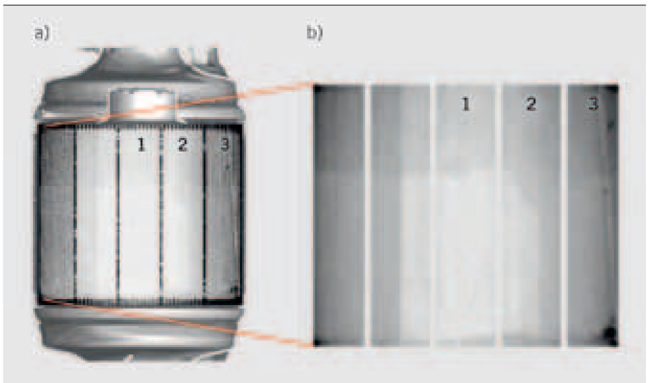

❸ Analysis of the tomography data: (a) vertical, centre section trough the DPF; the outer regions are loaded more abundant (darker) than the inner regions (bright), which are protected by the coverage; (b) Monolith region: for a better representation of the soot deposit, the image was processed by a Gaussian filter, which eliminated the channel structures; clearly visible are the two vertical lines as sharp boundaries between loaded and unloaded filters regions; similarly, a horizontal line is seen in the upper third, which is due to the catalytic zone coating

The procedure for the determination of the local soot and ash deposits is shown in ❸. ③ (a) depicts the local deposit as example of a vertical section through the middle of the filter. For a clearer representation, the monolith section was processed with a Gaussian filter, which eliminates the channel structures, as seen in ③ (b). The darker the areas appear the more abundant is the deposit. Two areas are particularly noticeable: Firstly, a vertically extended region below the coverage running through the whole monolith, which is separated by two clear vertical lines from the rest of the monolith. This area is brighter meaning there is less or no soot and ash deposits. Secondly, a horizontally extended region in the upper third of the filter, which is due to the catalytic zone coating. The upper third of the filter shows over the entire width a stronger contrast than the rest of the filter. A tomography measurement of the unloaded filter prior to the here described experiment has indicated this area before. The trend shows that the outer regions experienced a more abundant loading as expected. Noticeable in ③ (b) is the area below the cover at the bottom of the filter segments. These deposits are ash residues originating from the two regenerations, where the filter was loaded without using of the coverage.

In order to compare the local loading-level in different regions, a mean gray value of the cross-sectional area along the loading direction was calculated for individual segments, ❹. The degree of the loading is shown in an example of three segments: segment 1 (completely covered), segment 2 (partially covered), and segment 3 (not covered). It can be directly seen from the evaluated profiles that the amount of exhaust gas flowing through the filter, increases from the inner to the outer parts. Higher gray values and thus higher attenuation coefficients indicate a larger deposit. Four interesting regions in

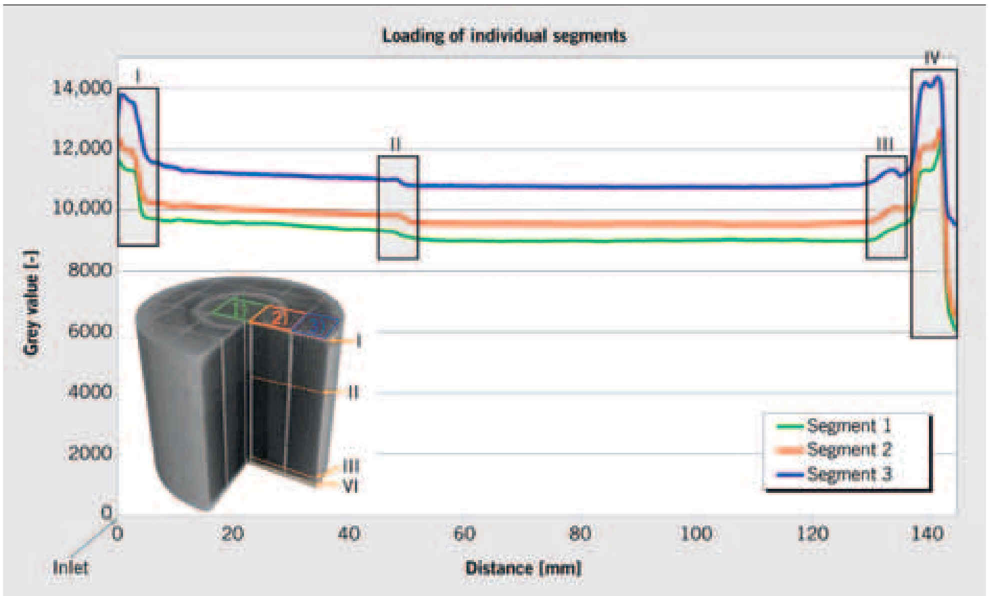

❹ Line profiles along three segments for the loading with the coverage, ③ (a); the higher the gray level, the more abundant the deposit: segment 1 (completely covered), segment 2 (partially covered) and segment 3 (not covered); the gray marked areas are: (I) plugs inlet-sided, (II) transition zone of the catalytic zone coating, (III) ash residues and (IV) plugs outlet-sided

the marked gray areas I – IV are highlighted. These are the plugs on the inlet and outlet regions I and IV. The region II represents the transition zone of the catalytic coating area, which is in all three profiles at the same position and detected as a step. In region III of all segments, an increase of the gray values towards the bottom regions can be seen, which arises from the ash and soot deposits. Moreover, the homogeneity of the deposits can be evaluated from the individual profiles of the particular segments. For instance in the upper third of the filter for all three profiles a certain drop in gray-scale intensity is noticeable suggesting an inhomogeneous loading. However, for the remaining parts of the filter the gray values remain constant.

3.2 MIDI SETUP

For the tomographic investigation of individual segments, the DPF had to be mechanically disassembled. A segment from the outer region, as seen in ③, the segment 3, was chosen. The bottom part of the segment was investigated. The NT results are shown in ❺ (a). For the tomography 625 projections were recorded over an angular range of 360° with an exposure time of 25 s per projection. The resolution is 50 µm/px with a given field of view of 100 × 100 mm². ⑤ (b) shows the 3D representation of the reconstructed volume data set. Therein, the horizontal planes as seen in ⑤ (c) and (d) are indicated. In the upper section the soot deposits are displayed on the monolith walls, ⑤ (c). In ⑤ (d) the ash deposits are detected in the filter channels. The bright dots in the channels are metallic particles.

3.3 MICRO SETUP

For the high-resolution tomography with the micro setup (resolution 13.5 µm/px), the sample had to be cut to fit the size to the field of view of the detector (27×27 mm²). The sample is shown in ❻ (a). 625 projections over an angular range of 360° with an exposure time of 90 s per projection were recorded. The three-dimensional representation of the tomography data is shown in ⑥ (b). With the help of the tomography data, the different materials could be segmented according to the histogram criteria, ⑥ (c). An animation of the high-resolution tomography can be downloaded from [6].

❼ shows two vertical, ⑦ (a) and (b), and two horizontal, ⑦ (c) and (d), cross-sectional images. It can be seen that the soot deposits on the walls and on top of the ash. Noticeable in ⑦ (a) and (c) is the partial removal of the soot layer from the filter wall. The bright spots indicate metallic particles.

4 USAGE OF DIESEL FUEL CONTAINING TRACER AGENT

A tracer agent was developed to enhance both, the contrast of the soot within the neutron images and thereby improve the detection

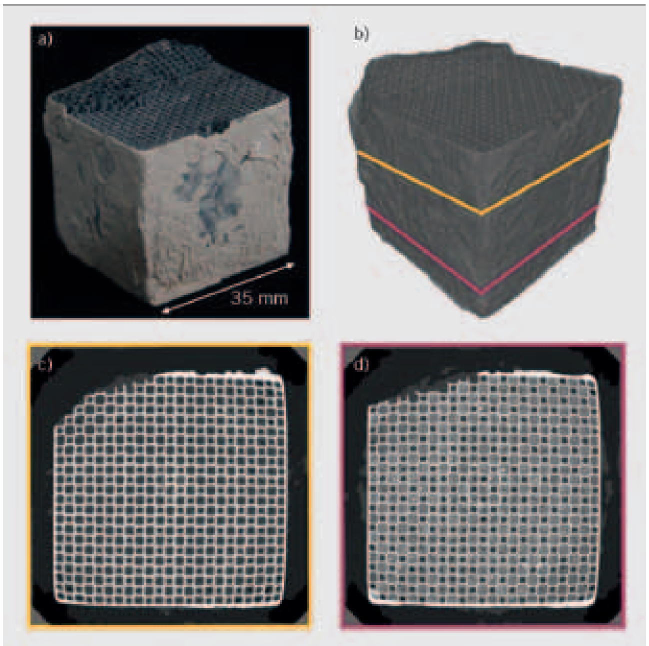

❺ Neutron tomography data of a single segment: (a) photo: (b) 3D visualisation, suggesting the cutting planes; (c) horizontal section through the segment, showing the soot loading on the walls; (d) horizontal section, showing the channels filled with ash; bright spots are metallic particles

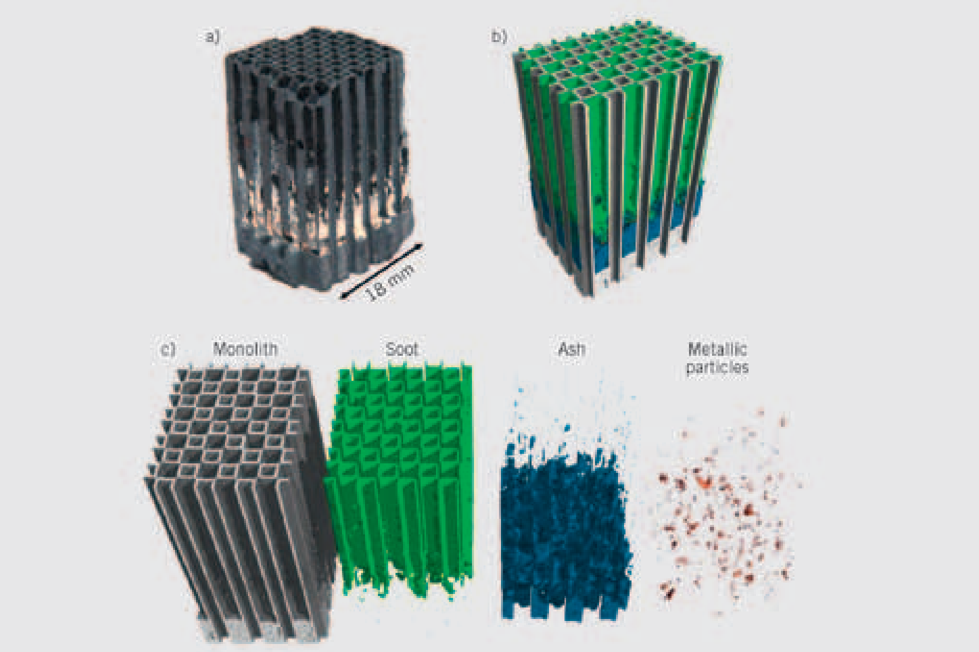

❻ High-resolution neutron tomography: (a) photo of the prepared sample; bright deposits are ash residues, black deposits result from the soot loading; (b) 3D representation; (c) segmentation of the individual components of the sample

accuracy. The tracer is based on a gadolinium (Gd) compound. Gd is an element showing one of the highest attenuation coefficients for neutrons ($\Sigma_{25meV} = 1500\ cm^{-1}$). Even smallest Gd concentrations (within the ppm-range) in the fuel are hence sufficient to increase the contrast. For the loading of the DPFs, 0.01 g pure Gd per litre diesel were sufficient.

❽ shows the NT data of a DPF loaded with normal diesel fuel (⑧ (a), (c)) and a DPF loaded with fuel containing the tracer agent (⑧ (b), (d)). The loading of the latter was achieved using an unloaded silicon-carbide monolith. The contrast enhancement of the soot containing the tracer with a layer thickness of 80 µm is clearly visible; this allows for a much more effective and precise visualisation of the soot layer within the filter. In ⑧ (b) no ash is observed as the filter had not yet been regenerated. Prominent features in ⑧ (d) are the crossing points of the monolith walls (small squares), which show clearly less soot inclusion than the filter walls between

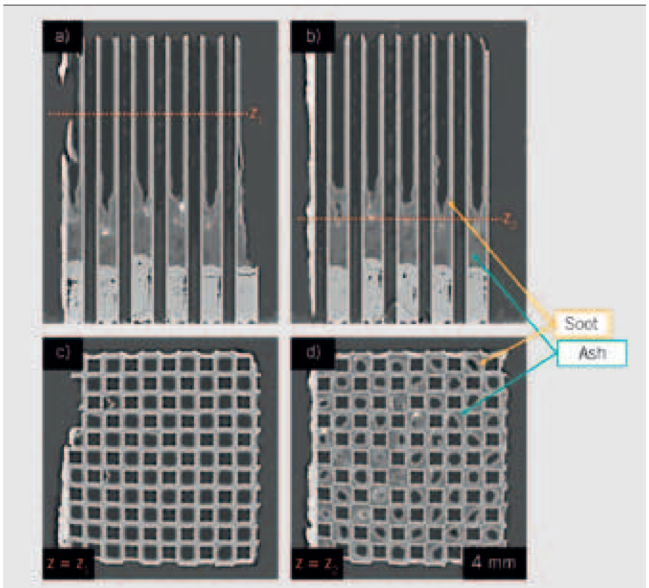

❼ Cross-sectional images of high resolution tomography: (a), (b) vertical sections at different positions; at the plug end one can clearly see the ash deposit, the soot is located on the wall and on top of the ash, bright spots are metallic deposits; (c) horizontal section through the upper part of the sample: soot deposit on the wall; (d) horizontal section through the lower part of the sample: soot and ash deposits

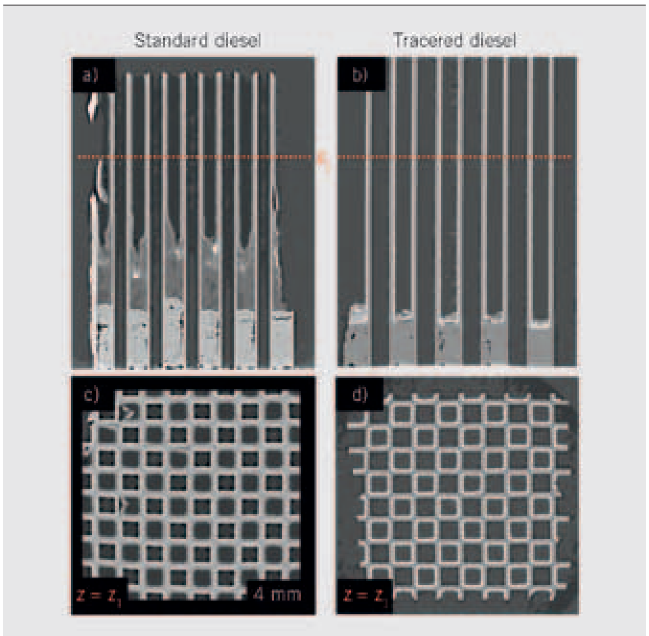

❽ Neutron-tomography data showing the comparison between a loaded DPF loaded using normal diesel fuel (left) and a DPF loaded with fuel containing a tracer agent (right); the contrast enhancement of the soot is clearly visible in (b) and (d) two channels. This means that it is possible to visualise the soot deposition within the filter walls using fuel containing the tracer agent. This would allow for example to study the filter effect of monoliths under variation of porosities.

A quantitative comparison between the loadings using normal fuel and fuel with the tracer agent can be seen in ❾. The histogram in the figure is based on the NT data shown in ⑧ and contains the occurrences of the absolute attenuation coefficient (Σ) values. The higher the peak the more material with this attenuation coefficient is in the sample volume. For the loaded DPF using the normal fuel one can distinguish between ash, soot and monolith material. Here, the ash shows the lowest Σ, followed by soot, whose Σ is slightly below the one of the monolith. This appears on a first glance not consistent with the relative attenuation coefficient from ①, where soot shows the highest Σ. For the calculation of the relative attenuation coefficient neither the density nor the porosity were considered. The measured attenuation coefficients, however, contain however information on the density and the porosity.

The DPF loaded with fuel containing the tracer agent shows remarkable differences. The peak of the soot with the tracer agent is now shifted to the right of the monolith peak in ⑨. The contrast of soot is increased by a factor of three. Depending on the Gd concentration used for the fuel, the soot peak can be moved and adjusted with regard to its attenuation coefficient. For the DPF loaded with the fuel containing the tracer, no ash peak is visible because no regeneration had been performed prior to the NT measurement. However, a considerable contrast enhancement would be expected.

5 SUMMARY AND OUTLOOK

The results of the neutron tomography investigations of the canned DPF showed that the three-dimensional ash and soot distribution can be visualised over an entire filter volume. Within single segments, the ash and soot distribution could also be monitored in discrete filter channels to gain information about the thickness of soot deposits. The application of a Gadolinium tracer additive resulted in a significant higher soot contrast and hence detection efficiency.

The results obtained from the static measurements will allow us to investigate dynamic charge and regeneration processes in particulate filters in real time.

Given that modern treatment of exhaust emissions comprises urea injection to optimise the conversion of nitrogen oxides, the sensitivity of neutrons towards hydrogen may also allow the visualisation of the urea distribution in DPFs.

The NI beam lines are available for industrial users after consultation to perform the here described or similar experiments.

THANKS

The authors want to thank Florian Schmid, Jan Hovind, Eberhard Lehmann und Peter Vontobel for the help during the measurements and visualisation of the data; Max Mehring for the chemical analyses; Hans-jörg Grützmacher for the development of the Gd-tracer additive, Pierre Comte und Jan Czerwinski for the loading of the DPF with the Gd-tracer additive; Verband der Schweizerischen Schmierstoffindustrie (VSS lubes) for the financial support of the tracer project.

REFERENCES

[1] Zandhuis, J. A.; et al.: SAE, DOI: 10.4271/2009-01-0289, 2009
[2] Mehring, A.; et al.: Journal of Thermal Analysis and Calorimetry, Volume 105, Number 2, pp. 545 – 552, 2011
[3] Kak, A. C.; Slaney, M.: Principles of Computerized Tomographic Imaging. SIAM, 2001
[4] Lehmann, E.; et al.: Nondestr. Test Eval. 16, 191-202, 2001
[5] Kaestner, A.; et al.: NIM A, Volume 659, Issue 1, pp. 387 – 393, 2011
[6] http://neutra.web.psi.ch/images/movie/DPF_Microtomo2_loQ.avi

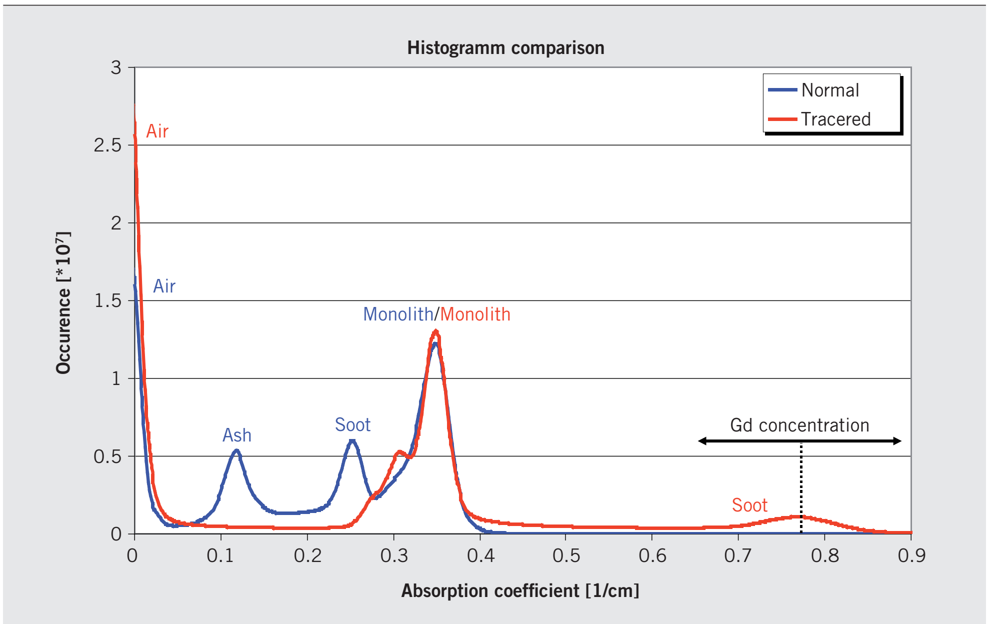

❾ Comparison of the attenuation coefficients for loadings with normal fuel and fuel containing the Gd tracer agent; for the normal loading ash, soot and monolith-material can be distinguished; remarkable is the increase of the attenuation coefficient of the soot containing the tracer by a factor of three

CORROSION PROTECTION OF ALUMINIUM IN BOILING COOLANT

For a future-orientated development of internal combustion engines regarding consumption optimisation with higher power densities coolants have to meet increased thermal stresses. The impact of local boiling on corrosion and corrosion protection due to added inhibitors was investigated at the Chair and Institute for Materials Technology (IfW), Technische Universität Darmstadt, in the context of the research project No. 969 "Boundary Temperature" assigned by the Research Association for Combustion Engines (FVV).

AUTHORS

DIPL.-ING. GEORG ANDERSOHN is a Research Associate in the Area of Expertise Surface Technology at Zentrum für Konstruktionswerkstoffe (MPA/IfW) of Technische Universität Darmstadt (Germany).

DR.-ING. TORSTEN TROSSMANN is Head of the Area of Expertise Surface Technology at Zentrum für Konstruktionswerkstoffe (MPA/IfW) of Technische Universität Darmstadt (Germany).

PROF. DR.-ING. MATTHIAS OECHSNER is Managing Director of Zentrum für Konstruktionswerkstoffe (MPA/IfW) and Professor for Materials Technology of Technische Universität Darmstadt (Germany).

PROF. DR.-ING. CHRISTINA BERGER is former Managing Director of Zentrum für Konstruktionswerkstoffe (MPA/IfW) of Technische Universität Darmstadt (Germany).

THE SEAL OF APPROVAL FOR SCIENTIFIC ARTICLES IN MTZ.
MTZ PEER REVIEW
RECEIVED 2011-10-26
REVIEWED 2011-11-30
ACCEPTED 2011-12-20
REVIEWED BY EXPERTS FROM RESEARCH AND INDUSTRY.

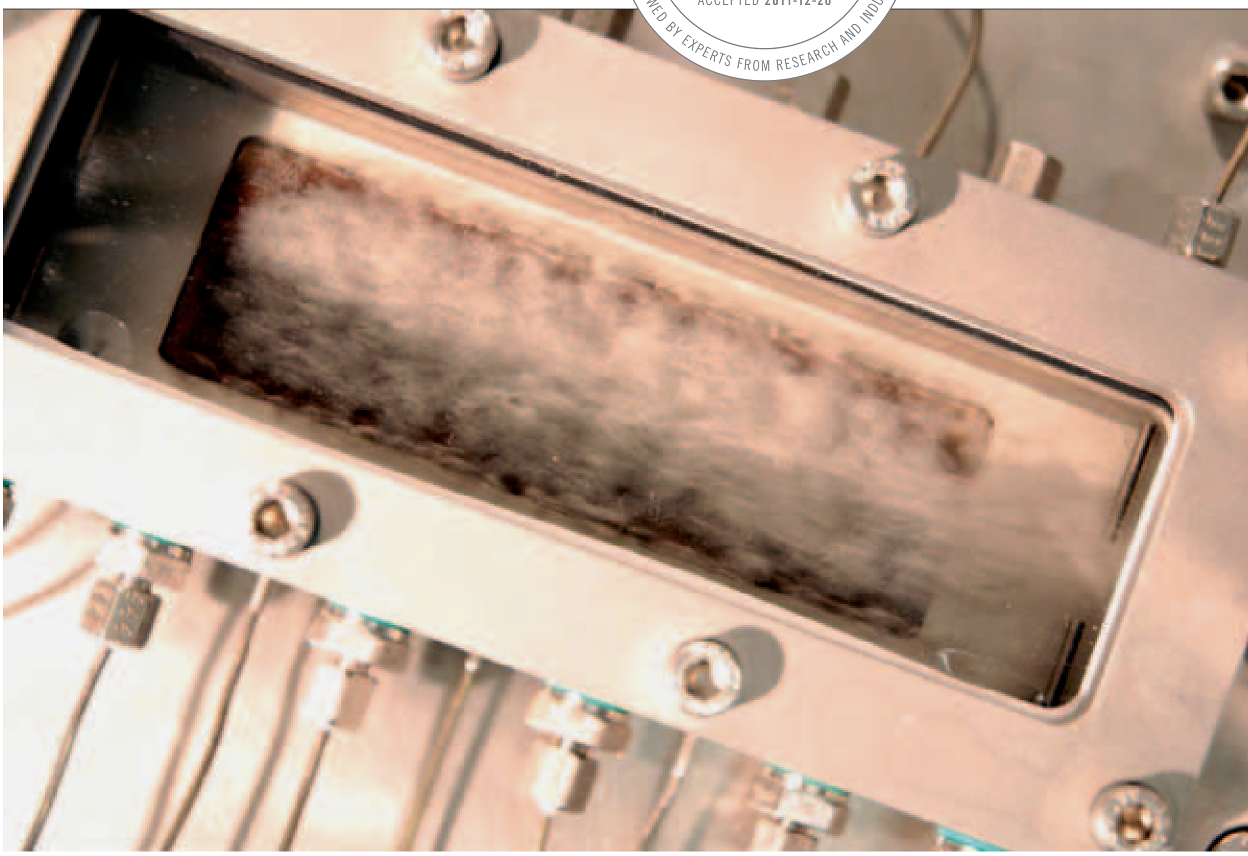

1 MOTIVATION

The highest priority in the development of future powertrains is the sustainable reduction of CO_2 emissions and the exploitation of potential savings regarding fuel consumption. The internal combustion engine as the key drive technology will not be replaced in the near future, especially not as part of a hybrid drive system. Therefore it has to fulfil the increased demands for efficiency and performance.

Towards more fuel-efficient automobiles the advanced direct injection for gasoline and diesel engines display a significant role, both in combination with turbocharging and downsizing concepts. The mentioned steps for optimisation generally result in a significant increase in combustion temperature, which on the other hand causes combined with an increasingly more compact design of engines an increase of the heat flux density and thus of the material temperatures [1]. Furthermore, due to an optimised thermal management of the cooling system, improved engine efficiency is achieved [2]. In this context, the stresses caused by various degrees of hybridisation have to be considered, such as start-stop systems, when a combustion engine of a vehicle under full load is suddenly switched off.

Consequence of these measures described above is an increased thermal load on the cooling system. The mean temperature of the coolant level is raised significantly, as well as the local coolant temperatures on hot surfaces. When the flow rate of the coolant is also controlled in order to achieve the optimum temperature of the units or even completely stopped because of the start-stop system, the local boiling and evaporation on hot material surfaces cannot be avoided.

Because of these local and temporarily different boundary conditions, like material and coolant temperatures, flow rates or boiling process, the electrochemical corrosion system consisting of the aqueous coolant and metallic materials is decisively affected. The formation and collapse of vapour bubbles or increased flow rates with local pressure drops can additionally promote the occurrence of cavitation and erosive effects [3]. Moreover, it is obvious that the boiling processes consisting of vapour bubble formation have an impact on the solubility and fouling of the additives and their corrosion protection abilities.

Within the scope of the research project "boundary temperature" the influence of such operating parameters and their effect on the interaction between material and coolant could be investigated under defined flow conditions on a relatively large specimen surface (30 cm^2). With the developed testing rig, called GTA, the corrosion and inhibition behaviour can be experimentally simulated in the laboratory depending on the selected test parameters and coolant additives using a high thermal loading, heat-carrying aluminium sample exposed to constant boiling of the passing coolant [4].

2 BOUNDARY-TEMPERATURE-RIG

The developed testing rig is a closed recirculation system designed with a separate air supply, ❶ (left). The turbulator in flow direction previous to the specimen chamber provides a defined type of flow. The heated aluminium specimen is pressed by means of the chamber on a copper block, which is heated by electric heating elements. The supplied electrical power is constant. This way, there is a heat flow, which dissipates through the specimen into the passing coolant, ① (right). Based on this specimen arrangement, the heat transport through a hot cylinder wall or liner into the coolant is simulated on laboratory scale.

The temperatures of the heater, the sample, and the coolant are detected with resistance thermometers. The temperatures within the specimen are measured through corresponding holes in a low-

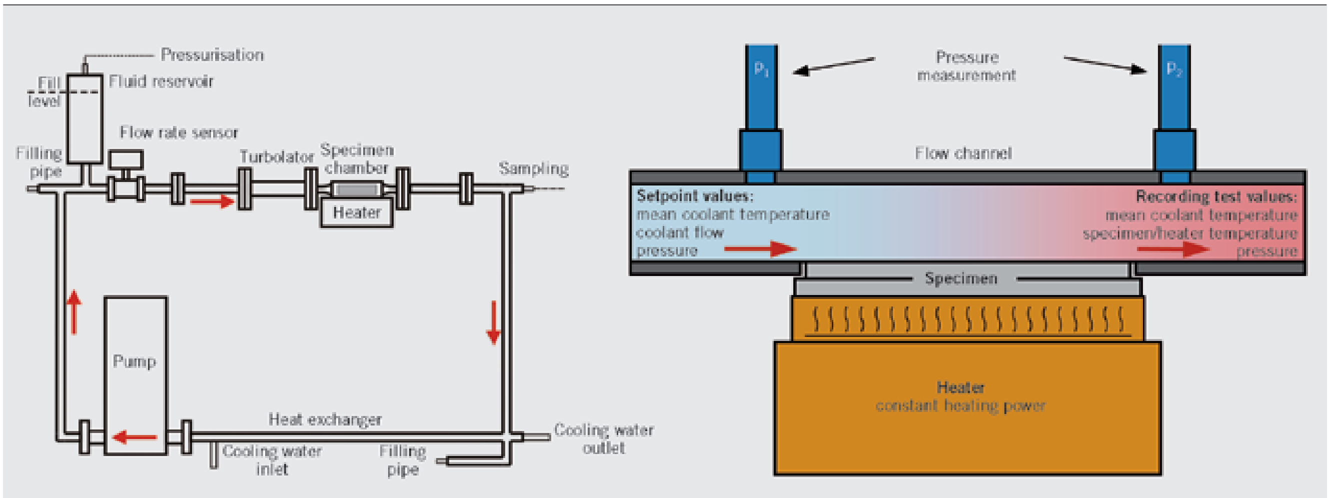

❶ Schematic view: recirculation system (left) and sectional view of heater/specimen/flow channel (right) er region (near the heater) and in an upper region (near the coolant-side surface of the specimen). Through a tubular heat exchanger, the heat introduced via the specimen is revoked exactly to allow a constant mean coolant temperature as a target value.

The three target values, namely average coolant temperature, flow rate, and pressure can be selected in certain areas and are precisely controlled throughout the test. The parameters used for the experiments are listed in ❷. Furthermore, the heating power and the test duration are input parameters. All measurements get stored during a test in 30-s intervals.

2.1 TEST PROCEDURE

The experimentation is carried out on the basis of FVV-Guideline R530-2005 [5]. This guideline includes detailed descriptions regarding the pre- and post-processing, purification and analysis of specimen as well as the test facility. The duration of an experiment is 96 h. The test run is separated in three heating periods of 12, 36 and 24 h and two 12-hour resting periods. The aluminium specimens are made of the material EN AC-Al Si6Cu4. Before each test run the specimen is being grinded (grain size 600) and purified (acetone).

2.2 COOLANT PREPARATION

In practical, coolants consist of 50 to 70 vol.-% water and 30 to 50 vol.-% coolant additive (glycol, inhibitors, additives). Due to the fact, that the relation between the wetted surface of the sample and the inhibitors concentration in the test is different to the praxis, an adjustment is needed. To achieve this, the concentration of inhibitors is reduced by adding mono ethylene glycol (MEG). The defined total proportion of MEG ensures that there are similar physical and thermodynamic properties. The used water is demineralised water to exclude a possible influence of the minerals present in tap water on the corrosion behaviour. The outcome of this is a mixing ratio for the tests of 20 vol.-% coolant additive, 20 vol.-% MEG and 60 vol.-% demineralised water. Among the three commercially available coolant additives are a silicate-containing product (coolant A: Si), one coolant additive based on organic acids (coolant B: OAT) and a hybrid coolant additive (coolant C: Si-OAT).

PARAMETER	Value
MEAN COOLANT TEMPERATURE	95 °C – 125 °C
FLOW RATE	20 l/min I 0.4 m/s
OVERPRESSURE	1.5 bar I 2.5 bar I 3.0 bar
HEATING POWER (ELECTRICAL)	2944 W
TEST DURATION	96 h
COOLANT VOLUME	4.5 l – 5.0 l
SPECIMEN SURFACE	30 cm²
HEAT EXCHANGER TUBE	565 cm²

❷ Test parameters

3 RESULTS

As influences on the corrosion behaviour following results on the variation of the mean coolant temperature and pressure are presented. The influence of the heat flux and coolant concentration is summarised.

3.1 EFFECT OF THE MEAN COOLANT TEMPERATURE

3.1.1 EVALUATION OF CORROSION BEHAVIOUR

❸ shows the change of mass of the specimens for different mean coolant temperatures and coolant additives A, B, and C. The experiments were performed at a pressure of 2.5 bar. An increase of mass is recorded in the experiments with coolant A (Si) at all samples due to formation of a surface layer. This layer formation is decreasing with increasing coolant temperature. All the specimens of the tests with coolant B (OAT) have a mass loss, which is lower at 95 °C than at 105 °C coolant temperature, and decreases again with increasing temperature level. Similar behaviour is observed when using coolant additive C (Si-OAT), but the absolute values for mass loss are higher by at least a factor of 3. With a total specimen weight of approximately 84 g the overall mass loss after a 96-hour test is up to about 1.2 %.

In particular, for the evaluation of the corrosion damage not only the integral value of dissolved material volume is important, but

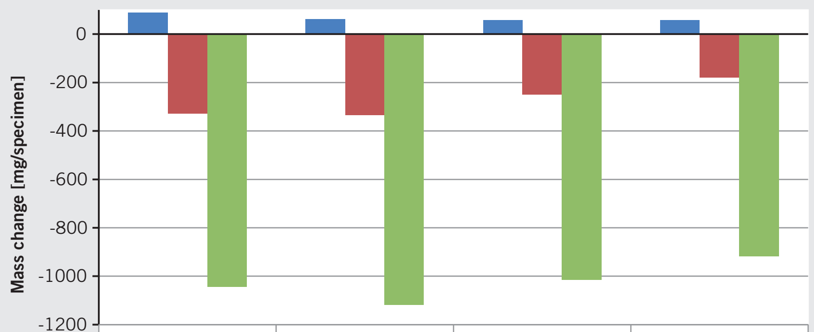

	95 °C	105 °C	115 °C	125 °C
Coolant A	88	60.8	56.2	56.5
Coolant B	-326.9	-334.8	-248.4	-180.1
Coolant C	-1043.4	-1117.9	-1013.9	-918.1

❸ Change in mass depending on the mean coolant temperature (96 h, 2.5 bar) also the depth of local corrosion attacks, which is more critical from a technical point of view. In addition, the formation of inhibition or reaction layers has to be evaluated, because these insulate thermally or reduce coolant flow to the point of blockage of the cooling channels.

To represent this, the appearance of the inhibition layer on specimens tested with coolant A (Si) at a temperature of 125 °C is shown in ❹ (top). The uniform thickness of the layer of 6 to 8 µm is visible in the cross section, ④ (below). For enhancement of contrast the specimens were previously coated with copper. Worth mentioning are the circular structures, which distinguish from the rest of the surface layer and are distributed on the entire specimen surface. The analyses by energy dispersive X-ray spectroscopy (EDX) detect predominantly silicon (Si) and oxygen (O) in the surface layer and in the circular structures. Thus, on the surface of the aluminium specimens a covering inhibition layer of aluminosilicates (Si–O–Al–O–Si) and silicates (O–Si–O) was formed. The circular structures are towering cylindrical shapes and typical for multi-chain silicates, for example poly silicates.

The micrographs using scanning electron microscope (SEM) document mostly surface corrosion on the specimens after the experiments with coolant B (OAT), ❺. The specimen at 105 °C also has pitting-like corrosion attacks. Hence, the corrosion phenomenon is dependent on the mean coolant temperature. The whole surface is covered by a reaction layer due to uniform corrosion with the specimen material. The intermetallic phases of the specimen material (Al_2Cu, Si) are integrated in the reaction layer, which predominantly consists of aluminium oxide or hydroxide with about 23 to 25 µm of thickness.

The specimens after the tests with coolant C (Si-OAT) have considerable uniform and pitting corrosion at all temperatures, shown for example in ❻. In comparison to the specimens in coolant B (OAT) the corrosion is a lot stronger, especially the depth of local corrosion attacks (correlation with mass loss). The most significant local attacks are 200 to 300 µm of diameter with hole depths of up to 200 µm. The only locally found reaction layer is about 10 to 18 µm thick and also mainly consists of aluminium oxide or hydroxide.

3.1.2 PRESSURE FLUCTUATIONS

During the experiments with coolants A (Si) and B (OAT) pressure fluctuations occurred solely at the mean coolant temperatures of 95 and 105 °C. In ❼, the pressure for all three coolants over the 96-hour test period at 105 °C coolant temperature is presented. The pressure fluctuations are an indication for changing boiling processes of the superheated coolant at the specimen surface.

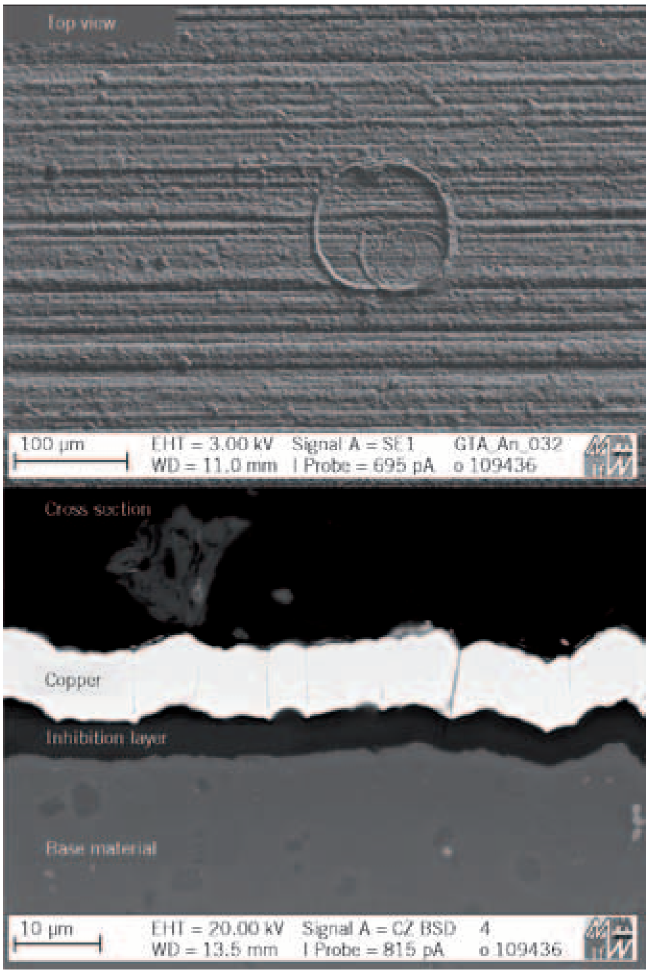

❹ SEM micrographs in top view and cross section, coolant A (Si), 125 °C

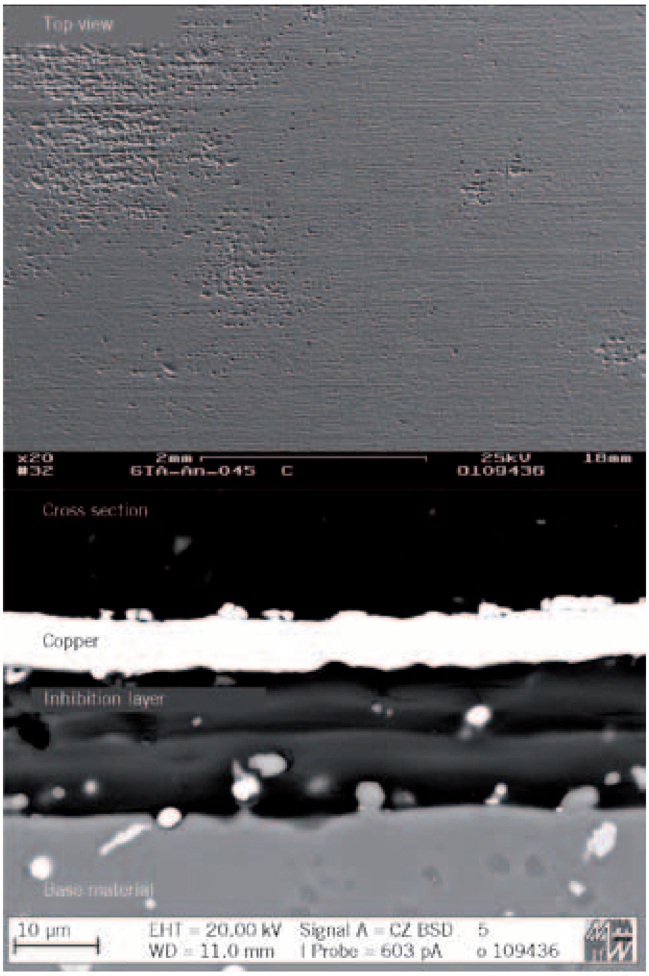

❺ SEM micrographs in top view and cross section, coolant B (OAT), 125 °C

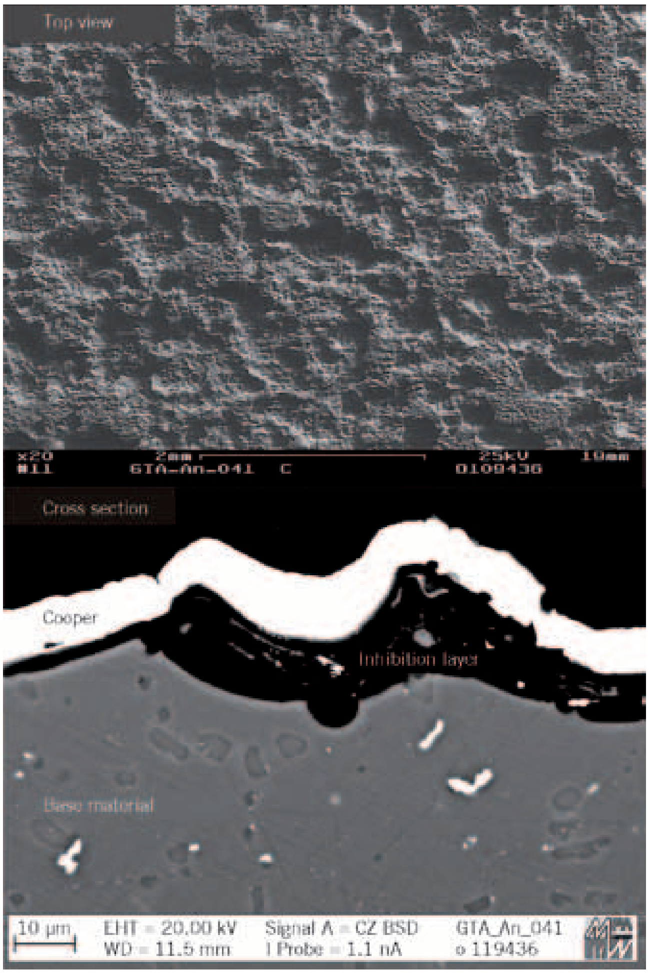

❻ SEM micrographs in top view and cross section, coolant C (Si-OAT), 125 °C

According to the measured temperatures in the range of 140 to 150 °C near the surface only water will evaporate at a relative pressure of 2.5 bars, since MEG has a boiling point of about 245 °C.

A detailed evaluation of the boiling was not subject of this research and is not possible by installed measurement techniques. However, it is assumed that in states with significant pressure fluctuations an unstable film boiling respectively a frequent change between stable and unstable boiling does exist. The pressure fluctuations are caused by the continuously changing number and size of itself forming and detaching vapour bubbles. In addition, it must be noted that the boiling state respectively the pressure fluctuations and their amount is depending on the formed reaction layers. During the tests with coolant C (Si-OAT), for example, no pressure fluctuations occurred. As influences on the boiling process the increased roughness of the sample surface due to considerable corrosion or the thermal insulating reaction layers have to be mentioned. These influences affect the heat transfer and lead to changed specimen temperatures.

In a direct comparison of pressure and specimen temperature correlations are observed: In a sudden decrease of pressure fluctuations the specimen temperature escalates. Pressure fluctuations are accompanied by a decrease in specimen temperature. Due to the measurement technique, it is not yet possible to determine which operation occurs first triggering further changes of the interactions. The initiation may be caused, for example, by degradation of heat transfer due to reaction layers formed on the sample surface, which subsequently means a further change in the boiling process, and thus induces the pressure fluctuations.

3.2 EFFECT OF THE PRESSURE

In order to specifically influence the boiling process, and to document the effect on the corrosion and inhibition behaviour, experiments were carried out at pressures of 1.5, 2.5, and 3.0 bar. Due to the increase of pressure, the boiling temperature of the coolant is higher, hence the boiling process and near-surface interactions between dissolved inhibitors and specimen are affected. As a result of the lower nucleate boiling the heat transfer is deteriorating, which implicates an increase of the specimen temperature.

The pressure rise leads to an increased formation of silicate layer in tests with coolant A (Si). The layer morphology is unchanged. On specimens examined in coolant B (OAT) an alternation of corrosion is documented. While at 1.5 bar prevails a local uniform corrosion, elevated pressure results in a local-depth corrosion attack, which is superimposed on the surface corrosion, ❽. Similar changes appear at the specimens tested in coolant C (Si-OAT): At elevated pressure a significant pitting corrosion attack can be documented instead of uniform corrosion, ❾.

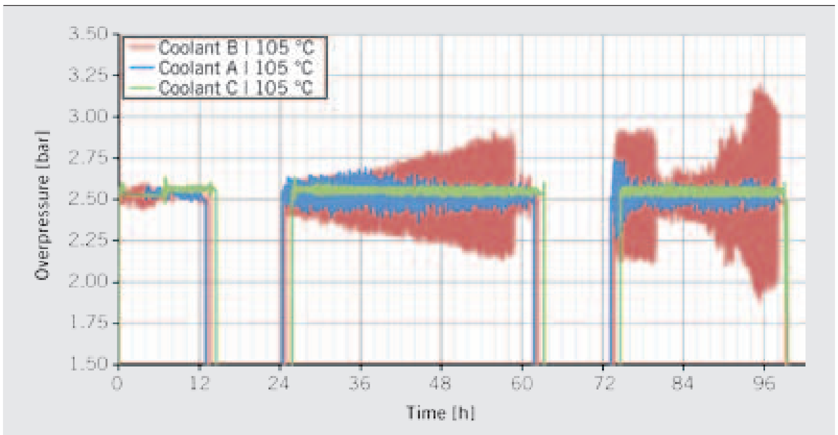

❼ Pressure measurement near the specimen, coolant A (Si)/ coolant B (OAT)/ coolant C (Si-OAT), 105 °C

4 CLASSIFICATION OF THE RESULTS

According to the results it is possible to make correlations between the key parameters influencing the corrosion and the corrosion protection. Specified and constant stress leads to an interaction at the boundary surface between material and coolant. Depending on the inhibition this causes a formation of an inhibition or reaction layer, and/or corrosion, which in return leads to damages of the material. These two factors are again dependent on the factors boiling and heat transfer. In addition, all four factors influence each other at the same time, ❿.

Using coolant A (Si) the formation of silicate layer is increased under permanent boiling conditions. This layer has a thermally insulating effect, so the heat dissipation deteriorates and the boiling process changes. As a result the sample temperature increases. This in turn means a self-reinforcing effect for the formation of silicate layers. The increasing thickness of the layer can lead to overheating and to corrosive damage of the material. A disruption of the layer by thermal expansion is additionally feasible. Due to the permanent regeneration and healing of the layer the inhibitor depletion is also relevant in this context. The silicate reserves in the coolant are exhausted and there is no longer (adequate) corrosion protection.

In coolant B (OAT) a reaction layer is formed in addition to mass loss and uniform corrosion, which also acts thermally insulating, and thus constantly influences and changes the boiling and the heat dissipation. A depletion of inhibitors does not occur. Only a local reaction layer and mostly significant pitting-like corrosion attacks with high mass loss are documented when using coolant C (Si-OAT). The pressure reduction clarifies, that the corrosion behaviour is dependent on the boiling process, the heat dissipation, and thus the sample temperature, because the type of corrosion is alternating from pitting to uniform corrosion. The predominant mechanism of silicate additives and organic acids or the interaction between both cannot be definitively assessed.

5 SUMMARY

Due to the successful testing with the developed "Boundary-Temperature-Rig" the interactions between materials and coolants could be investigated. The corrosive damage and the inhibition were estimated at defined and practically relevant constraints on

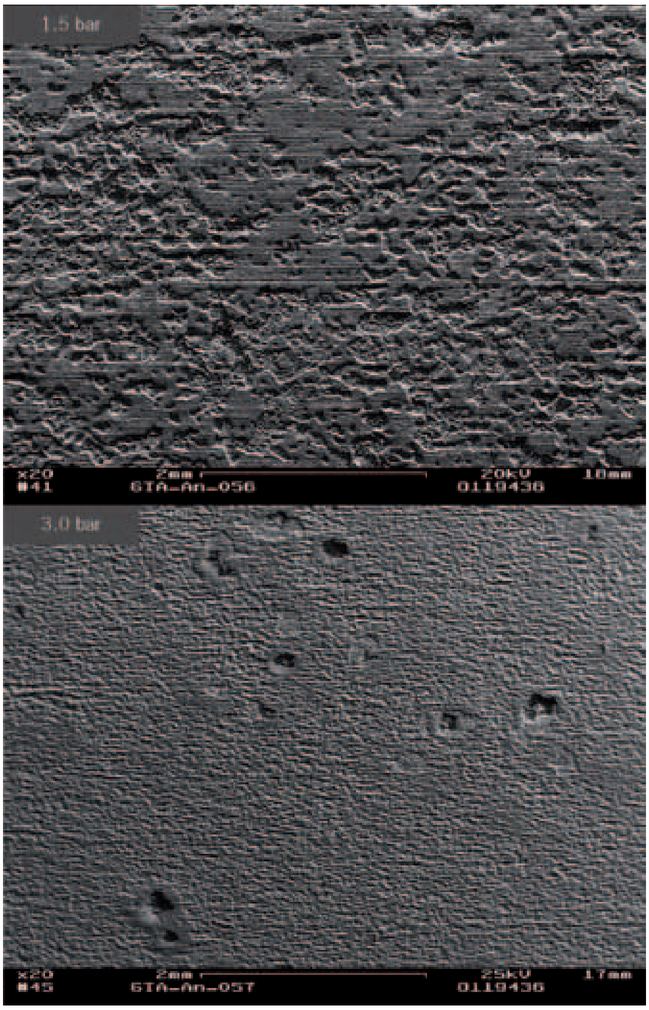

❽ SEM micrographs of the specimen surface, coolant B (OAT), 115 °C, 1.5/3.0 bar

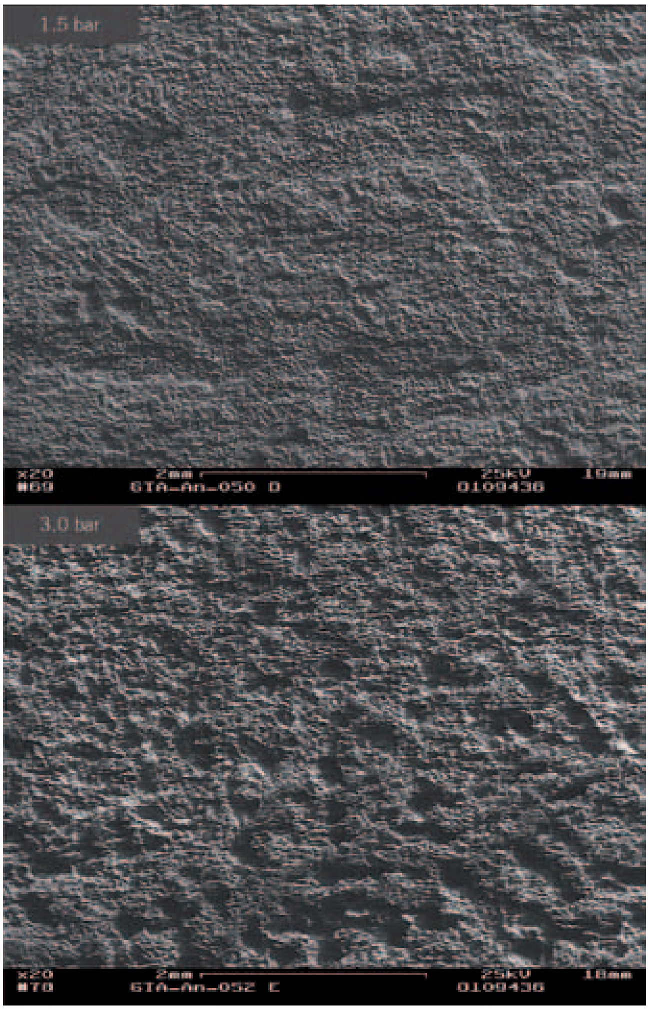

❾ SEM micrographs of the specimen surface, coolant C (Si-OAT), 115 °C, 1.5/3.0 bar

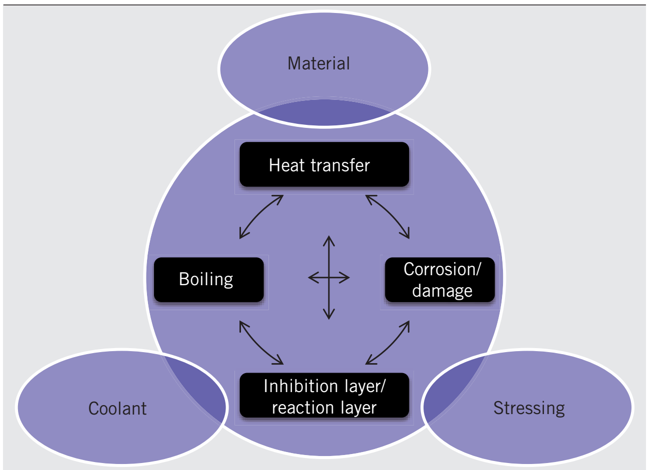

⑩ Interactions between the parameters influencing corrosion behaviour

THANKS

The IGF-project (15627 N/1) of the Research Association for Combustion Engines (FVV) was supported by the AiF in the framework of the program to promote industrial research and development (IGF) by the Federal Ministry of Economics and Technology based on a decision of the German Bundestag. The authors thank the FVV for the opportunity to implement the project, and the BMWi and the AiF for the financial support. The project was accompanied by a working group of the FVV under the leadership of Hans Koch, Behr GmbH & Co. KG. This working group deserves our thanks for the great support.

a relatively large specimen surface. From the corrosion point of view the decisive factors, which were assessed within the scope of the research project, are heat flux, near-surface sample temperature, inhibitor concentration and local boiling conditions. In this context the mean coolant temperature is only a minor influencing factor. Combinations of stress, that promote a high material removal or local corrosion attacks, have to be avoided. The question, if stress limits in terms of corrosion protection were already exceeded with the investigated coolant additives and the selected parameters, cannot be answered at this point. However, the partly significant corrosion attacks give reasons to further investigations. The developed testing rig, called GTA, is a tool for component and coolant manufacturers in order to identify possible thermal limitations of the corrosion system "material/coolant" under permanent boiling conditions. Knowledge of the consequences in modern engine and cooling system developments can be assured.

Further studies on the corrosion behaviour with local boiling and complete evaporation of the coolant are currently in progress as part of the follow-up project "boundary temperature II". Hereby, the flow of the coolant is varied, even to zero, in order to investigate the effects of an optimised thermal management.

REFERENCES

[1] Robert Bosch GmbH: Der Verbrennungsmotor hat Zukunft. Presse-Information, September 2009
[2] Röser, P.: Energetisch optimiertes Kraftfahrzeugkühlsystem. Schriftenreihe des Instituts für Verbrennungsmotoren und Kraftfahrwesen der Universität Stuttgart, Band 31, Stuttgart: Vieweg, 2006
[3] Berger, C.; Troßmann, T.; Kaiser, M.: Heißkühlung – Kühlmittelzusätze auf dem Prüfstand. In: MTZ 69 (2008), No. 2, pp. 146 – 153
[4] Andersohn, G.; Troßmann, T.; Eppel, K.; Oechsner, M.; Berger, C.: Grenztemperatur – Thermische Einsatzgrenzen für die Anwendung von Kühlmittelzusätzen. FVV-Abschlussbericht zum Vorhaben Nr. 969, Heft 937-2011, Frankfurt, 2011
[5] Forschungsvereinigung Verbrennungskraftmaschinen e. V.: Prüfung der Eignung von Kühlmittelzusätzen für die Kühlflüssigkeiten von Verbrennungsmotoren. Prüfrichtlinie, Heft R530-2005, Frankfurt, 2005